MAXIMISING THE PHOTOBIOLOGICAL PRODUCTION OF HYDROGEN USING LEACHATE, WHILE MONITORING ALGAL PHOTOSYNTHESIS USING PAM FLUOROMETRY

Sarah Anne White

Supervisor:

Professor Cristina Trois

University of KwaZulu Natal

Co-Supervisor:

Professor Akash Anandraj

Mangosuthu University of Technology

Submitted in fulfilment of the Doctor of Philosophy degree, College of Agriculture, Engineering and Science, University of KwaZulu-Natal, Durban

March 2014

MAXIMISING THE PHOTOBIOLOGICAL PRODUCTION OF HYDROGEN USING LEACHATE, WHILE MONITORING ALGAL PHOTOSYNTHESIS USING PAM FLUOROMETRY

Sarah Anne White

I hereby declare that the dissertation represents my own work. It has not been submitted before for any diploma/degree or examination at any University.

_____

Sarah Anne White

As the candidate's Supervisor I agree/do not agree to the submission of this thesis

_____   _____

Prof Cristina Trois   **Prof Akash Anandraj**

Supervisor   Co-Supervisor

College of Agriculture, Engineering and Science Centre for Algal Biotechnology

University of KwaZulu Natal   Mangosuthu University of Technology

This _____ day of _____ 2014, at the University of KwaZulu Natal.

ABSTRACT

Hydrogen is universally known as the most efficient renewable energy source capable of meeting global energy demands. *Chlamydomonas reinhardtii* has the ability to produce biohydrogen during the metabolic engineering of the photosynthetic pathways. The aim of this study was to 1) use leachate as a feedstock to enhance microalgal biomass and subsequent hydrogen production, 2) use Pulse Amplitude Modulated (PAM) Fluorometry to elucidate the role of photosystem one during hydrogen production, 3) use Nicotinamide Adenine Dinucleotide Phosphate (NADPH) fluorescence as an indicator of hydrogen production and 4) design a modular pilot scale biohydrogen bioprocessing system implementing experimental findings into a conceptual model. This resulted in a cost effective source of renewable hydrogen produced from waste. The use of 16% landfill leachate was found to increase biomass production by 26% as compared to using Tris-Acetate Phosphate (TAP) media alone. Hydrogen induction resulted in an increased gas synthesis of 37% as well as an increased production period of 8 days compared to the normal 5 days. Landfill leachate further reduced the costs as it acted as a free nutrient source with the added ecological advantage of leachate treatment. Hydrogen production was induced by sulphur depletion and physiological parameters were measured using PAM Fluorometry. Photosystem I was found to be dominant during hydrogen production while photosystem II was down-regulated due to the sulphur depletion and damaged D1 proteins. NADPH fluorescence was significantly correlated to hydrogen yields allowing for NADPH to be utilised as a molecular indicator for hydrogen synthesis. The overall functionality of this bioprocessing system relies on the optimum physiological functioning of cells. The above findings were implemented into a pilot scale design, maximising the physiological performance during hydrogen production. This study has contributed knowledge regarding the production of hydrogen gas from leachate, the physiological changes of photosystem I during hydrogen production and the use of NADPH fluorescence as an indicator. The fundamental theories of bioprocessing incorporate a firm understanding of cellular and biochemical processes. The use of molecular indicators determined from physiological studies can be used at pilot scale to improve overall efficiency of hydrogen production.

COLLEGE OF AGRICULTURE, ENGINEERING AND SCIENCE

DECLARATION 1 - PLAGIARISM

I, Sarah Anne White declare that

1. The research reported in this thesis, except where otherwise indicated, is my original research.

2. This thesis has not been submitted for any degree or examination at any other university.

3. This thesis does not contain other persons' data, pictures, graphs or other information, unless specifically acknowledged as being sourced from other persons.

4. This thesis does not contain other persons' writing, unless specifically acknowledged as being sourced from other researchers. Where other written sources have been quoted, then:
   a. Their words have been re-written but the general information attributed to them has been referenced
   b. Where their exact words have been used, then their writing has been placed in italics and inside quotation marks, and referenced.

5. This thesis does not contain text, graphics or tables copied and pasted from the Internet, unless specifically acknowledged, and the source being detailed in the thesis and in the References sections.

6. The Turnitin Report produced a Similarity Index of 10% (Appendix 3).

Signed

_____

Sarah Anne White

COLLEGE OF AGRICULTURE, ENGINEERING AND SCIENCE

DECLARATION 2 - PUBLICATIONS

Details of contribution to publications that form part and/or include research presented in this thesis are as follows:

Publication 1:

White, S., Anandraj, A. & Trois, C. 2013. The effect of landfill leachate on hydrogen production in *Chlamydomonas reinhardtii* as monitored by PAM Fluorometry. International Journal of Hydrogen Energy 38, 14214-14222 (Appendix 1).

Sarah White undertook all the experimental work and writing of the draft article. Profs Cristina Trois and Akash Anandraj assisted with the development of the experimental protocol and the finalisation of the manuscript. They were also responsible for the overall supervision of this project.

Publication 2: (Submitted)

White, S., Anandraj, A. & Trois, C. 2013. Photosynthetic Shift Towards Photosystem I Up-Regulation during Hydrogen Production in *Chlamydomonas reinhardtii*. International Journal of Hydrogen Energy.

Sarah White undertook all the experimental work and writing of the draft article. Profs Cristina Trois and Akash Anandraj assisted with the development of the experimental protocol and the finalisation of the manuscript. They were also responsible for the overall supervision of this project.

Publication 3:

White, S., Anandraj, A. & Trois, C. 2013. NADPH fluorescence as an indicator of hydrogen production in the green algae *Chlamydomonas reinhardtii*. International Journal of Hydrogen Energy. 39: 1640 -1647. (Appendix 2)

Sarah White undertook all the experimental work and writing of the draft article. Profs Cristina Trois and Akash Anandraj assisted with the development of the experimental

protocol and the finalisation of the manuscript. They were also responsible for the overall supervision of this project.

Publication 4: (In Preparation)

White, S., Anandraj, A. & Trois, C. Design of a Modular Pilot Scale Biohydrogen Processing System.

Publication 5: (In Preparation)

White, S., Anandraj, A. & Trois, C. A Critical Review of Biohydrogen Production Technology and its Latest Advancements. Renewable and Sustainable Energy Reviews.

Signed:

_____

Sarah Anne White

SANPAD Research Capacity Initiative (RCI) 2011/2012 Cohort

The South Africa Netherlands research Programme on Alternatives in Development (SANPAD) has since 1997, been financed by the Netherlands Ministry of Foreign Affairs (www.sanpad.co.za). SANPAD has facilitated and financed research projects, search capacity building and research support activities over the past ten years. The specific outcome for the 7 week RCI programme is an assessed proposal for a PhD that can be registered in the year of completion of the RCI Programme.

I was selected to be part of this programme as a member of the 2011/2012 cohort.

Modules included:

Survey of Theories

Identifying a Good Research Question

Survey of Qualitative Methods

Evaluating Research Designs and Research Proposal Writing

Dealing with Data

Mentoring and Dissemination

Composing and Defending the Research Proposal

The programme was successful and graduation was the 7 September 2012 (Appendix 3).

ACKNOWLEDGEMENTS

TABLE OF CONTENTS

LIST OF FIGURES

LIST OF TABLES

ABBREVIATIONS AND NOTATIONS

Pulse Amplitude Modulated Fluorometry

AL	Actinic Light
Alpha (α)	Maximum photosynthetic efficiency
CEF	Cyclic Electron Flow
F	Dark fluorescence yield
F_o	Minimum fluorescence in a dark adapted sample
F'_o	Minimum fluorescence in a light adapted sample
F_m	Maximum fluorescence in a dark adapted sample
F'_m	Maximum fluorescence in a light adapted sample
Fluo	Fluorescence
F_v	Variable fluorescence (F_m-F_o)
F'_q/F'_m	PS II operating efficiency
F_v/F_m	Maximum quantum yield of PSII
LEF	Linear Electron Flow
ML	Measuring Light
NPQ	Non Photochemical Quenching
PAM	Pulse Amplitude Modulated Fluorometry
P-I Curves	Photosynthesis – Irradiance Curves
P_m	Maximal change of P700 in a dark adapted state
P'_m	Maximal change in P700 in a light adapted state
PPFD	Photosynthetically Active Photon Flux Density
PS I	Photosystem One
PS II	Photosystem Two
P700 red	Fraction of P700 that is reduced in a given state
rETR	Relative Electron Transport Rate
ETR_{max}	Maximum Relative Electron Transport Rate
RLC	Rapid Light Curve
YI	PSI photochemical quantum yield
YII	Effective PSII quantum yield
Y (NA)	Nonphotochemical quantum yield of PS I (fraction of P700 that cannot be oxidized)

Y (ND)	Nonphotochemical quantum yield of PS I (fraction of oxidized P700)
Y(I) :Y(II)	Quantum yield ratio

Units

A	amp
cm	centimetre
cB	centiBarrer
d	day
g	gram
hr	hour
kg	kilogram
kWh	kilowatt hour
L	litre
m	metre
m^3	cubic metre
mg	milligram
mL	millilitre
mPa	milliPascals
mS	milliSiemens
nm	nanometre
NTU	Nephelometric Turbidity Unit
ppm	parts per million
ppt	parts per thousand
psi	pounds per square inch
s	seconds
t	ton
Tg	terragram
μg	microgram
μs	microseconds
kL	kilolitre
V	volts
W	Watt
Wh	Watt Hour
°C	degree Celsius

Chlamydomonas Growth Media

dH$_2$O	distilled water
TAP	Tris-Acetate Phosphate
TAP-S	Tris-Acetate Phosphate minus sulphur

Molecular

ATP	Adenosine Triphosphate
Chl *a*	Chlorophyll *a*
CO$_2$	Carbon Dioxide
DCMU	3-(3,4- dichlorophenyl)-l,l-dimethylurea
H$_2$	Hydrogen
NADP$^+$	Nicotinamide Adenine Dinucleotide Phosphate (oxidised form)
NADPH	Nicotinamide Adenine Dinucleotide Phosphate (reduced form)
NH$_4$	Ammonium
NH^3	Ammonia ion
NO$_3$	Nitrate
NO^{3-}	Nitrate ion
NO^{2-}	Nitrite ion
O$_2$	Oxygen
PO^{4+}	Phosphate ion

Elemental

Cd	Cadmium
Cl	Chloride
Co	Cobalt
Cr	Chromium
Fe	Iron
H	Hydrogen
Hg	Mercury
K	Potassium
Mg	Magnesium
Mn	Manganese
Mo	Molybdenum
Na	Sodium
Ni	Nickel

P	Phosphorus
Rb	Rubidium
Rh	Rhodium
Ru	Ruthenium
S	Sulphur
Zn	Zinc

Technical/Instrumentation

AC	Alternating Current
Ah	Amp hour
AVR-RISC	Advanced Virtual RISC
DC	Direct Current
EDX	Energy Dispersive X-Ray
GPRS	General Packet Radio Service
IED	Intelligent Electronic Devices
LED	Light Emitting Diode
MBT	Mechanical Biological Treatment
MHz	Mega Hertz
NiMH	Nickel Metal Hydride
PC	Personal Computer
PEMFC	Proton Exchange Membrane Fuel Cells
PLC	Programmable Logic Controller
PTFE	Polytetrafluoroethylene
RTU	Remote Terminal Unit
SEM	Scanning Electron Microscope
SCADA	Supervisory Control and Data Acquisition
USB	Universal Serial Bus
WAP	Wireless Application Protocol
WtE	Waste to Energy

General

HyTEC	Hydrogen Transport for European Cities
SHLP	Shanghai Hydrogen Lighthouse Project
SUV	Sports Utility Vehicle
USA	United States of America

CHAPTER ONE
General Introduction

1.1 Sustainable Energy

The effects of fossil fuel utilisation cause global climate change, energy conflicts and energy shortages. There negative effects have been observed throughout all levels of society i.e. global, regional and local. The result is that energy is know considered a key player towards sustainable development (Yuksel and Kaygusuz, 2011). This means that sustainable development requires the supply of affordable and clean renewable energy that does not cause a negative impact on society. Investigations into alternative energy sources such as solar, wind, hydro and wave power have recently showed popularity. A new trend of research into waste from agriculture, industry and domestic sources is been converted into useful energy namely biohydrogen, biogas and bio-alcohol. This occurs through waste to energy technologies and is currently underway on a global perspective (Yuksel and Kaygusuz, 2011, Kothari et al., 2010). The use of waste and biomass to produce renewable fuels is a high quality solution to energy security, especially when coupled to energy recovery technology (Ciccoli et al., 2010). Ciccoli et al, 2010 also state that waste fuels are generally poor in energy content which requires maximum efficiency in the utilization in order to obtain a usable amount of energy. One of the most important factors of renewable energy is their environmental compatibility. Inline with this characteristic, renewable energy sources (mainly organic waste materials) are likely to become one of the more attractive substitutes in the near future.

It has been shown that 4 energy paths are considered to attain sustainability. These paths are 1) continuation of current energy use technologies and amendments; 2) universal adoption of advanced technologies for transportation and electricity generation; 3) the production of alternative renewable energy sources from waste and biomass resources to supplement conventional energy production processes and 4) the development of centralized clean energy production routes and distribution systems (Kothari et al., 2010). With regard to path 3, various agricultural waste types (animal and plant wastes), industrial (dairy wastes, sugar refineries, paper and pulp, tanneries and slaughter houses) as well as kitchen and garden waste have been found to be potential renewable energy sources, able to attain sustainability

with regard to Waste-to-Energy. These waste types are generally considered as solid waste and are placed in landfill sites as a main waste management technique. In developing countries landfills are often the only economic form of waste disposal (El-Fadel et al., 2012).

1.1.1 Global Waste to Energy from Landfills

Municipal solid waste constitutes an important and escalating environmental problem. It has been estimated that waste production varies from 0.5 kg to 4.5 kg per person in different regions of the world (Bakare et al., 2005). Many developing and developed countries use landfills as a waste management technique in which to dispose their waste (Fig 1.1). It can be seen that South Africa ranks landfills approximately 90% of its waste, with only about 10% been recycled (Department of Environmental Affairs (2012)). There are numerous methodologies to treat municipal solid waste. The most well established methods include thermal Waste-to-Energy (WtE) or mass grate combustion as well as different Mechanical-Biological Treatments (MBT) (De Gioannis et al., 2009). Here the energy is recovered and the residual biomass is disposed through landfilling (Cimpan and Wenzel, 2013). Other methods include waste pyrolysis, gasification and mechanical heat treatment however these methods have proven less efficient. Over the years methane from landfill has been extracted and used for various energy processes such as electricity generation or as a direct fuel source (Bolan et al., 2013). Global methane emissions from landfill have been estimated to be between 9 - 18 to 30 - 70 Tg/year (Salomon and Silva Lora, 2009).

1.1.2 Environmental Issues of Landfills

Landfills have been found to cause environmental degradation through the production of leachate (Lou and Nair, 2009). Leachate is caused by the percolation and infiltration of runoff water, rain, ground water and flood water through the landfill biomass (Kjeldsen et al., 2002). It has been previously reported that leachate, even in small quantities can pollute large quantities of fresh water rendering them toxic for commercial and in particular domestic use (Trois et al., 2010b). This makes landfill leachate a recognised environmental problem requiring appropriate treatment and processing. Leachate treatment methods include nitrification-denitrification, chemical oxidation, aerobic-anaerobic decomposition, active carbon, reverse osmosis, coagulation-flocculation and adsorption or a combination of these methods (Trois et al., 2010a). Biological processing of leachate produces biogas (methane,

carbon dioxide and small quantities of hydrogen sulphide) which can be used as an energy source (Balmant et al., 2014).
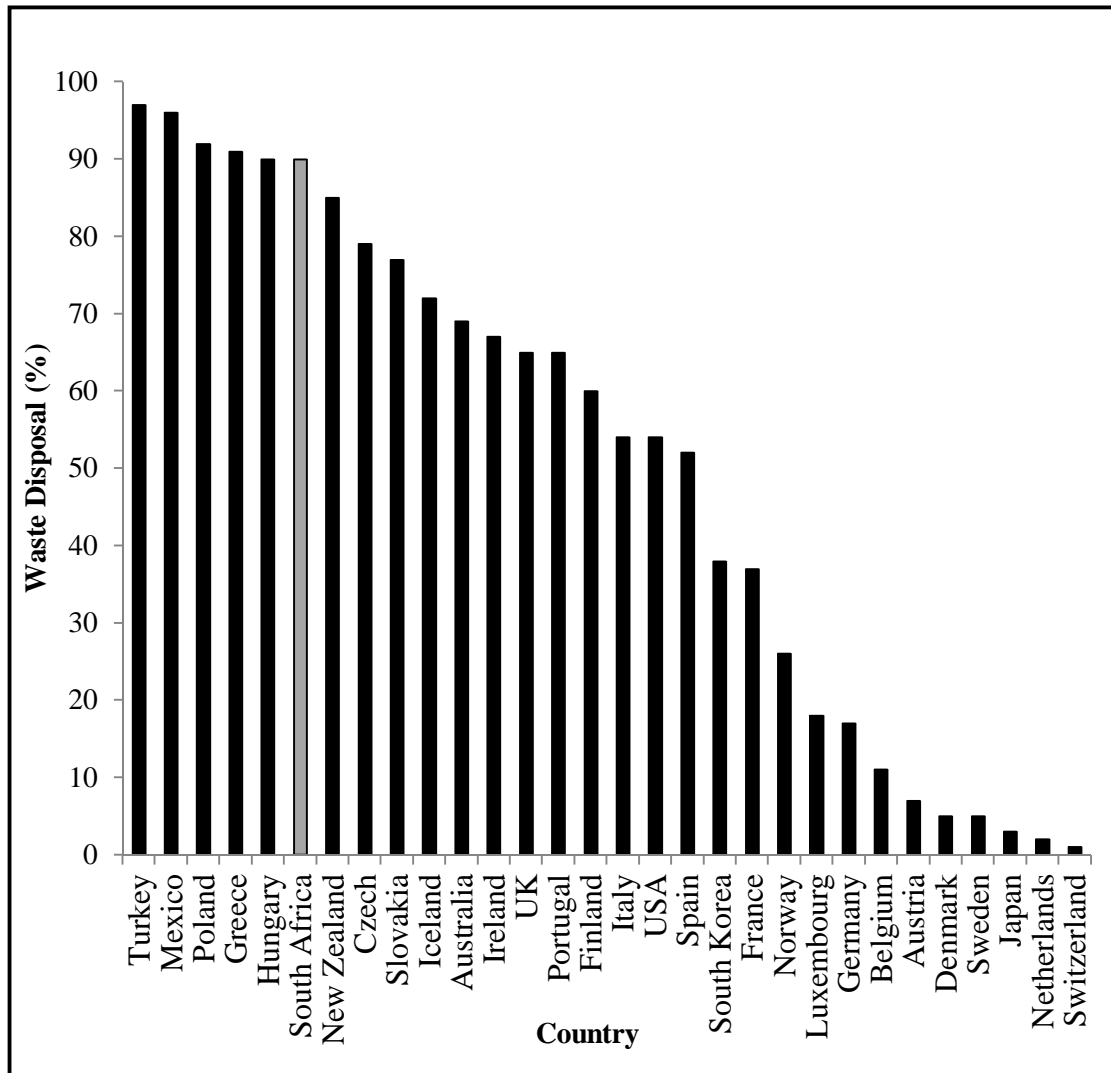
Figure 1.1: Percentage Waste Disposal in landfills in both developed and developing countries (Bolan et al., 2013)

1.1.3   Landfill and Leachate Processing in Durban, South Africa

The eThekwini Municipality in Durban, has a population of over 3.5 million people (2010 census) and generates approximately 1.2 million tonnes of municipal solid waste per annum (Trois et al., 2007). eThekwini has three projects underway to produce landfill gas which was converted to electricity (Couth et al., 2011). These projects are stationed at the Bisasar

Road, La Mercy and Marianhill landfill sites. A total of 9 MW was produced from these sites.

In Durban the high rainfall results in the generation of large volumes of leachate (Trois et al., 2007). Research has taken place to treat the leachate using a denitrification process using pine bark as the carbon source (Trois et al., 2010a). Leachate consists of high concentrations of dissolved and finely suspended organic matter and inorganic compounds with the main compound being ammonia (Singh et al., 2013). Leachate has also been found to contain large quantities of various organic constituents such as nitrogen and phosphorus, tannins, phenols, humic acids and heavy metals (Lin et al., 2007, Zhang et al., 2009, Trois et al., 2010a). There is a characteristic trait of leachate to be excessive in these nutrients, particularly ammonia (Robinson et al., 2005, De Gioannis and Muntoni, 2007). This chemical make up of leachate will fluctuate over time depending on the degradation stage of the waste, type of waste and landfill technology as well as seasonal changes and the of amount of rainfall, however large quantities of nutrient will remain (Kawai et al., 2012). The treatability of landfill leachate depends on its composition and characteristics which is highly dependant on the age of the landfill site. Stabilized or young landfills have very different characteristics (Kurniawan et al., 2006).

1.1.4   Leachate as a Feedstock for Microalgae

Microalgae are unicellular, microscopic, polyphyletic, organisms that have the ability to convert solar energy, carbon dioxide and water to biomass. It is for this reason that it can be cultured as an energy crop (Greenwell et al., 2009). A growing range of studies have been conducted exploring techniques and procedures to produce large quantities of biomass for numerous applications (Harun et al., 2010). Since microalgae are photosynthetic organisms, the chlorophyll and bioactive compounds can be utilized for food and cosmetic purposes (Spolaore et al., 2006). The high lipid content of some microalgae has made then a favourable source for biodiesel production (Chisti, 2007). Numerous other energy sources have been produced from microalgae namely biomethane (Chynoweth et al., 2001), bioethanol (Chisti, 2008) and biohydrogen (Ghirardi et al., 2000).

Microalgae are favoured other biomass sources as they require less water than terrestrial crops and can be grown in freshwater, saline or brackish environments (Chisti, 2008). Microalgae have a generation time of between 4-24 hours allowing for continuous biomass

formation (Chisti, 2007). The feasibility of microalgal cultivation depends on optimising the external parameters. These include light, carbon dioxide, water and inorganic salts (Chisti, 2007). Temperature is also important as it must remain in a range conducive to algal growth (normally 20 to 30 °C in South Africa). Maintaining optimal levels of nutrients will also increase biomass production with the most important nutrients being nitrogen (N), phosphorous (P), iron (Fe).

The increasing costs of nitrogen and phosphorous fertilizers is putting stress on maintaining feasible large scale production systems (Bhatnagar et al., 2011). Thus it is essential to find alternative sources of nutrients for the production of microalgal biomass and consequently renewable energies (Bhatnagar et al., 2011). Maturation ponds at wastewater treatment plants have shown promise to provide a rich supply of nutrients (Clavier et al., 2005, Cho et al., 2013). Recently studies have shown the use of leachate as a feedstock for microalgae (Lin et al., 2007, Richards and Mullins, 2013). Specific microalgal strains have been found to be tolerant of environmental stressors such as the harmful components of landfill leachate, namely high ammonia and heavy metal concentrations. This allowed strains to be able to maintain internal homeostasis while being able to assimilate nutrients and grow (Power, 1999). It has been found that microalgal treatment methods supersede bacterial treatment methods in decreasing the amount of NH_4 (Munoz and Guieysse, 2006). Microalgae have preferentially developed the production of extracellular peptides and polysaccharides capable of binding heavy metals. These compounds are then partitioned internally for appropriate assimilation, thereby mitigating the potential toxic effect (Lesmana et al., 2009). Identifying a suitable microalgal strain able to withstand the leachate characteristics is key to exploiting microalgal technology for leachate treatment. High levels of ammonia have been found to inhibit algal growth therefore optimization of leachate is required prior to treatment (Lin et al., 2007).

It is important to note that there are limitations to the use of alternative biodegradable materials such as leachate, wastewater effluent or animal waste. Sterilization may be necessary in order to minimize the negative effects of bacteria and pathogens on algal growth (Cai et al., 2013, Richards and Mullins, 2013). Various micropollutants have also been identified in leachate (Xu et al., 2008). It is for this purpose that compounds extracted from this algae cannot be utilized for human/animal consumption. Some waste sources i.e. leachate contain heavy metals which will accumulate in the algae cells. One has to be cautious as to not induce microalgal toxicity with high levels of metals (Richards and

Mullins, 2013). This metal uptake may also influence the utilization of biomass. It would be preferred to use the biomass as a renewable energy source compared to a protein/lipid source due to heavy metal contamination. Process flows therefore need to be designed with this in mind.

1.1.5 *Chlamydomonas reinhardtii* as a suitable candidate for leachate treatment

Chlamydomonas reinhardtii is a widely distributed single celled green algae that has one large cup-shaped chloroplast that is biochemically and structurally similar to vascular plants and a mitochondria with respiratory activity (Merchant et al., 2006). The chloroplast allows autotrophic cultivation (CO_2 and light) and the mitochondria allows for heterotrophic cultivation (no light and acetate) or a combination of the two process can occur (Cardol et al., 2005, Blaby-Haas and Merchant, 2012). *Chlamydomonas* is one of the best reference organisms for the research into algal biology, physiology and photosynthesis (Dent et al., 2001). Its genome has been fully sequenced (Merchant et al., 2007) allowing for proteomic and genomic manipulation and metabolic engineering (Grossman et al., 2007). *Chlamydomonas* has the ability to use multiple different nitrogen sources (nitrate, nitrate) and in particular, ammonium, urea and nitrogen from purines or ureides (Merchant et al., 2006). Numerous studies have monitored metal assimilation in *Chlamydomonas* with special reference to its compartmentalisation, homeostasis and recycling (Blaby-Haas and Merchant, 2013). The most important and documented feature regarding *Chlamydomonas* is its ability to produce hydrogen gas. It was for this reason that Chapter 2 investigated the effect on landfill leachate on biomass production and subsequent hydrogen production. Table 1.1 shows a comparison of the top hydrogen producing microalgal species and the hydrogen related characteristics. It is worth noting that due to the interplay between experimental conditions (nutrients, light intensity, cell density etc) it is difficult to critically compare hydrogen yields from various studies due to the variability (Yeager et al., 2011).

Table 1.1: Summary of Hydrogen Producing Microalgae Species with Their Respective Characteristics

Microalgae	Hydrogen yield (ml/L/h)	Chlorophyte	Genome Sequenced	Ability to use multiple Nitrogen sources (ammonia)	Dominant Photosystem	Autotrophic Heterotrophic and Mixotrophic growth	References
Chlamydomonas reinhardtii	2.9	Y	Y	Y	II	Y	(Cardol et al., 2005, Merchant et al., 2006, Merchant et al., 2007, Yeager et al., 2011, Blaby-Haas and Merchant, 2012, Kundu et al., 2012, Kosourov et al., 2012, He et al., 2012, Blaby-Haas and Merchant, 2013, Ferreira et al., 2013b)
Scendesmus sp.	0.065	Y	N	N	II	N	
Chlorella sp.	1.37	Y	N	N	II	N	
Cyanobacteria sp.	2.2	N	N	N	I	N	

1.1.6 Hydrogen Gas as a Source of Energy

Hydrogen has always been perceived of as a fuel of the future. It has the potential to play a key role in the production of sustainable renewable energy, particularly from renewable sources (De Gioannis et al., 2013). It is a clean energy carrier that has the highest specific energy density, is recyclable and non polluting and is therefore considered the best alternative energy source to fossil fuel (Das and Veziroglu, 2001, Wang et al., 2014). Hydrogen is used as a feedstock for Proton Exchange Membrane Fuel Cells (PEMFC). Fuel cells have recently received a great deal of attention and show promising results as a energy producer due to their high efficiency (Murray et al., 1999, Hou et al., 2014). PEMFC have a high power density, simple structure, rapid response capability and are therefore favoured when compared to other fuel cells (Kim et al., 2014). In a fuel cell, hydrogen and oxygen are combined in an electrochemical reaction generating electrical power with water as a by-product (Kim et al., 2014). Currently 96% of hydrogen is produced from hydrocarbon sources (Balat, 2008), in particular from steam methane reforming. To be environmental compatible, non fossil fuel sources need to be employed. Here the electrolysis of water could prove to be an option however, conversion losses, storage and re-electrification reduce the efficiency of this method (Rosner and Wagner, 2012). Another possibility is the use of biological organisms capable of producing hydrogen (McKinlay and Harwood, 2010, Chou et al., 2011). Biohydrogen has been found to be less energy intensive and environmentally friendly compared to current methodologies (Orhan et al., 2011).

1.1.7 Current Fuel Cell Technologies

Fuel cells can be utilised in three main applications namely, transportation, stationary installations, and portable uses. Research into using hydrogen fuel cells in vehicles instead of conventional petroleum based fuels is growing daily (Hwang, 2013, Li et al., 2013, Raine, 2013). These include vehicles such as cars, buses, scooters and sport utility vehicles (SUV'S). Some of the world leading car manufacturers believe that quite a significant number of hydrogen vehicles will be present on the road by the year 2015 (Daimler et al., 2009). A transition from gasoline combustion engines vehicles to hydrogen fuel cell vehicles is likely to be the key in the strategy for greenhouse gas reduction, fuel independence and energy security goals (Stephens-Romero et al., 2011). This would require the roll-out of adequate infrastructure to support this hydrogen economy. Numerous countries are on board

with pilot programmes such as the HyTEC project at the 2012 London Olympic games and the HyCO4 project in the Netherlands as well as hydrogen fuelling stations in Germany and the USA (Raine, 2013). Brazil is currently developing the Brazilian Fuel Cell Bus Project in which the first commercial hydrogen fuelling station will be built and the first fleet of fuel cell buses will be licensed (Neves Jr and Pinto, 2013). Shanghai has introduced the "Shanghai Hydrogen Lighthouse Project" (SHLP) in which a small network of hydrogen refuelling station is planned throughout the city (Weinert et al., 2007). In Spain a medium sized refinery is being planned in which it will have a capacity of 70 000 Nm^3h^{-1} and be able to satisfy the requirement of 270 000 hydrogen cars providing enough fuel to refuel 34 000 times a day (del Mar Arxer and Martinez Calleja, 2007). Numerous studies have been done to determine models allowing the formation of refuelling stations networks in Florida and the Orlando metropolitan area (Kuby et al., 2009). This shows a world-wide agreement that hydrogen fuel cell vehicles are only a few years away and we need to develop the infrastructure to smooth the transition. This hydrogen network continues to grow including other transportation types. Boats are also incorporating hydrogen fuel cells into there designs with boats being made in Turkey and Austria (Barrett, 2012). The aviation industry is using fuel cell technology in small general aircraft (Romeo et al., 2013) as well as in commercial aircraft (Pratt et al., 2013). The main application for fuel cells is to replace hydraulic or pneumatically driven components in the avionic discipline with fuel cell driven electric means (Peters and Samsun, 2013). Stationary fuel cell uses include back up energy systems for telecommunication or radio towers or other technology that requires uninterrupted power (hospitals, banks, airports etc.) (Cottrell et al., 2011) . Fuel cells are proven to be more beneficial when compared to on site generators and standard valve-regulated lead acid batteries with regard to start up time and cost and maintenance (Cottrell et al., 2011). Portable uses of fuel cells include any electronic device such as cell phones, video recorders, laptops or hearing aids. These are generally consumer products targeting small-scale use. Such devices usually have a power rating less than 100 W with certain larger scale devices having a rating of 300 W (Shaw et al., 2013). Smaller portable fuel cells have been designed for appliances with a power rating of 12.5 W to 17 W for charging cellular phones and portable media devices (iPods, MP3 players etc) (Inman et al., 2011). The uses for fuel cells are vast and new technologies are appliances are being converted to use this hydrogen fuel cell technology.

1.1.8 Hydrogen Synthesis from *Chlamydomonas reinhardtii*

A select group of photosynthetic organisms have evolved the ability to produce hydrogen from water and solar energy when subjected to specific metabolic and physiological conditions (Costa and Greque de Morais, 2011). The production of hydrogen gas from microalgae was originally demonstrated in experiments performed by Hans Gaffron and co-workers (Gaffron and Rubin, 1942). Since then, numerous studies have taken place showing hydrogen production from various microalgae species. (Ghirardi et al., 2000, Florin et al., 2001, McKinlay and Harwood, 2010). The enzyme catalysing this reaction was found to be inactivated by trace amounts or oxygen that is co-evolved during photosynthesis. Because of this, hydrogen was found to be produced for only a short period of time (Ghirardi et al., 1997). Several years ago it was found that if you cultivated *Chlamydomonas* deprived of inorganic sulphur, the hydrogen production is sustained for up to 120 hours (Wykoff et al., 1998). This process induces the partial and reversible inhibition of the water oxidation activity from photosystem II in the electron transport chain (Wykoff et al., 1998) (Figure 1.2). Initially it was not understood how the participation of photosystem II came into play.
Later it was found that the partial and reversible inhibition of the water oxidation activity from photosystem II limits the evolution of O_2 due to the reversible damage caused on the D proteins (Melis et al., 2000, Ghirardi et al., 2000). These D proteins have a photo protective function for photosystem II. In the absence of sulphur, the D proteins cannot be repaired and the activity of PS II is progressively reduced thereby reducing the oxygen production (Jorquera et al., 2008). Further research found that *Chlamydomonas* underwent five different phase during sulphur depletion namely; aerobic, oxygen consumption, anaerobic, hydrogen producing and termination phases (Kosourov et al., 2002).

This process has been found to have no effect on cellular respiration and the culture changes from aerobic to anaerobic within 1-2 days (Ghirardi, 2006, Kosourov et al., 2007). The anaerobic conditions induce the expression of the [Fe-Fe]-hydrogenase (O_2 or aerobic conditions will inhibit expression) which redirects the electron flow from normal carbon fixation towards proton reduction. Thus, hydrogenase acts as an H/e$^-$ release mechanism by recombining H from the medium and e$^-$ from reduced ferredoxin to produce a gas that is excreted from the cell (Kruse et al., 2005). This results in the production of hydrogen gas for 4-5 days (Ghirardi et al., 2000, Ghirardi, 2006). Since this was discovered, the conventional manner in which to produce hydrogen is induced by the deprivation of sulphur (Melis et al., 2000, Kosourov et al., 2002, Melis, 2007).
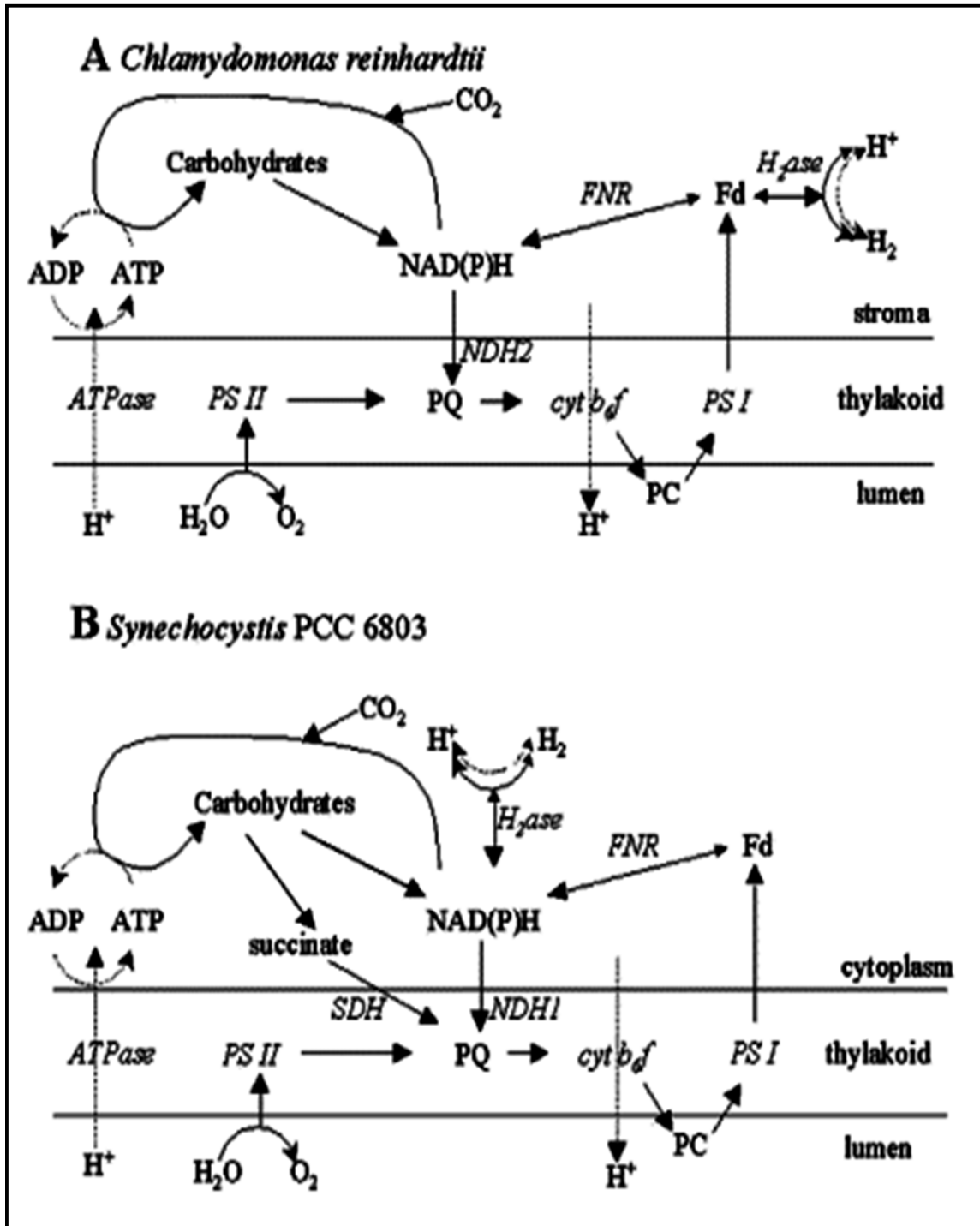
Figure 1.2: Production of hydrogen gas from the electron transport chain under anaerobic conditions in *Chlamydomonas* (A) and *Synechocystis* PCC 6803 (B) (Cournac et al., 2002).

Since the initial research, several approaches have been investigated in an attempt to increase hydrogen yields. These approaches included increasing the duration of H_2 production (Federov et al., 2005), synchronising cell division (Tsygankov et al., 2002), optimization of media components (Jo et al., 2006), optimization of light and pH (Kosourov et al., 2007, Laurinavichene et al., 2002, Kosourov et al., 2003) as well as techniques where small amounts of sulphur was added back into the culture medium (Kosourov et al., 2002, Zhang et al., 2002). The use of *Chlamydomonas* mutants has also increased the knowledge base regarding hydrogen production (Kruse et al., 2005). The next stage of research involved the use of physiological parameters in an attempt to increase hydrogen yields. This required an understanding of the electron transport chain and the key proteins involved. A review paper has been published summarising the history of photosynthetic hydrogen research from the pioneering studies of Hans Gaffron to the potential exploitation that has arisen today (Melis and Happe, 2004).

1.1.9 *Chlamydomonas reinhardtii* Electron Transport Chain

Figure 1.2 shows that all electrons originate from the PS II in the electron transport chain and are driven to PS I and are then transported through the ATPase pump producing ATP.

When photons of light are captured by PSII, oxygen is being produced from PSII with the breakdown of H_2O into O_2. (Figure 1.2A) It is important to note that this oxygen induces the inhibition of the hydrogenase enzyme thereby reducing hydrogen production. During hydrogen production, it can be seen that electrons are channelled from PSII to Plastoquinone to PSI to Ferrodoxin and then to then finally to the hydrogenase enzyme. Here H protons are converted to H_2 in the stroma and are released as a gas (Figure 1.2A). Because the activity of PS II is reduced during hydrogen production, numerous physiology studies have taken place to monitor this process (Melis et al., 2000, Antal et al., 2003, Ghirardi, 2006, Jorquera et al., 2008). There is an incomplete understanding of the exact physiological changes that take place during hydrogen production. At the onset of hydrogen production, transfer of electrons at PSII and the subsequent transfer to PSI abruptly decreases (Antal et al., 2003). The transfer of electrons from PSII to PSI during hydrogen production has yet to be measured showing the need to investigate the role of PSI. The hydrogen production process was mapped using an S-System modelling approach which showed the interactions of all components during hydrogen production (Jorquera et al., 2008). In this model PSII was used as a variable and PSI was depicted as a constant. This shows a need to verify the role of PSI

during hydrogen production. A better understanding of the physiological changes occurring during hydrogen production will possibly assist in improving hydrogen yields and this was investigated in Chapter 3.

Minimal studies have recorded the physiological functioning of PS I probably due to the availability of technology during the passed 10-15 years. Generally information regarding photosystems is measured using advanced fluorescence measurements. Early fluorescence emission and excitation technology measured only maximum and minimum fluorescence from PS II and not PS I. Present technological advances have now allowed for the differentiation between fluorescence parameters of PSI and PSII.

1.1.10 Nicotinamide Adenine Dinucleotide Phosphate (NADPH) Fluorescence

Another technological advancement regarding fluorescent measurement is the ability to monitor cellular Nicotinamide Adenine Dinucleotide Phosphate (NADPH) fluorescence. NADPH has an excitation spectrum at approximately 340 nm and an emission peak around 465nm (Schreiber and Klughammer, 2009). This cellular molecule is actively involved in the electron transport chain. As can be seen in Fig 1.2B, NADPH is the carrier molecule to the hydrogenase enzyme in *cyanobacteria* (Cournac et al., 2002). This implies NADPH has a pivotal role in the hydrogen production process. In *Chlamydomonas*, the photosynthetic pathway uses NADPH as the terminal electron acceptor during conventional photosynthesis (Fig 1.2A). During hydrogen production, however, the electrons are further driven to [FeFe]-hydrogenase (Sakurai et al., 2013). NADPH must be involved in this process which is yet to be fully described in literature. Chapter 4 monitored NADPH fluorescence during hydrogen production in an attempt to use NADPH as an indicator of hydrogen production.

Fluorescence provides an extremely sensitive tool for examining energy metabolism in photosynthetic cells (Oxborough et al., 2000). Both photosystems and NADPH can be measured using fluorescence protocols. The most effective manner in which to monitor photosystem fluorescence is to use Pulse Amplitude Modulated (PAM) Fluorometry.

1.1.11 Pulse Amplitude Modulated (PAM) Fluorometry

PAM Fluorometry has become one of the most non-invasive and rapid techniques to record the variability in chlorophyll fluorescence, indicative of photosynthetic performance. This has been demonstrated in terrestrial plants (Juneau et al., 2005) and microalgae (Hartig et al., 1998, Oxborough et al., 2000, Schreiber et al., 2002, Baker, 2008, Stirbit and Govindjee, 2011). In recent years, chlorophyll fluorescence techniques have become ubiquitous in plant ecophysiology (Juneau et al., 2002, Juneau et al., 2005, Schreiber et al., 2007). The main attraction of chlorophyll fluorescence is its ability to give a relative measure of photosynthesis (Maxwell and Johnson, 2000).

With advancements on fluorometric technology, a dual channel PAM was developed, which is able to distinguish between PS I and PS II fluorescence (Schreiber et al., 2002). A specific module for this system was also developed with allows the instantaneous measurement of NADPH fluorescence (Schreiber and Klughammer, 2009). This allows the PAM to detect light induced changes in NADPH fluorescence in suspensions of isolated chloroplasts, microalgae and cyanobacteria (Schreiber and Klughammer, 2009). The software will allow for simultaneous measurements of chlorophyll and NADPH fluorescence providing a surplus of information regarding photosynthesis and in particular the changes in the electron transport chain during hydrogen production.

Studies have used fluorometry in monitoring toxicity testing (Schreiber et al., 2002, Schreiber et al., 2007, Herlory et al., 2013), acclimation processes (Grossman, 2000, Kuster et al., 2004) as well as nutrient stress (Beardall et al., 2001, White et al., 2011, Gao et al., 2013). This will make PAM Fluorometry not only a fundamental tool in monitoring changes during hydrogen production, but also in acclimation to leachate as a nutrient feedstock.

1.1.12 Pilot Scale Bioprocessing Systems

A bioprocess usually consists of a feedstock pre-treatment, fermentation or biocatalysis, and downstream processing or separation for product recovery, purification and delivery (Yang, 2007). Bioprocessing has gained commercial interest because of the perceived environmental advantages of using biomass rather than fossil fuels. This process also

becomes sustainable due to a renewable feedstock and is able to reduce green house gas emissions.

Mass cultivation of microalgae occurs either by open raceway ponds or photobioreactors. Photobioreactors are the preferred choice due to the closed environmental system, maximum light absorption and precise controllability of culture parameters (Chisti, 2007). Hydrogen production favours photobioreactors as there is the control to switch from aerobic to anaerobic conditions. Outdoor photobioreactors have shown promise of hydrogen production using sunlight (Scoma et al., 2012). Few studies have explored the scale up effects from laboratory scale to pilot/large scale production for large scale (Rosner and Wagner, 2012, Oncel and Sabankay, 2012, Scoma et al., 2012). Overall challenges were reported to be the photobioreactor design and low hydrogen yields (Pulz, 2001, Levin et al., 2004, Rashid et al., 2013). Other challenges included light delivery, land and water availability, harvesting procedures as well as the interactive nature of the culture parameters (nutrients, temperature, pH, oxygen, mixing and light) (Fouchard et al., 2008, Christenson and Sims, 2011, Oncel and Sabankay, 2012). The findings report that scalability is possible due to continued advancements in research of the individual components in the bioprocess designs. It is worth noting that one can design and build the 'perfect' reactor however if the algae doesn't produce hydrogen, this system design will still fail.

Microalgae have been described as "Little Cell Factories" capable of producing a vast amount of various biochemical compounds (Leon-Banares et al., 2004). It is this reason that microalgae have been used in numerous bioprocess applications for energy sources such as biodiesel, bioethanol, biomethane and biohydrogen etc. (Harun et al., 2010, Blanch, 2012). Bioprocess engineering can be thought of as an interdisciplinary challenge. It consists of different components that all require optimization to make the system work effectively. These include items such as computer systems, software writing, infrastructure engineering, specifications of industrial equipment and most importantly, an understanding of the intricacies during biohydrogen production from *Chlamydomonas* for maximum manipulation and exploitation.

The microalgal cellular factories have to be performing in an optimized manner before its hydrogen production can be up-scaled to a pilot-scale system. This means that the overall functionality of a bioprocessing system relies on the functionality of the individual cells. Because the system relies on a biological organism requiring manipulation of its

photosynthetic pathways to produce hydrogen, a full understanding of the organism is required to be able to fully manipulate it. Following this, the bioprocessing plant can then be designed and optimized for maximum biomass and hydrogen production. This understanding was achieved in the physiological studies shown in Chapter 2, 3 and 4 prior to being combined into a pilot scale bioprocessing system in Chapter 5 to exploit the findings for the large scale production of biohydrogen from *Chlamydomona*s. It is worth noting that limited studies have produced hydrogen gas on a pilot scale and no studies have produced microalgal hydrogen from large scale production. This is due to the numerous application problems previously listed. This study is therefore one the few having a conceptual design for a pilot scale processing system based on concrete findings from lab scale research.

In summary the main objectives of the whole study were as follows:

1. To determine how landfill leachate will effect the growth and hydrogen production of *Chlamydomonas reinhardtii*.

2. To determine the role of Photosystem I in the electron transport chain during hydrogen production.

3. To determine the use of NADPH fluorescence as an indicator of hydrogen production.

4. To design a modular pilot scale biohydrogen processing system based on the findings from the previous chapters.

CHAPTER TWO

The Effect of Landfill Leachate on Hydrogen Production in *Chlamydomonas reinhardtii* as monitored by PAM Fluorometry

Abstract

This study investigated the effect of landfill leachate on biomass and biohydrogen production from *Chlamydomonas reinhardtii*. Maximum biomass and cell viability was recorded in 16% leachate medium with a corresponding growth rate of 927 μg/L chl *a* d^{-1} as compared to the control of 688 μg/L chl *a* d^{-1}. *Chlamydomonas* cultured in leachate-supplemented medium was subsequently induced to produce 37% more biohydrogen compared to the control culture. The spurge in growth can be a consequence of abundant essential elements in the diluted leachate. Energy Dispersive X-ray analysis of cells in a 16% leachate medium had the highest accumulation of Cr, Mn, Fe, Co, Ni, Mo and Cd. The benefits of the leachate medium were further shown during the hydrogen production phase using Pulse Amplitude Modulated Fluorometry. This period was extended to 8 days in comparison to the control. Leachate therefore increases both the biomass and biohydrogen yield of *Chlamydomonas.*

Keywords*: Chlamydomonas reinhardtii*; Leachate; Biohydrogen; Pulse Amplitude Modulated Fluorometry; Renewable Energy.

2.1 Introduction

Hydrogen has always been thought of as the fuel of the future, mainly due to its high conversion efficiency, recyclability and non polluting nature (Das and Veziroglu, 2001). Hydrogen is used in fuel cells which constitute an attractive power generation technology, converting chemical energy into electricity at a high efficiency (60%-70%) (Murray et al., 1999). Sustainability and renewability of hydrogen production can be achieved if the source is biological, such as bacteria (*Rhodopseudomonas palustris, Clostridium butyricum and Bacillus thermoamylovorans*) *(Chou et al., 2011)* or algae (*Scenedesmus obliquus, Chlamydomonas reinhardtii* and *cyanobacteria)* (McKinlay and Harwood, 2010). Biohydrogen has been found to be less energy intensive and environmentally friendly compared the current thermochemical and electrochemical processes (Orhan et al., 2011).

Microalgae have been identified as a leading feedstock for biodiesel and jet fuel (Parmar et al., 2011) and recently extensive research has been undertaken to produce biohydrogen (Melis et al., 2000, Amos and Ghirardi, 2004). For the production of biohydrogen, photosynthetic microalgae are cultured in conditions to induce an anaerobic environment where, microalgae use solar energy to split water into protons and electrons, producing hydrogen as the proton carrier (Kruse et al., 2005). Currently photobiological production of hydrogen by microalgae is of interest as it holds the promise of generating the most environmentally friendly renewable energy from one of the most plentiful resources, light and water (Melis et al., 2000). There are however constraints with regard to the production of hydrogen from microalgae effecting the feasibility of this process. The increasing cost of nitrogen and phosphorus fertilizers is putting stress on maintaining feasibility of large scale microalgal biomass production (Bhatnagar et al., 2011). Copious amounts of water are required for cultivation creating a water demand on the system. Continuous biohydrogen production from algae is not yet sustainable as it is only produced for a short duration under specific stress conditions. Currently the reported rates of hydrogen production by the conventional sulphur-deprived method are below the theoretical maximum for algal systems (Amos and Ghirardi, 2004). The conditions to produce maximum hydrogen are still being investigated with advancements in this technology occurring daily. (Kosourov et al., 2007). Thus it is essential to find alternative sources of nutrients for the production of microalgal biomass and consequently renewable energies (Bhatnagar et al., 2011).

Landfill leachate is generated by infiltration and percolation of runoff water, rain water, ground water and flood water through the waster layers of the landfill site (Kjeldsen et al., 2002). The composition of leachate can vary depending on the degradation stage of the waste, the type of waste and landfill technology. Leachate can have a variety of inorganic and organic constituents such as nitrogen and phosphorus, heavy metals, tannins, phenols, ammonia and humic acids (Lin et al., 2007, Trois et al., 2010a). It has been previously reported that small amounts of leachate could pollute large amounts of water rendering them unusable and toxic for domestic or commercial use (Trois et al., 2010b). It is for this reason that leachate is recognized as an important environmental problem and appropriate treatment and processing of this liquid is crucial. Current leachate treatments methods include nitrification-denitrification processes, chemical oxidation, aerobic-anaerobic decomposition, active carbon, reverse osmosis, coagulation-flocculation and adsorption or a combination of these methods (Trois et al., 2010a).

Reports on the use of microalgae as a treatment for wastewater are readily available (Cho et al., 2013) where the wastewater becomes a nutrient source for the algae. Some algal strains are sensitive to environmental contaminants generally found in waste waters and are commonly used in toxicity testing (Lin et al., 2007). In contrast, other algal species have been found to be tolerant of environmental stresses such as high heavy metal concentrations, high ammonia concentrations or high salinities and are able to treat leachate with the removal of heavy metals and nutrients as well as organic matter assimilation and degradation (Lin et al., 2007, Richards and Mullins, 2013). It is also worth noting that algal based treatments generally lower the amount of NH_4 than NO_3 when compared to other bacterial treatment methods (Munoz and Guieysse, 2006) .

Microalgae have preferentially developed the production of extracellular peptides capable of binding heavy metals. These hydroxyl, carboxyl, sulphate and amino groups in the cell wall polysaccharides act as the binding site for the metals. It is also to be noted that biomass characteristics, pH of the solution, as well as the physico-chemical properties of the target metal have a impact on the rate of biosorption (Lesmana et al., 2009). These compounds which form as organometallic complexes, are partitioned inside vacuoles to facilitate the appropriate control and assimilation of the metals in the cytoplasm preventing the potential toxic effect (Lesmana et al., 2009). Heavy metals have been found to be strong inhibitors of microbial photosynthesis and can also cause morphological changes in the size and shape of microalgal cells (Munoz and Guieysse, 2006). Finding a suitable microalgal strain that is

able to withstand the stress of high heavy metals concentrations and high nutrient concentrations is the key to success when using microalgae in leachate treatment. Leachate levels that were too high have been found to inhibited microalgal growth and nutrient removal (Lin et al., 2007). The need for optimization of leachate concentrations is therefore crucial for nutrient removal and maximum biomass production possibly increasing the potential for hydrogen production.

Tolerance to environmental stresses in microalgae can be monitored using Pulse Amplitude Modulated (PAM) Fluorometry (Maxwell and Johnson, 2000, Schreiber et al., 2002). PAM Fluorometry has become one of the most well used, rapid and non-invasive techniques to obtain information regarding photosynthetic performance and chlorophyll fluorescence variability. This has taken place in both terrestrial plants (Juneau et al., 2005) and particularly in microalgae (Baker, 2008, Schreiber et al., 2002, Oxborough et al., 2000, Stirbit and Govindjee, 2011). Recently, the technique of chlorophyll fluorescence has become universal in the analysis of plant ecophysiology (Juneau et al., 2005). One of the main attractions of chlorophyll fluorescence is its ability to give a relative measure of photosynthesis (Maxwell and Johnson, 2000). In this study a DUAL-PAM fluorometer was utilized. The DUAL-PAM is a highly sensitive research instrument having the ability to employ strong light for excitation of chlorophyll fluorescence and for driving photosynthetic energy conversion. This system is suited for assessments of photosystem II via chlorophyll fluorescence as well as photosystem I via P700 measurements. Furthermore it can be extended to assess other informative photosynthetic parameters such as the change in transthylakoid pH, the thylakoid membrane potential and NADPH fluorescence. A crucial feature is the ability to simultaneously monitor PSI and PSII with the modulated measuring light with minimal disturbance (www.walz.com/downloads/manuals/dual-pam-100/Dual-PAM1e.pdf). PAM Fluorometry works on a model developed for PS II photochemistry in which the photochemistry competes with processes of fluorescence and heat loss for excitation energy in the pigment antennae of PS (Butler, 1978, Baker, 2008). This model proposed that electron transfer from the reaction centre of PS II to the primary quinone acceptor of PS II quenches fluorescence. Increases in the heat loss result in non-photochemical quenching of fluorescence. This model therefore predicts that PS II fluorescence emission could be used to monitor changes in photochemistry. This makes it a fundamental tool in monitoring nutrient stress (White et al., 2011) with the application of monitoring the effect of leachate on microalgae physiology, based on the photosynthetic potential and functioning.

This study therefore investigated the feasibility of increasing biomass and biohydrogen production in *Chlamydomonas reinhardtii* using diluted landfill leachate.

2.2   Materials and Methods

2.2.1   Leachate pre-treatment

Raw leachate was collected from the Bulbul Drive Municipal Landfill Site, in KwaZulu-Natal, South Africa. The leachate was filtered through a 0.22μm vacuum pump filtration system to remove particulate matter, followed by sterilisation at 121°C for 15 minutes. This leachate was utilized for all experimental procedures throughout the study.

2.2.2   *Chlamydomonas* Cultivation

The freshwater unicellular chlorophyte *Chlamydomonas reinhardtii* CC125 was cultured in Tris-acetate-phosphate (TAP) media (pH 7.0) until early logarithmic phase was reached. Samples were then transferred to TAP media with leachate varying from a concentration of 0% to 100% in 10% intervals. Subsequent leachate optimization studies involved leachate percentages of 10% to 20% in 2% intervals. Leachate experiments were conducted over 22 days. Samples were cultured at an irradiance of 200 μmol m^{-2}s^{-1} with a 12:12 hour light: dark cycle at a constant temperature of 25 ± 1 ℃. Experiments were repeated twice for validation purposes.

2.2.3   PAM Fluorometry

A DUAL-PAM 100 Chlorophyll Fluorometer (Heinz Walz Gmbh, Effeltrich, Germany) was used to obtain simultaneous fluorescence measurements for Photosystem II (PSII) and Photosystem I (PSI). Rapid light curves were generated from 3 ml microalgal aliquots placed in quartz cuvettes (10 x 10 x 40 cm). The relative Electron Transport Rates (rETR) vs. irradiance contours were obtained by incubating the microalgal cells under actinic light at 40 s intervals. The actinic light ranged from 0 μmol photons m^{-2} s^{-1} to 2630 μmol photons m^{-2} s^{-1} over a series of 20 increments. A blue light saturation pulse (0.6 s at 10 000 μmol photons m^{-2} s^{-1}) was used to determine the rETR at each irradiance level. Rapid light curves were used to extract detailed information regarding the saturation characteristics of both PSI and PSII. This was then used to infer information related to the overall photosynthetic

performance of the microalgae (Ralph and Gademann, 2005). All PAM data and generated RLCs (Baker, 2008) were obtained using Dual PAM software (v 1.11).

The rETRs were determined using the formula:

$$rETR = F'_q/F'_m \text{ x PPFD} \qquad (1)$$

In this formula $F'_q = (F'_m - F')$ and the segment (F'_q/F'_m) is termed the PS II operating efficiency and estimates the efficiency at which light absorbed by PS II is used. At specific photosynthetically active photon flux densities (PPFD) an approximation of the quantum yield of linear electron flux through PS II and PS I was determined (Baker, 2008).

The maximum quantum efficiency from PS II was determined from the formula:

$$F_v/F_m = (F_m - F_o)/F_m \qquad (2)$$

Where F_o and F_m are defined as the minimal and maximal fluorescence yields of a dark-adapted sample, respectively.

Non photochemical quenching (NPQ) was calculated from PS II ΔF_m compared to the final value F_m in dark adapted samples using the formula (Schreiber, 2004):

$$NPQ = (F_m - F_m')/F_m' \qquad (3)$$

The initial slope of the RLC is termed the alpha (α) value (Ritchie, 2008) and represents the maximum photosynthetic efficiency of the microalgae sample.

The effective PS II quantum yield (YII) is calculated according to Genty (1989) by the formula (Genty et al., 1989):

$$Y(II) = (F_m' - F)/F_m' \qquad (4)$$

Analogous to the Y(II) is the PS I photochemical quantum yield Y(I) derived from (Klughammer and Schreiber, 2008). It is calculated from the complimentary PS I quantum yields of nonphotochemical energy dissipation Y(ND) and Y(NA) via the formula :

$$Y(I) = 1 - Y(ND) - Y(NA) \qquad (5)$$

Where Y(ND) and Y(NA) can be determined directly from the saturation pulse method. Y(ND) and Y(NA) are calculated as follows:

$$Y(ND) = 1 - P700 \text{ red} \qquad (6)$$

$$Y(NA) = (P_m - P_m')/P_m \qquad (7)$$

The ratio of quantum yields was calculated by: Y(I) / Y(II)

2.2.4 Chlorophyll *a* determination

Microalgal biomass was quantified by chlorophyll *a* (chl *a*) fluorescence, using a Trilogy Fluorometer (Turner Designs, California). Chlorophyll *a* from microalgal samples (10ml) was extracted in 90% acetone at 4 ℃ for 24 hours (Parsons et al., 1984). Chlorophyll *a* standard (Sigma) was used to calibrate the Trilogy fluorometer.

2.2.5 Scanning Electron Microscope (SEM) and Energy Dispersive X-ray (EDX)

Microalgal samples cultured at specific leachate concentrations were centrifuged at 3000 rpm for 15 minutes and washed with distilled water three times to remove salt and media precipitates. Samples were then freeze dried using liquid nitrogen and incubated at - 80 °C for 3 days. Cells were then mounted onto aluminium stubs on thin carbon tape and subsequently sputter coated with gold. Samples were then observed by a scanning electron microscope (SEM) at an accelerating voltage of 20 kV and analysed using the coupled energy dispersive X-ray (EDX) digital controller (Zeiss FEGSEM Ultra Plus).

2.2.6 Hydrogen production using leachate

Chlamydomonas reinhardtii CC125 cells were grown until late exponential phase in Tris-acetate-phosphate (TAP) media with 16% leachate (pH 7.0) under 100μmol m^{-2}s^{-1} in a 12:12 light : dark cycle. A control culture consisted of *Chlamydomonas* cells cultured in 100% TAP media. Cells were harvested and centrifuged at 3000 rpm for 15 minutes before being washed three times in TAP-S media. Cells were then resuspended in TAP minus sulphur (TAP-S) media in duplicate 1L modified Schott (Schott, Duran) bottle with 3 sealed ports at a concentration of 6401.11 ± 162 chlorophyll *a* μg/L. These bottles were then placed on magnetic stirrers and incubated at a light intensity of 100 μmol m^{-2}s^{-1} at a light cycle of 12:12 light: dark and a temperature of 23 ± 1°C. PAM Fluorometry was conducted as previously discussed.

2.2.7   Hydrogen Evolution measurements

Hydrogen was collected from the sealed modified Schott bottle by the upward displacement of water in a 50ml burette (Laurinavichene et al., 2002). Measurements were recorded daily. The hydrogen gas was collected in a Hamilton gas-tight syringe and injected into a gas chromatograph (Shimadzu GC 2014, Shimadzu, North America) equipped with a thermal conductivity detector and a Porapak Q column.

2.2.8   Statistics

Statistical comparisons were performed using SPSS version 11.5.1 for Windows. All values were logarithmically (log_{10}) normalised to meet the requirements for parametric statistical tests. One way analyses of variance (ANOVA) were used to test for differences in data ($p < 0.05$).

2.3   Results and Discussion

Chlamydomonas reinhardtii cultured at specific leachate concentrations (16%) (Fig 2.1) showed the ability to increase its biomass yield by 26% (Fig 2.2) compared to the TAP control and showed enhanced photosynthetic functioning with increases in $rETR_{max}$ PSI and $rETR_{max}$ PS II of 46% and 51% respectively (Fig 2.3). Furthermore, a biohydrogen yield improvement of 37% was found with the addition of 16% leachate and an extended period of 8 days of production was observed in this study (Fig 2.4) compared to 4-5 days shown in previous studies (Melis et al., 2000, Kosourov et al., 2007).

Initially, *Chlamydomonas reinhardtii* was grown in TAP media with the addition of leachate in concentrations ranging from 0% up to 100%. The growth rates as depicted below (Fig 2.1) showed positive growth from 10% to 30% leachate. Maximum growth was shown at a concentration of 20% leachate. Negative growth was experienced from 40% to 100% leachate. This corresponds to previous studies where algal cultures showed negative growth rates for cells cultured at leachate percentages ranging from 30% - 100% (Lin et al., 2007). Although maximum growth (1208 ± 15.24 chl *a* μg/L d^{-1}) occurred at 20% leachate (Table 2.1), an extended incubation period of 45 days resulted in an 80% reduction in chlorophyll *a* content from 5742.25 ± 30.25 chl *a* μg/L d^{-1} to 1131.09 ± 160.45 chl *a* μg/L d^{-1}. The $rETR_{max}I$ showed a reduction of 89% from 496.63 to 52.78 while the $rETR_{max}II$ showed a reduction of 87% from 315.86 to 38.35. The F_v/F_m value was reduced by 60% from 0.1 to 0.04 and the α value showed a reduction of 33% with a change from 0.23 to 0.16. This depicts a reduction in cell viability after 45 days and showed the need to determine the point where maximum growth was reached and where culture viability was maintained. Cell viability is crucial, as the cells will need to be photosynthetically active and have enough time to be fully acclimated to the leachate media in order to be produce adequate hydrogen. *Chlamydomonas* has shown the ability to efficiently utilise limiting nutrients or adjust there metabolic rate in order to survive high levels of nutrients. Research has shown that they are able to make adjustments in the metabolic pathways that favour cellular survival when the potential for cell growth and division is reduced due to external conditions (Grossman, 2000).
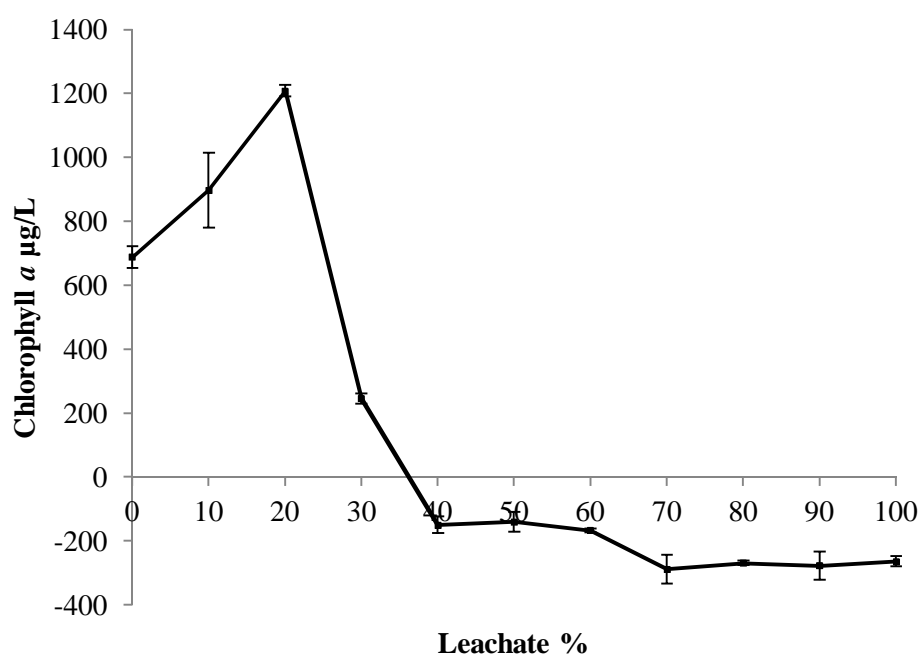
Figure 2.1: Growth rates of *Chlamydomonas reinhardtii* cultured in TAP media with the addition of leachate at concentrations ranging from 0% to 100% (Averages ± SD).

Chlamydomonas reinhardtii cultured in normal TAP media was subsequently grown in TAP media supplemented with 12%, 14%, 16% and 18% leachate. At these concentrations maximum rate of growth and biomass was recorded between days 5 and 8 of the growth period (Fig 2.2). The respective growth rates of 752.21 ± 50.3 chl *a* μg/L d^{-1}, 948.06 ± 182.8 chl *a* μg/L d^{-1}, 927.20 ± 6.9 chl *a* μg/L d^{-1} and 1037.44 ± 48.5 chl *a* μg/L d^{-1}, were recorded (Table 2.1). However, significantly lower rates ($p < 0.05$) 657.84 ± 34.1 chl *a* μg/L d$^{-1)}$ were observed in control cultures (TAP medium). After 22 days growth, the culture in 16% leachate had the highest chl *a* content showing greater biomass acclimation at this leachate level. There was no significant difference evident in the final chlorophyll *a* values between the 12%, 14% and 18% cultures after a 22 day incubation period ($p < 0.05$).
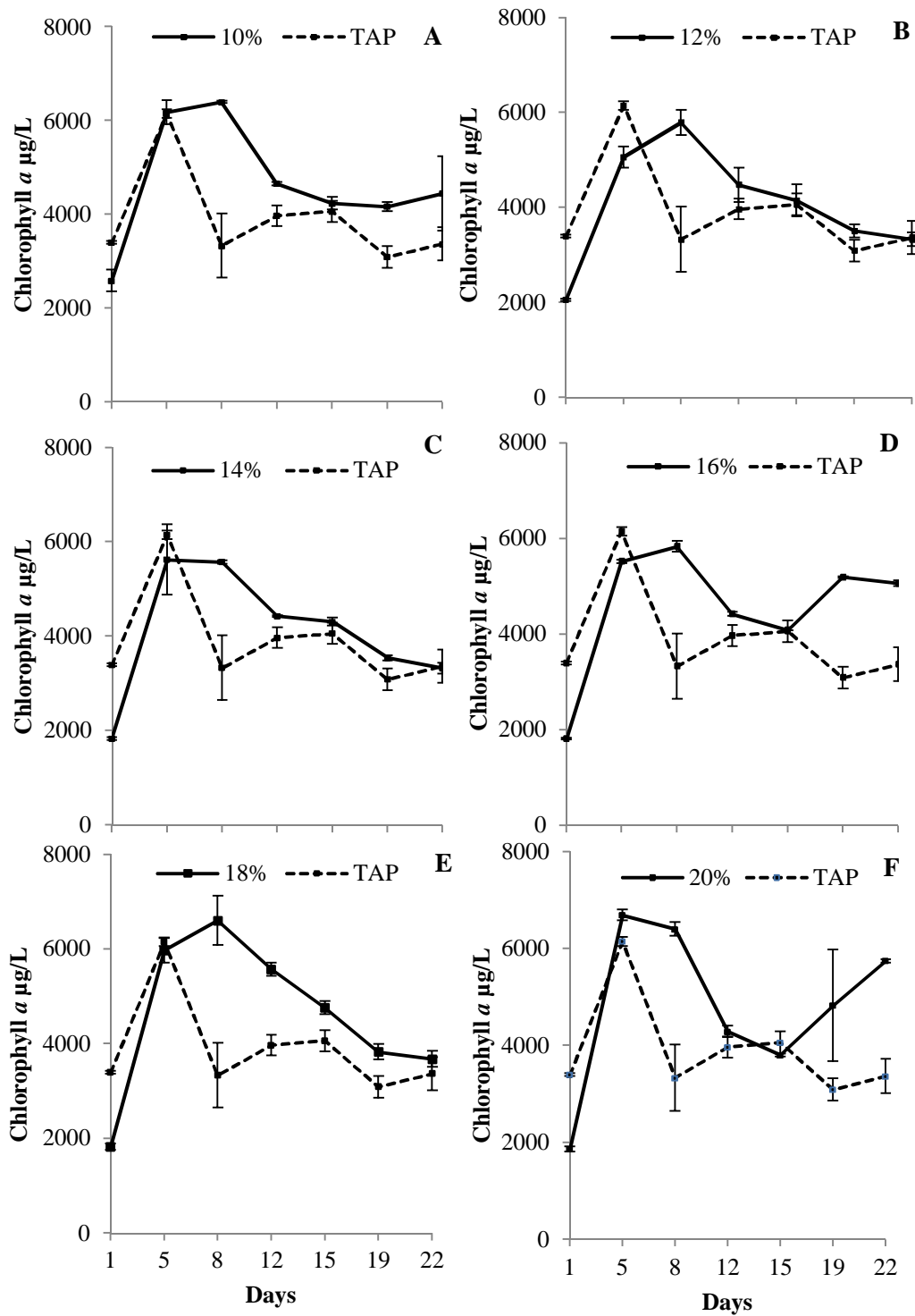
Figure 2.2: Chlorophyll *a* growth curves of *Chlamydomonas reinhardtii* cultured in leachate concentrations of 10% (A), 12% (B), 14% (C), 16% (C), 18% (D) and 20% (E) for a duration of 22 days (Averages ± SD).

Table 2.1: Growth Rates of Microalgae cultured with varying leachate percentages

Leachate %	Growth Rate (chl a μg L^{-1}d^{-1})
0 (TAP)	657.84 ± 34.1
10	1002.76 ± 121.83
12	752.21 ± 50.3
14	948.06 ±182.8
16	927.20 ± 6.9
18	1037.44 ± 48.5
20	1208 ± 15.24

The physiological data obtained using PAM Fluorometry (rETR$_{max}$ PS I, rETR$_{max}$ PS II, F_v/F_m, NPQ, α and YI:YII yield ratio) showed an increase in physiological functioning when the 16% diluted-leachate media was used (Fig 2.3). This was evident by the increase of 45 % in the rETR$_{max}$ PS I value and 51% increase in the rETR$_{max}$ PS II value (Fig 2.3A and B). The F_v/F_m value showed a reduction from 1 to 0.12 in the leachate-diluted media when compared to the control showing a reduction from 0.71 to 0.46 (Fig 2.3C). The use of leachate-dilute media resulted in more biomass therefore a greater proportion of the nutrients will be assimilated and utilised for growth. This will decrease the F_v/F_m value as nutrients are depleted and nutrient stress starts occurring. The α value which depicts efficiency, was show to be 44% lower in the leachate-diluted media than the TAP control (Fig 2.3E). The α value has been previously shown to inversely correlate with lipid yields (White et al., 2011). This may justify the decrease in photosynthetic efficiency by a possible metabolic shift to produce lipids. This will provide a greater internal energy source (lipids and carbohydrates) which will favour the energy intensive hydrogen production process (Hemschemeier and Happe, 2011, Richards and Mullins, 2013). The YI:YII yield ratio showed no significance difference between the leachate-diluted media and the TAP control throughout the 22 day period (Fig 2.3F). The physiological data also showed evidence of acclimation to the leachate-diluted media. This was evident by the 87% increase of rETR$_{max}$ PS I from initial values (day 1) to acclimated values at day 5 (Fig 2.3A). Further evidence of acclimation was shown in the maximum NPQ value of 10, recorded on day 1 in the 16% (Fig 2.3D). This showed that majority of light, was converted into heat and not into energy for electron transport. This value then decreased by 98% to 0.15 after acclimation whereby marginal difference were evident compared to the control TAP culture. This provided evidence for an acclimation that needed to occur, before logarithmic growth can occur (Grossman, 2000).
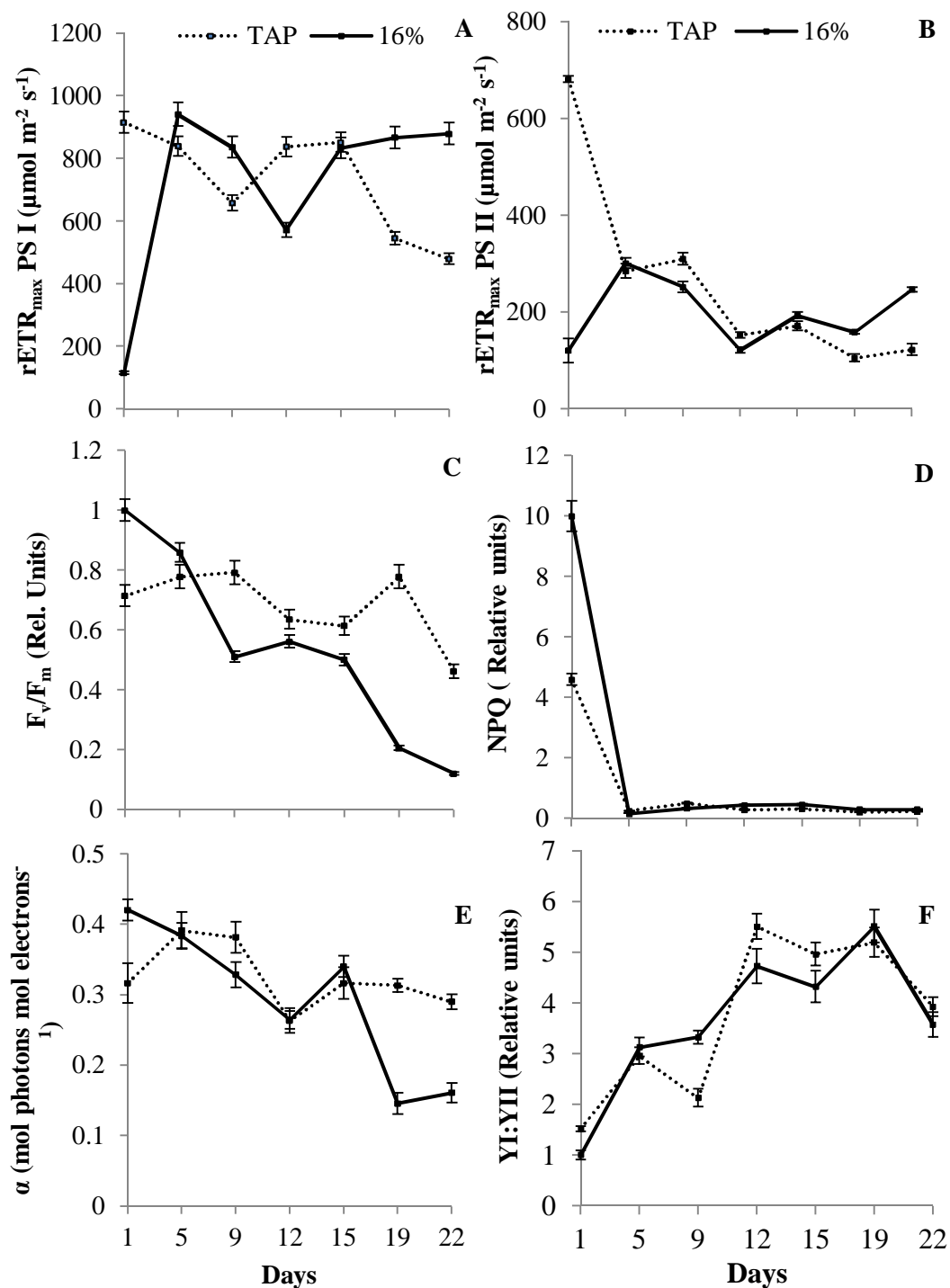
Figure 2.3: PAM fluorometric parameters of *Chlamydomonas* cells cultures in 16% leachate-diluted media (solid line) and TAP media (dotted line). PAM parameters used include rETR$_{max}$ PS I (A), rETR$_{max}$ PS II (B), F$_v$/F$_m$ (C), NPQ values (D), alpha (E) and yield ratio YI:YII (F) (Averages ± SD).

The production of hydrogen gas from *Chlamydomonas* cultured in 16% leachate was then induced (Fig 2.4) using the conventional method of a sulphur free TAP medium (Antal et al., 2003) and verified using gas chromatography. Approximately 3 grams of microalgae was inoculated into TAP-S. This deprivation is known to limit the recovery of the D1 protein and therefore causes the partial and reversible inhibition of PS II water oxidation (Kosourov et al., 2007). This then induces the expression of two (FeFe)-hydrogenases which redirect the flow of electrons coming from the photosynthetic electron transport chain in the chloroplast from carbon fixation toward proton production. As a result, H_2 is produced for several days (McKinlay and Harwood, 2010).

Using the conventional method to produce hydrogen through sulphur depletion, the H_2 gas was produced for 5 days, commencing from day 3 until day 8 whereby production then ceased. This was expected as generally the removal of sulphur induces hydrogen production for approximately 120 hrs (Antal et al., 2003). When a leachate-diluted media was used, the hydrogen production phase was extended to 8 days starting at day 2 and ceasing on day 10 (Fig 2.4A). Daily hydrogen production peaked at 8.25 x10^{-4} ml H_2 chl a^{-1} d^{-1} on day 7 when cultured in leachate-diluted media compared to a peak production of 5.16 x 10^{-4} in the conventional method at day 5. Cumulative hydrogen yields were shown to increase by 37% in the leachate-diluted media (16% leachate) compared to cells initially cultured in TAP media (Fig 2.4B). This is due to the longer hydrogen production phase of three extra days as well as the greater production rates. A possible explanation to the extended hydrogen production phase and greater hydrogen yields is the increased amount of nickel (Ni) present in the leachate. Ni is a key micronutrient used in the production of the dehydrogenase enzyme (Daday et al., 1985, Hausinger, 1987). The nickel may induce a greater activity or allow for the production of a greater supply of enzyme.
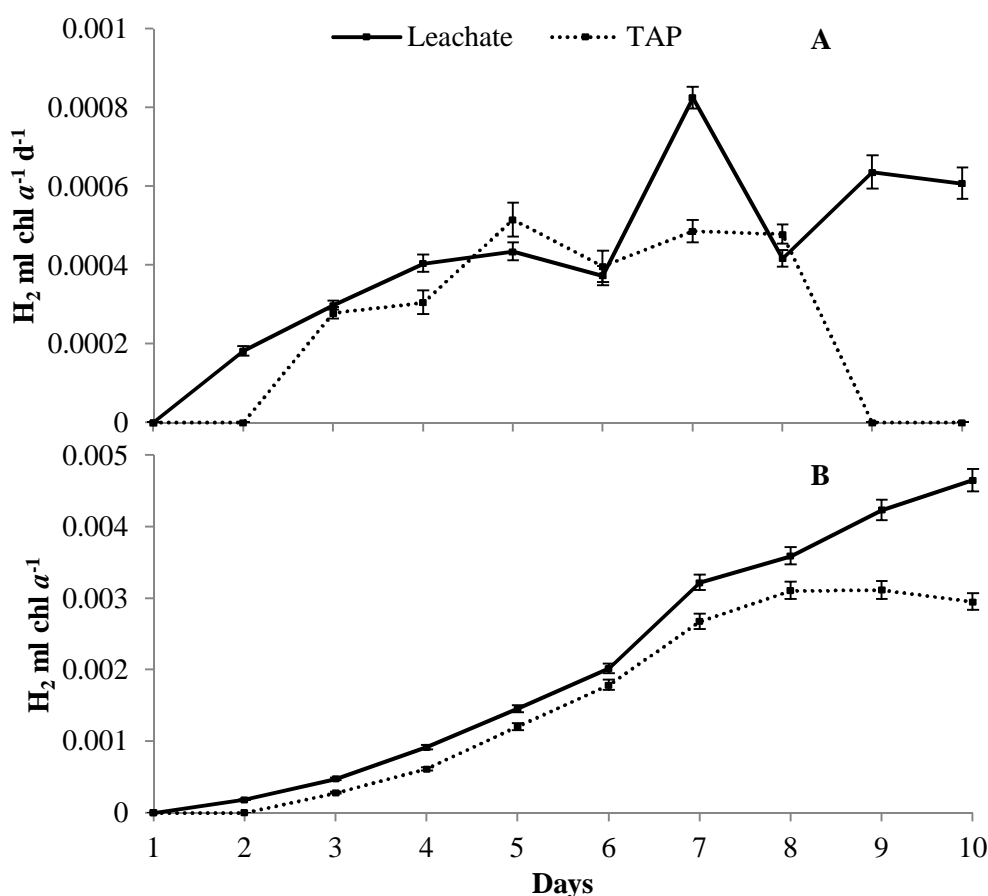
Figure 2.4: Hydrogen yields of *Chlamydomonas* cultured in 16% leachate in TAP media and biohydrogen produced in TAP-S (black line) and *Chlamydomonas* cells cultured in TAP media (dotted line). Hydrogen yields expressed as cumulative values (A) and daily hydrogen yields normalized by chlorophyll *a* concentration (B) (Averages ± SD).

The physiological data obtained from PAM Fluorometry (F_v/F_m, $rETR_{max}$ PS I, $rETR_{max}$ PSII, YI:YII yields and NPQ) shows that less physiological stress was evident in cells cultured in 16% leachate than in TAP media alone when subjected to hydrogen producing conditions (Fig 2.5). This is possibly due to the increased availability of essential elements from the leachate required for cellular maintenance. This allows for an increased tolerance to unfavourable conditions such as the induction of hydrogen.

The maximum quantum efficiency F_v/F_m indicates nutrient limitation. Values between 0.6 and 0.7 have been reported under eutrophic conditions when nutrient limited stress was absent. (Kromkamp and Peene, 1999). The same study revealed that the F_v/F_m value has been

found to be relatively constant in non-stressed cultures, and decrease in nutrient stressed cultures. *Chlamydomonas* cells induced to produce H_2 the conventional way showed a decrease in F_v/F_m from 0.7 to 0.3. Cells cultured in 16% leachate showed a decrease in the F_v/F_m value from 0.7 to 0.4 throughout the ten day incubation period (Fig 2.5A). Cells cultured continually in TAP media showed an increase in F_v/F_m from 0.3 to 0.6 throughout the experimental period. This shows that cells in TAP media are not nutrient stressed whereas hydrogen inducing conditions cause nutrient limitation stress. From day 4 until day 8 no significant difference was evident between the TAP and leachate cells showing minimal nutrient stress as compared to conventional hydrogen inducing methods. This may be due to essential nutrients assimilated from the 16% leachate medium. This shows that less nutrient stress was physiologically evident when leachate was used during biomass generation, compared to cells cultured in conventional TAP media before being induced to produce H_2 via sulphur depletion.

Relative electron transport rates obtained from light curves represent the rate of electron transfer through the photosystems as is used as an indicator of photosynthetic efficiency. This was measured for both PS II and I. In PS I, cells cultured in TAP media were shown to have increased $rETR_{max}$ values during incubation in TAP-S media as compared to cells incubated in TAP media alone (Fig 2.5B). Cells cultures in leachate showed an increase in $rETR_{max}$ of 47% compared to conventional methods having an increase of 17%. This is possibly due to the increased assimilated elements during cultivation from the diluted leachate media. The $rETR_{max}$ values of photosystem II (Fig 2.5C) show that under conventional methods, the $rETR_{max}$ values remains unchanged ($p > 0.05$) for six days at approximately 0.01 μmol m^{-2}s^{-1} chl a^{-1} followed by a reduction to 0.006 μmol m^{-2}s^{-1} chl a^{-1} until day ten. This was expected as it is known that PS II is down regulated during hydrogen production due to the damaged D1 protein (Melis et al., 2000). Cells cultured in leachate showed a significant decrease in $rETR_{max}$ value from day 1 to day 2 of 57%. This is due the delayed PS II down regulation as the microalgal cells potentially contain more sulphur as the leachate used during growth has high sulphur content. They are therefore able to repair the photosynthetic machinery for a longer duration before irreparable damage takes place due to the sulphur deprivation for induced H_2 production. After day six the $rETR_{max}$ II values increases marginally. This is possibly due to a greater stress tolerance of the cells originally incubated with leachate. The cells are therefore able to withstand harsher conditions without having a great reduction in photosynthetic functioning. Cells cultured in TAP media also

show a significant reduction from day one to day two and then remain unchanged for the duration of the experiment.

The yield ratio (YI:YII) is a novel parameter that can determine regulation between photosystem I and II and the variability within this regulation. When cells were induced to produce hydrogen under the conventional method, the yield increased significantly ($p < 0.05$; 82%) during the hydrogen production phase (Fig 2.5D). This is compared to an increase of 50% in the cells incubated with leachate. This shows that PS I tend to be up regulated during hydrogen production while PS II is down regulated. Cells incubated in TAP media only, showed no increase in the yield ratio and remain between 0.002 and 0.003 throughout the ten day period. This shows the increased stress during hydrogen induction and the resulting tolerance experienced via the up-regulation of PS I. The use of leachate decreased this physiological stress evident by the smaller yield ratio increase.

The NPQ value depicts the light energy that is emitted as heat from the photosynthetic apparatus. NPQ values showed that the production of hydrogen increase the stress placed on the cells (Fig 2.5E). Conventional methods showed significantly high NPQ values having a maximum value of 1.08 compared to 0.24 of the TAP control. This shows that physiological stress is evident when hydrogen inducing conditions are maintained. Conventional methods showed the NPQ values to increase when hydrogen production commenced on day three and then decreased after the cessation of hydrogen production. The addition of leachate during the growth of the inoculum has shown to decrease the NPQ values by an average of 72% compared to the conventional methods. No significant differences ($p < 0.05$) were observed in the NPQ values between cells incubated in leachate and cells in normal TAP media.

The PAM Fluorometry parameters show that during hydrogen production there is an increase in physiological stress measured by the YI:YII yields, NPQ and $rETR_{max}$ values. The use of leachate-diluted media has shown to reduce the effect of the stress. Leachate is known to contain large amounts of nutrients and metals (Trois et al., 2010b) . In this study, the incorporation of these essential nutrients during growth may allow the *Chlamydomonas* cell to withstand greater stress than normal cells. It is therefore important to identify the nutrient and metals present in the leachate in order to determine its suitability to supplement media.
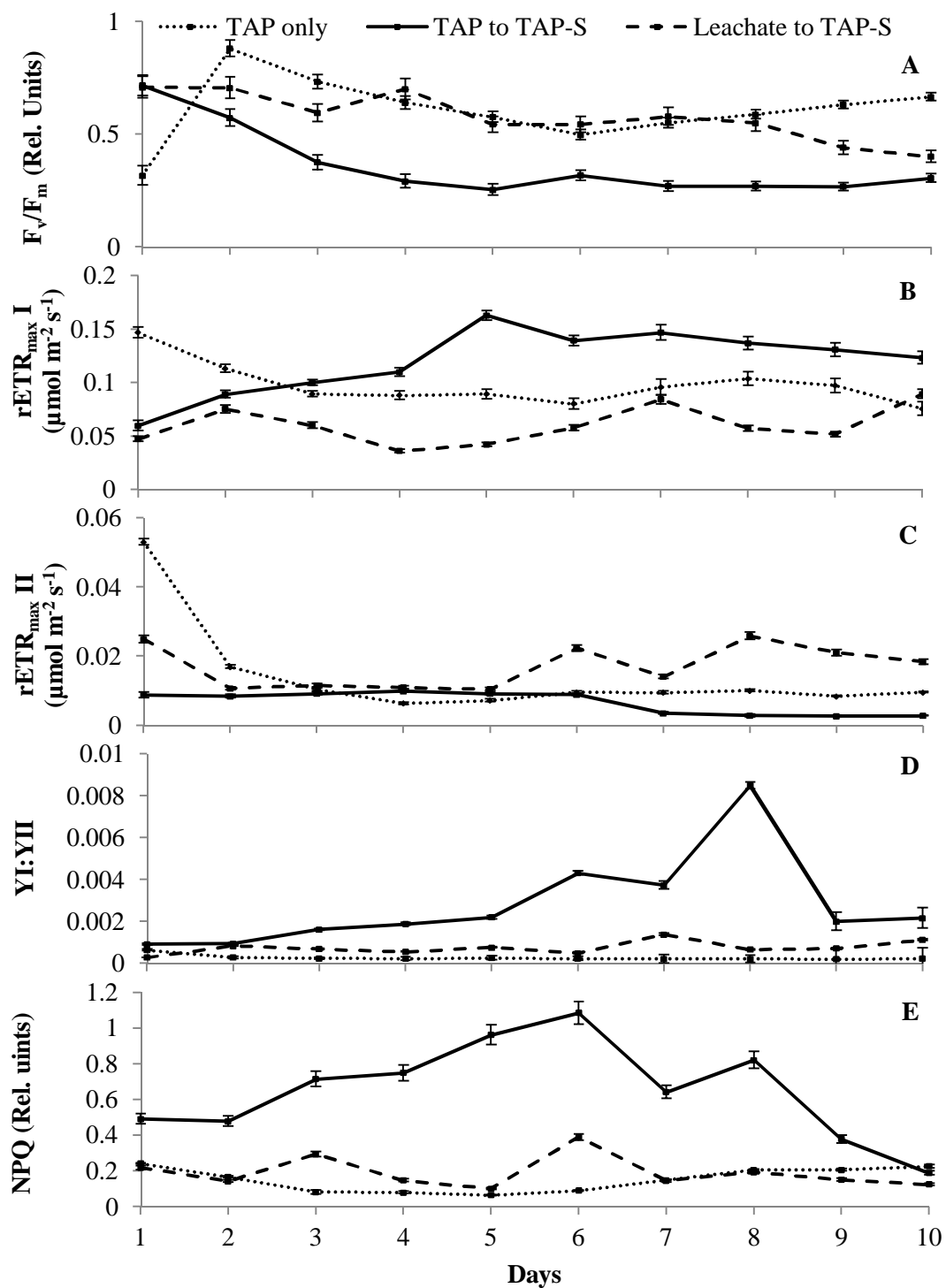
Figure 2.5: PAM fluorometric parameters of *Chlamydomonas* cells cultures in TAP media as an inoculum (solid line), TAP plus 16% leachate (dashed line) and cells incubated in TAP media (dotted line). PAM parameters used include F_v/F_m (A), $rETR_{max}$ PS I (B), $rETR_{max}$ PS II (C), yield ratio YI:YII (D) and NPQ values (E) (Averages ± SD).

A general trend was identified where *Chlamydomonas* cells at 20% leachate showed a greater accumulation of the nutrients needed for growth such as Mg, P, S, K. (Fig 2.6A).To maintain homeostasis, the microalgal cells had to increase the growth inducing elements to assist in withstanding the effects hyper-nutrient stress (White et al., 2011). This was not a sustainable process as the hyper-nutrient stress was excessive at 20% leachate. This was evident in the loss of viability (80%) after 45 days extended incubation. The cells at 16% showed the lowest amounts of these elements present on the surface. This is possibly due the lower hyper-nutrient stress and easier ability to maintain homeostasis with the inclusion of only 16% leachate. The result of this was the increased biomass production, evident by the higher growth rates and chl *a* value. The heavy metals on the cellular surface of the microalgae showed that cultures at 16% leachate had higher concentrations of metals and heavy metals (Fig 2.6B). In particular, Cr, Mn, Fe, Co, Ni, Cd and Mo showed the highest values. This shows that at 16% leachate, the cells are under less stress than the 20% leachate cells and are able to regulate heavy metal uptake while maintaining homeostasis and not affecting the biomass production. Further experiments were conducted using SEM EDX to determine the effect of the leachate with specific reference to the elements and the accumulation by the *Chlamydomonas* cells. The leachate sample contained elements depicted in Fig 2.6 as well as Na, Cl, Zn, Ru, Hg, Rb and Rh. Hg and Rh were only present in the leachate and not on the extracellular surface of the microalgal cells.
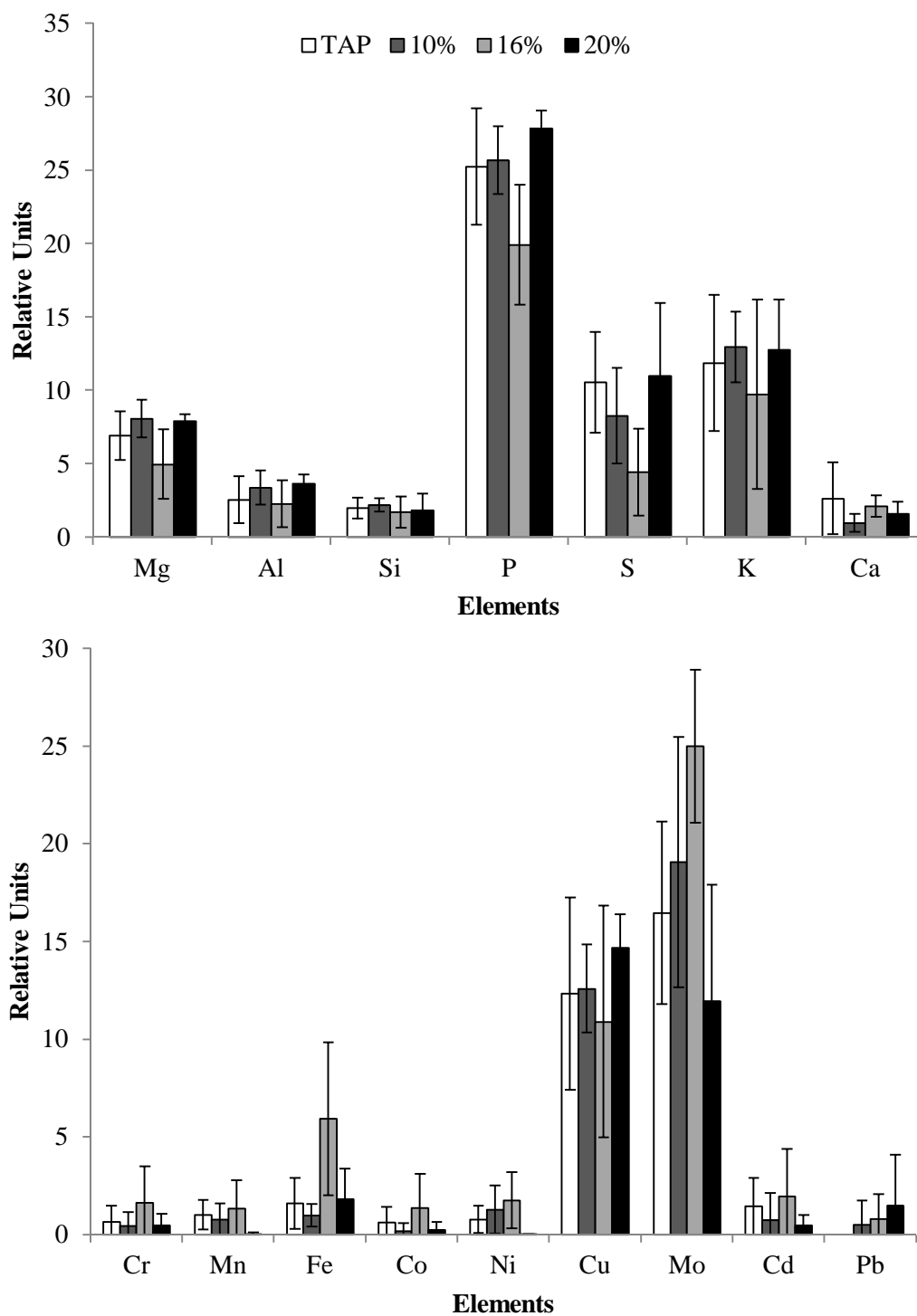
Figure 2.6: SEM EDX analysis of the elements presented on *Chlamydomonas* cells cultured at 10%, 16%, 20% leachate and a TAP control. Growth inducing elements shown in (A) and heavy metals in (B) (Averages ± SD).

2.4 Conclusions

A 16% leachate concentration has shown to be effective in increasing biomass by 26%, biohydrogen by 37% and prolonging the duration of hydrogen production by 3 days. This increases feasibility of the current biohydrogen production process due to reduced costs of nutrients and water, and increased production of biohydrogen as a renewable energy source. *Chlamydomonas* cultured at 16% leachate showed the greatest potential for heavy metal uptake and assimilation whereas cultures at greater stress had a higher affinity for growth stimulating elements. Future studies will investigate further optimising the use of leachate to increase biohydrogen in a continuous sustainable system.

CHAPTER THREE

Photosynthetic Shift Towards Photosystem I Up-Regulation during Hydrogen Production in *Chlamydomonas reinhardtii*

Abstract

This study investigated the effect of hydrogen synthesis on Photosystem I and Photosystem II in *Chlamydomonas reinhardtii* as monitored by Dual Pulse Amplitude Modulated (PAM) Fluorometry. Cultures were incubated in TAP-S for ten days, where the physiological parameters (rETR, Y (I), Y(II), NPQ, α, F_v/F_m and YI:YII) and hydrogen evolution yields were monitored. Photosystem I $rETR_{max}$ and YI: YII values were found to be up-regulated by 66% and 77%, respectively. Direct correlations (Pearson's) were recorded when comparing hydrogen evolution yields to the $rETR_{max}$I, YI: YII and α values, showing correlation coefficient values of 0.895, 0.912 and -0.917 respectively. Rapid light curves were used to optimize growth conditions and hydrogen yields based on light intensities. The synergistic approach of up-regulation of PSI may prove invaluable when combined with PSII down-regulation methods e.g. sulphur depletion or the use of oxygen scavengers to increase hydrogen yields and subsequent process feasibility.

Keywords: Biohydrogen; Pulse Amplitude Modulated (PAM) Fluorometry; Photosystem I up-regulation; *Chlamydomonas reinhardtii*; Renewable Energy.

3.1 Introduction

Renewable energy alternatives are fast becoming a favourite energy source over the conventional fossil fuels. The second generation renewable energy sources originating from forest residues, corn and sugarcane are limited with regard to land usage, water scarcity and food security issues (Sims et al., 2010). Third generation energy sources derived from microalgae have been shown to be advantageous over first and second generation fuels (Costa and Greque de Morais, 2011). These fuels include biodiesel, jet fuel and biohydrogen.

The production of hydrogen from green algae species has been occurring for the last 65 years in experiments originally performed by Hans Gaffron and his co-workers (Gaffron and Rubin, 1942). Microalgae have been found to be a candidate for such a process as they are able to produce hydrogen gas under specific metabolic and physiological conditions (Costa and Greque de Morais, 2011). A major limitation of this hydrogen production is that the expression of the hydrogenase enzyme and its activity are inhibited in the presence of O_2 (Chochois et al., 2010). To date hydrogen photoproduction is generally induced by depriving the *Chlamydomonas reinhardtii* cells of sulphur (Kosourov et al., 2007). This deprivation causes the partial and reversible inhibition of PS II water oxidation. This limits the evolution of O_2 due to the reversible damage occurring on the D proteins which have a photo protective function for PSII. In the absence of sulphate, the repair of the D proteins are impaired and the activity of PSII is progressively reduced (Jorquera et al., 2008). This has no effect on the respiration rate and results in an anaerobic state. Two (FeFe)-hydrogenase enzymes are then expressed, redirecting the flow of electrons coming from the photosynthetic electron transport chain from carbon fixation towards proton production (Antal et al., 2003). As a result, H_2 is produced for several days.

Several microalgal species (*Scenedesmus obliquus, Chlamydomonas reinhardtii* and *cyanobacteria)*, have shown the ability to produce hydrogen gas from the low-potential electrons produced in the photosynthetic electron transport chain (McKinlay and Harwood, 2010). Consequently microalgae have shown the potential to produce renewable energy when used in hydrogen fuel cell technology. This technology has proven to be very efficient with only water as a by-product. This concept has prompted major research into the field of renewable hydrogen from microalgae, with the ultimate goals of increasing yield, feasibility and sustainability of the process.

The foundations for exciting new breakthroughs have been provided by the work on the genome sequence (Merchant et al., 2007) , genes relevant to hydrogenases (Hemschemeier and Happe, 2011, Srisangan et al., 2011), the understanding of *Chlamydomonas* in an anoxic environment (Laurinavichene et al., 2002, Laurinavichene et al., 2006, Tsygankov et al., 2006) and most importantly, a better understanding of the physiology during the hydrogen production process (Santabarbara et al., 2007, Hemschemeier and Happe, 2011).

Physiological studies have found that during hydrogen production there is a reduction in the photochemical yield of PSII from 0.4 to 0.1 and an increase in Non Photochemical Quenching (NPQ) values (Antal et al., 2003). Overall this study found a decrease in PSII activity after the onset of anaerobiosis and during the production of biohydrogen. Another study confirmed these findings with a decrease in PSII functioning evident by the decrease in the photochemical yield (Kosourov et al., 2007). It can be seen that numerous studies have monitored H_2 production and correlated this with PS II fluorescence responses, however very little is known regarding the functioning and fluorescence behaviour of PSI. If electrons originating from the water-splitting process are transported from PSII to the Fe-Fe-hydrogenase through PSI (Kosourov et al., 2007), the functioning of PSI would be critical in understanding and optimising the production of hydrogen gas from *Chlamydomonas.*

It has been stated that at the onset of hydrogen production, electron transfer from PSII to PSI abruptly decreases (Antal et al., 2003). Electron transfer has yet to be simultaneously measured in PSII and PSI showing the need to investigate the role of PSI in the hydrogen production process. A metabolic map of the hydrogen production process during sulphur deprivation was devised, which included all the photosynthetic components (Jorquera et al., 2008). For this S-system modelling, PSII was used as a variable due to the change according to the sulphate concentration. The activity of PSI was made a constant as it had been previously reported to have marginal variations when exposed to varying sulphate concentrations (Melis et al., 2000, Ghirardi, 2006).

Research has started focusing on PSI and the role it plays in hydrogen production (Hoshino et al., 2012). A new strategy has been developed where specific wavelengths of light were used to individually stimulate photosystem I in an attempt to drive a steady flow of electrons along the photosynthetic chain. These electrons would be delivered to the hydrogenase enzyme for photo-hydrogen production (Hoshino et al., 2012). This strategy was found to prove successful in allowing cells to switch between hydrogen production and a recovery

period by stimulation with a specific PS I stimulating light source. Another study used spectral light having a distribution greater than 680nm which resulted in a hydrogen production due the termination of oxygen production (Hamada et al., 2003). The physiological reason for this was however not fully understood.

The limited information about PSI may be attributed to availability of technology during the last 10-15 years. Early fluorescence emission and excitation technology measured only F_o and F_m of PSII. Present technological advances differentiate between fluorescence of PSII and PSI. This simultaneous measurement of relative electron transports rates allow for the assessment of energy conversion efficiencies in both PSII and PSI (Klughammer and Schreiber, 2008). These technological advances encourage further research into the functioning, role and variation in PSI during changes in metabolic functioning of microalgae and in particular, during hydrogen production.

This study therefore investigates the physiological role of PSI and PSII during hydrogen production using Dual PAM 100 Fluorometer (Heinz Waltz).

3.2 Materials and Methods

3.2.1 Culture Conditions

Chlamydomonas reinhardtii CC125 cells were cultured until late exponential phase in Tris-acetate-phosphate (TAP) media (Gorman and Levine, 1965) (pH 7.0) between 100- 200 μmol m^{-2}s^{-1} in a 12:12 light: dark cycle. Cells were harvested and centrifuged at 3000 rpm for 15 minutes before being washed three times in TAP-S media and placed under three experimental conditions as follows: 1) Cells were resuspended in duplicate 1L culture bottles (Schott, Duran) with TAP media at a concentration of 644.42 $\pm$ 36 chlorophyll *a* μg/L. 2) Cells were re-suspended in duplicate in TAP minus sulphur (TAP-S) in modified Schott bottle with 3 vacuum sealed ports at a concentration of 5543.11 $\pm$ 228 chlorophyll *a* μg/L. 3) Cells were resuspended into TAP media with 3-(3,4- dichlorophenyl)-l,l-dimethylurea (DCMU) at a concentration of 5683.06 $\pm$ 72 μg/L chlorophyll *a*. These culture bottles were then placed on magnetic stirrers and incubated at a light intensity of 200 μmol m^{-2}s^{-1} at a light cycle of 12:12 light: dark (Laurinavichene et al., 2006). Experiments were repeated twice for validation purposes.

3.2.2 PAM Fluorometry

Simultaneous fluorescence measurements for Photosystem I (PSI) and Photosystem II (PSII) were obtained from a DUAL-PAM 100 Chlorophyll Fluorometer (Heinz Walz Gmbh, Effeltrich, Germany). The Rapid Light Curves (RLCs) were generated by applying a sequence of increasing actinic irradiance in 20 preset discrete increments ranging from 0 μmol photons m^{-2} s^{-1} to 2630 μmol photons m^{-2} s^{-1}. Each actinic light (AL) incubation lasted for 40 s before a saturation pulse of blue light (0.6 s at 10 000 μmol photons m^{-2} s^{-1}) was applied to determine the rETR at each irradiance level. Rapid light curves were used to extract detailed information regarding the saturation characteristics of both PSI and PSII and to infer information related to the overall photosynthetic performance of the microalgae (Ralph and Gademann, 2005). All PAM data and generated RLCs (Baker, 2008) were obtained using Dual PAM software (v 1.11).

The rETRs were determined using the formula (Baker, 2008):

$$rETR = F'_q/F'_m \text{ x PPFD} \qquad (1)$$

The maximum quantum efficiency from PS II was determined from the formula:

$$F_v/F_m = (F_m - F_o)/F_m \qquad (2)$$

Non photochemical quenching (NPQ) was calculated from PS II ΔF_m compared to the final value F_m in dark adapted samples using the formula (Schreiber, 2004):

$$NPQ = (F_m - F_m')/F_m' \qquad (3)$$

The initial slope of the RLC is termed the alpha (α) value and was calculated accordingly (Ritchie, 2008). The effective PS II quantum yield (YII) is calculated according to Genty (1989) by the formula (Genty et al., 1989):

$$Y(II) = (F_m' - F)/F_m' \qquad (4)$$

Analogous to the Y(II) is the PS I photochemical quantum yield Y(I) derived from (Klughammer and Schreiber, 2008). It was calculated via the formula:

$$Y(I) = 1 - Y(ND) - Y(NA) \qquad (5)$$

Where $\quad Y(ND) = 1 - P700$ red and $\qquad (6)$

$$Y(NA) = (P_m - P_m')/P_m \qquad (7)$$

The ratio of quantum yields was calculated as Y(I) / Y(II).

3.2.3 PAM Calibration to Photosynthetic Oxygen Curves (P-I Curves)

Cells were cultured in TAP media for a duration of ten days with daily recording of oxygen measurements and simultaneous monitoring of the Dual PAM parameters. The oxygen measurements were made using an optical oxygen meter – Firesting O_2 (Pyro-science, Germany). Medical oxygen was used for the upper 100% calibration and argon used for the 0% calibration. Light curve measurements were recorded every 40 seconds and coincided with the increase in light intensity from the PAM light curves. The rate of oxygen evolution was measured as a function of increasing light intensity. Light saturation curves were normalised to chlorophyll *a*.

3.2.4 Oxygen measurements

Oxygen measurements were recorded using an optical oxygen meter – Firesting O_2 (Pyroscience, Germany) Argon and medical Oxygen were used as the 100% and 0% calibrations. Recordings were set to occur hourly for the 14 day experimental period.

3.2.5 Chlorophyll *a* determination

Microalgal biomass was quantified by chlorophyll *a* (chl *a*) fluorescence, using a Turner Designs Trilogy Fluorometer. A 90% acetone solution was used to extract the chlorophyll for 24 hrs at 4°C. (Parsons et al., 1984). Chlorophyll *a* standard (Sigma) was used for calibration of the instrument.

3.2.6 Hydrogen measurements

Hydrogen was collected from the sealed modified Schott bottle by the upward displacement of water in a burette (Laurinavichene et al., 2002). Measurements were recorded on a daily basis. The hydrogen gas was collected in a Hamilton gas-tight syringe and injected into a gas chromatograph (Shimadzu GC 2014, Shimadzu, North America) equipped with a thermal conductivity detector and a Molecular Sieve 5A column.

3.2.7 Statistics

Statistical comparisons were performed using SPSS version 11.5.1 for Windows. All values were logarithmically ($\log_{10}$) normalised to meet the requirements for parametric statistical tests. One way analyses of variance (ANOVA) were used to test for significant differences in data ($p < 0.05$). Pearson's bivariate correlation was used to determine the relationship between the corresponding PAM parameters and hydrogen production ($p < 0.01$).

3.3 Results and Discussion

Photosynthesis – Irradiance (P - I) curves were correlated to PAM light curves to determine the accuracy of light curves as a relative measurement of photosynthesis (Fig 3.1). Oxygen and rETR data points were found to correlate in three distinct phases based on the growth phases on *Chlamydomonas*. The first phase corresponded to the lag phase (days 1) (Fig 3.1A). A significant correlation was found between samples on day 1 ($r = 0.817$, $p < 0.05$). Significant correlations were found between days 3 and 7 which corresponded directly with the microalgal growth phase ($r = 0.843$, $p < 0.05$) (Fig 3.1B). During the third phase, the oxygen and rETR values showed significant correlation during the stationary growth phase during days 8-10 ($r = 0.912$, $p < 0.05$) (Fig 3.1C). These correlations show that measurement of relative electron transport rate can be used as an accurate indicator of photosynthesis for further experiments.

The culturing of *Chlamydomonas reinhardtii* in TAP-S media resulted in the temporary transition of metabolic functioning and the production of hydrogen gas (Fig 3.2). PAM Fluorometry showed a distinct difference between PSI and PSII light curves (Fig 3.3) with PSI having a significantly higher electron transport rate than PSII (Fig 3.4). During hydrogen production photosynthetic apparatus showed distinct changes in PSII (Fig 3.5) and PSI (Fig 3.6) with an up-regulation in PSI visible. A summary of the regulation shifts can be seen in Table 3.1.
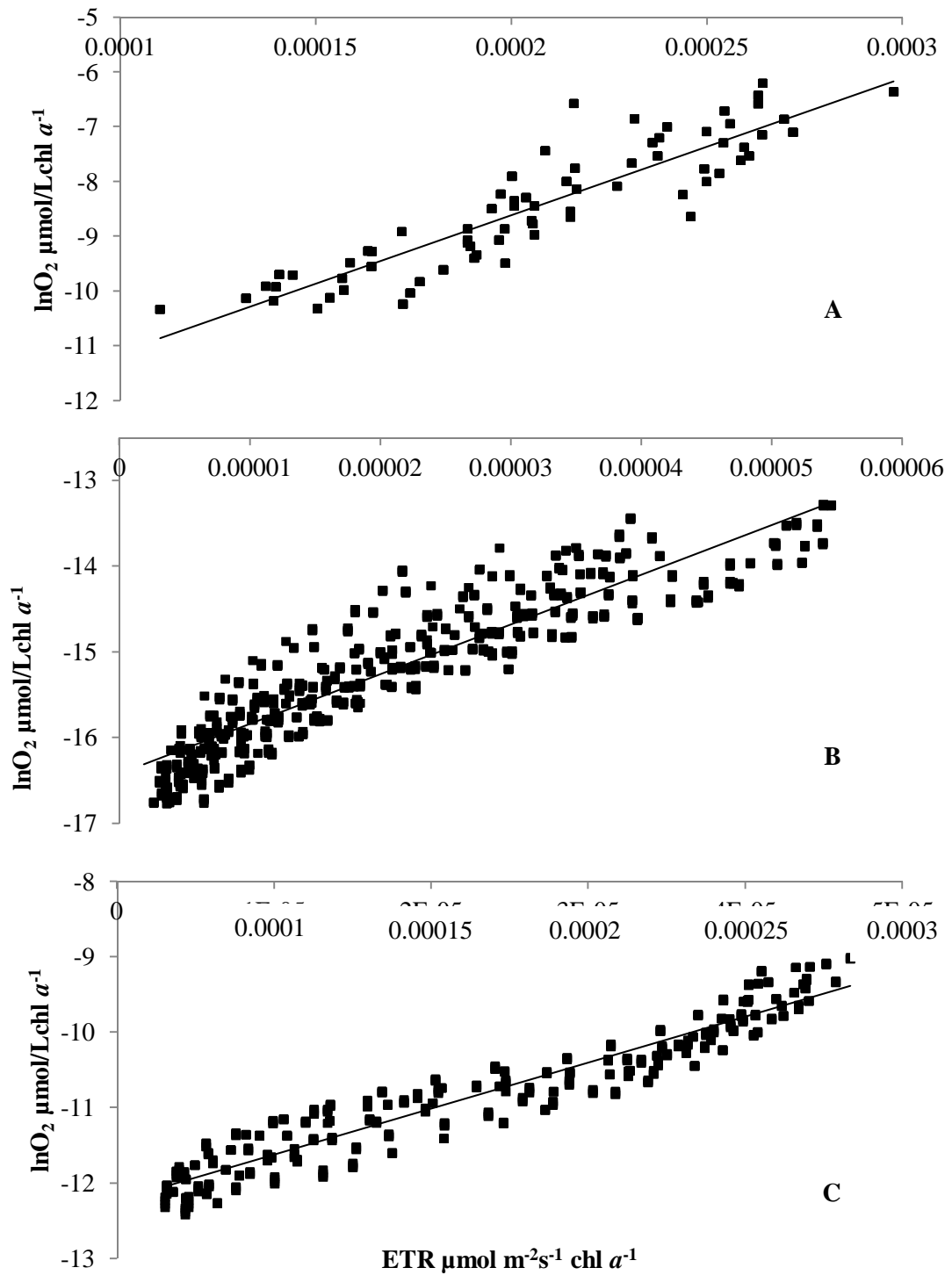
Figure 3.1: Correlation of Photosynthesis – Irradiance curves (P-I) compared to PAM rapid light curves during lag phase (n = 288) (A), logarithmic growth phase (n = 1073) (B) and stationary phase (n = 572) (C).

For the production of H$_2$, *Chlamydomonas* cells were incubated in TAP-S media, which initially lowered oxygen production (Fig 3.2). This reduction continued until day 3 where the respiration rate was greater than the oxygen production rate resulting in minimal oxygen levels (less than 1 μmol/L). This marked the end of the aerobic period and the start of the anaerobic period or hydrogen production period. The hydrogen production phase maintained an oxygen level of about 0.6 – 0.9 μmol/L while hydrogen was being produced. Hydrogen production was verified using gas chromatography. Previous studies found similar results (Degrenne et al., 2011). However, because of the high respiration rate, anaerobic conditions were maintained in the culture. Post H$_2$ production showed the recovery of oxygen by the inactivation of the hydrogenase enzyme. From these findings, three distinct phases were identified during ten days of no sulphur availability, namely 1) pre-H$_2$ production phase, 2) H$_2$ production phase and 3) post- H$_2$ production phase. A similar phase structure has been previously found (Kosourov et al., 2002) however the pre-H$_2$ production phase and H$_2$ production phase were further differentiated.
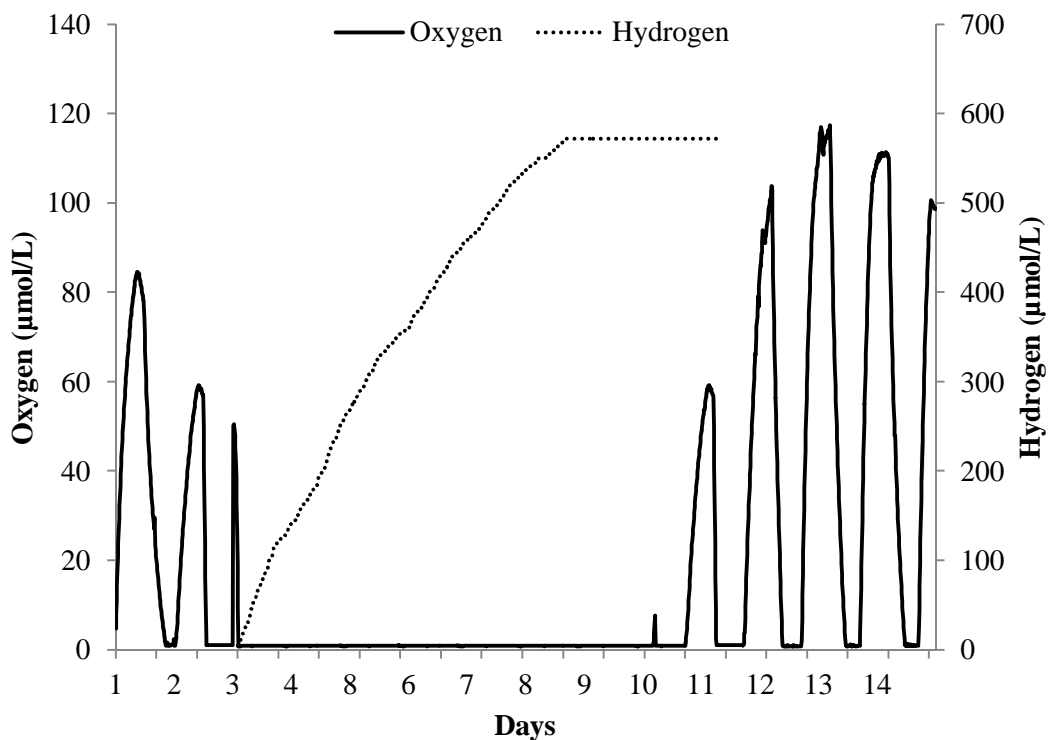
Figure 3.2: Oxygen and hydrogen values monitored over 14 days. Oxygen measurements were taken hourly and hydrogen measurement daily.

Comparing light curves obtained from the DUAL-PAM showed the relative electron flow rate of PSII and PSI (Fig 3.3). However, PSI electron transport rate was significantly greater ($p < 0.05$) than PSII for all control and experimental cultures. During RLC experiments, when PAR levels reached $\pm$ 200 μmol m^{-2}s^{-1}, the rETR of PSI was always significantly greater than PSII ($p < 0.05$). On average, a 6-fold increase in the rETR values of PSI compared to PSII was observed when incubated under direct sunlight ($\pm$2000 μmol m^{-2}s^{-1}). The reason maybe because PSI does not photo inhibit in PAR levels below 2000 μmol m^{-2}s^{-1}. This shows that PSI is able to function at higher light intensities and is not as photo sensitive as PSII. At light intensities above 500 μmol m^{-2}s^{-1}, PSII exhibited photoinhibition (Fig 3.3). At over-saturating PAR intensities the D proteins offer photo protection of PSII generating excess electrons which have been found to react with cellular oxygen forming oxygen radicals (Murata et al., 2007).

Over the 10 day duration (Fig 3.3A-J) PSII rETR decreased due to the sulphur limited media. It can also be seen that PSI activity increased considerably under high light intensities (500 – 2000 μmol m^{-2}s^{-1}). Previous studies show that hydrogen production needs to occur under low light intensities (25 μmol m^{-2}s^{-1} PAR (Tsygankov et al., 2006, Kosourov et al., 2007)), (200-250 μmol m^{-2} s^{-1}(Antal et al., 2003)) to minimise oxygen production by a down-regulated PSII. It can therefore be seen from Fig 3.3 that the optimum PAR varied daily, due to culture age and nutrient levels during the hydrogen production phase. A higher light intensity may be more favourable due to a higher PSI electron transport rate at the respective light PAR levels.

It has been found that at a PAR of 2000 μmol m^{-2}s^{-1}, hydrogen was produced when PSII experienced photoinhibition and reduced functionality (Markov et al., 2006). Figure 3.3 shows that at such a high light intensity only PSI is functional, showing that PSI must have a pivotal role in the production of hydrogen. A previous study showed that internal starch accumulation can be increased by up to 8-fold by variations in the photon flux density (Tolstygina et al., 2009). As starch accumulation has been found to increase in the pre-H$_2$ production phase and be used as an energy source for hydrogen, optimising its production at a favourable light intensity increases hydrogen yields (Melis et al., 2000, Chochois et al., 2010).

Biomass was optimised using light curves in the stages prior to sulphur depletion. At appropriate PAR levels during the growth stage electron transport peaked and subsequently

increased biomass. Greater biomass produces greater yields of hydrogen (Kosourov et al., 2002). The technique of using rapid light curves is a useful tool for increasing microalgal growth and hydrogen production.
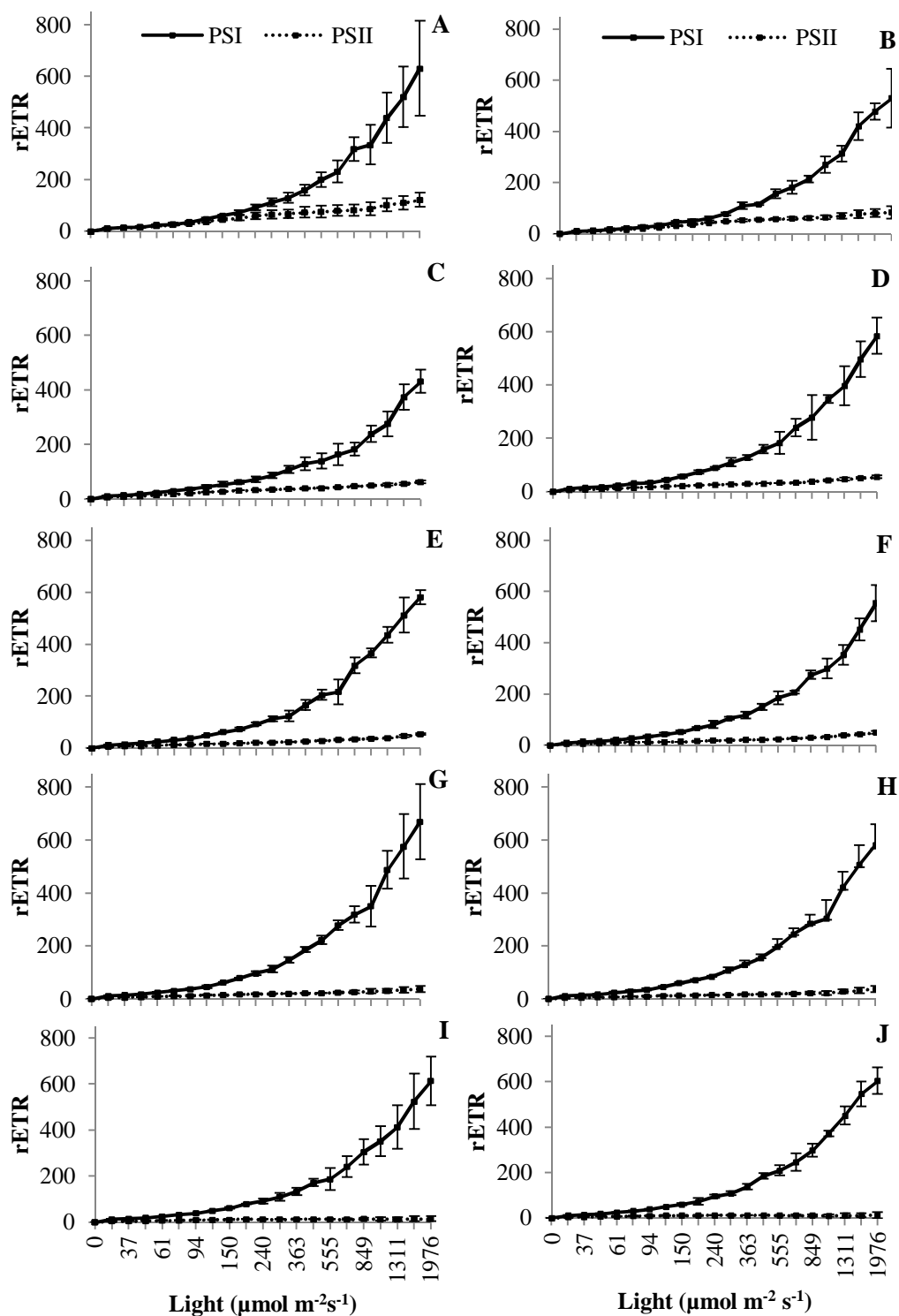
Figure 3.3: Rapid Light Curves of *Chlamydomonas reinhardtii* showing the differences in Photosystem I and Photosystem II when cultured in TAP-S media. Curves represent day 1 (A) to 10 (J) respectively (values are averages ± standard deviation).

When all rETR values were normalised to daily chl a, the rETR$_{max}$ of PSI was 70% higher than PSII (Fig 3.4A). This further increased to 90% from day 3-10. The photosynthetic yield showed further evidence of PSI having a greater stability and electron transport flow (Fig 3.4B).
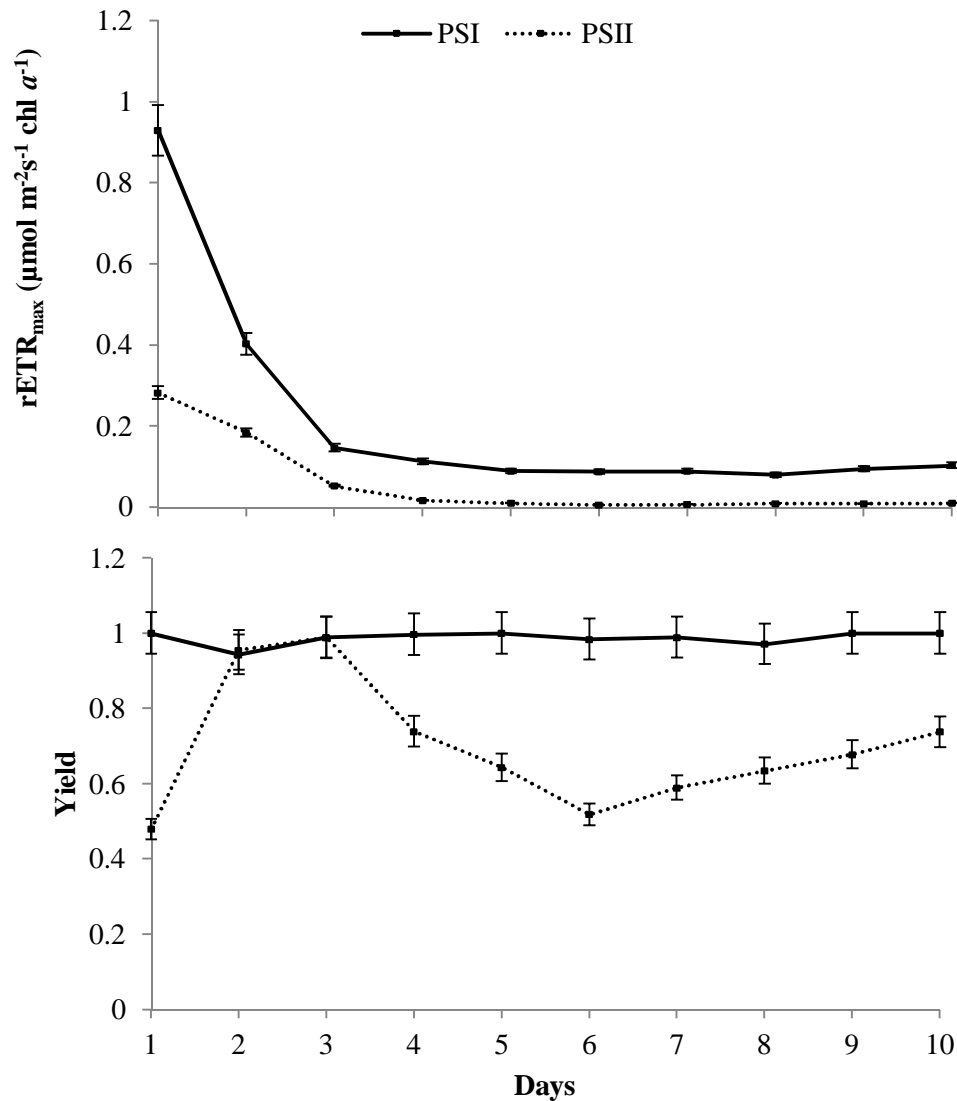
Figure 3.4: A comparison of PSI to PSII evident from the rETR$_{max}$ values (A) and the yields obtained from rapid light curves of *Chlamydomonas* (values are averages ± standard deviation).

Initially the Y(I) value of PSI was 52% higher than PSII. During logarithmic growth phase (day 2-3) the Y(I) and Y(II) values were equal showing maximum electron flow required for ATP production during cell division (Fig 3.4B). PSI Y(I) remained relatively unchanged

from day 3-10 having an average value of 0.98. PSII Y(II) decreased by 47% from 0.98 to 0.51 during day 3 – 6. Y(I) value then increased by 30% until day ten. These higher recordings in PSI compared to PSII is probably a consequence of electrons from cyclic electron flow (CEF) that occurs around PSI compared to the liner electron flow (LEF) at PSII (Alric et al., 2010, Cardol et al., 2011). ATP and NADPH are synthesised during LEF while CEF causes the production of ATP without a net increase in NADPH (Cardol et al., 2011). Eventually these electrons can be directed towards other metabolic pathways, possibly involved in the hydrogen production process (Geigenberger et al., 2005).

From chlorophyll *a* profiles, three phases were identified over the ten day experimental period (Fig 3.5A), which can be attributed to the physiological changes occuring during the hydrogen production phases identified in this study. During the pre-H_2 production phase the chlorophyll *a* increased by 23% from 5543 ± 228 μg/L chl *a* to 7202 ± 105 μg/L chl *a*. This increase was due to the internal storage of sulphur resulting in 2 days of growth and cellular division. During the five day H_2 production phase, chlorophyll *a* decreased by 42% to 4112 ± 158 μg/L chl *a* suggesting a break down of internal cellular components. Subsequently chlorophyll *a* stabilised at approximately 4219 ug/L chl *a* during the post H_2 production phase (day eight to ten). When compared to the TAP media control, it was found that cells had a logarithmic growth phase until day 6, resulting in the production of 6262 μg/L chl *a* followed by the stationary phase until ten where the biomass averaged 6873 μg/L chl *a*.

The PAM parameters measured (F_v/F_m , α , NPQ and F_o) gave further indication of the pre H_2, H_2 production and post H_2 production phases as well as the down regulation of PS II. This was evident in the efficiency (α) values (Fig 3.5B). Cells incubated in TAP-S showed a 50% reduction compared to the 47% increase in cells incubated in TAP media. When compared to cells suspended in the presence of the PS II electron transport inhibitor 3-(3,4-dichlorophenyl)-l,l-dimethylurea (DCMU) in TAP media, α values were negligible due to the high F_m value from the temporarily damaged PSII.

In this study, NPQ values were shown as evidence of down-regulation in PSII due to the increase in emitted thermal energy (Fig 3.5C). This occurs when the rate of photon capture exceeds the LEF resulting in a large proportion of the energy being dissipated as heat (Muller et al., 2001). During hydrogen production, NPQ increased significantly by 55% (p < 0.05). This was followed by a sharp decrease of 82% once the production of hydrogen ceased and cells began to recover. In comparison, cells cultured in TAP media showed a total

decline of 9% throughout the ten day period. Cells incubated in DCMU showed low NPQ values averaging 0.175. This low value is due to the down-regulation of PSII where minimal electrons are flowing through the photosynthetic system and even less are emitted as thermal energy.

Maximum quantum efficiency (F_v/F_m) showed that nutrient stress was evident in cells producing hydrogen (Fig 3.5D). Values decreased steadily from 0.77 to 0.31 over the ten day period. Alternatively minimal ATP availability during LEF may inhibit assimilation of nutrients which is energy (ATP) demanding. Cells in TAP media only showed an initial significant increase over two days to 0.77 followed by a decrease to 0.51 after logarithmic growth. This value then stabilised increasing marginally to 0.69. The down - regulation of PSII is evident by the increase in the F_o value (Fig 3.5E) resulting in a decrease in the quantum efficiency statistic. The increase in F_o value shows an overall increase is fluorescence under normal conditions. Here, light energy is being emitted as thermal energy and not being transported into the electron transport chain. This is known and previously reported in numerous instances (Muller et al., 2001).
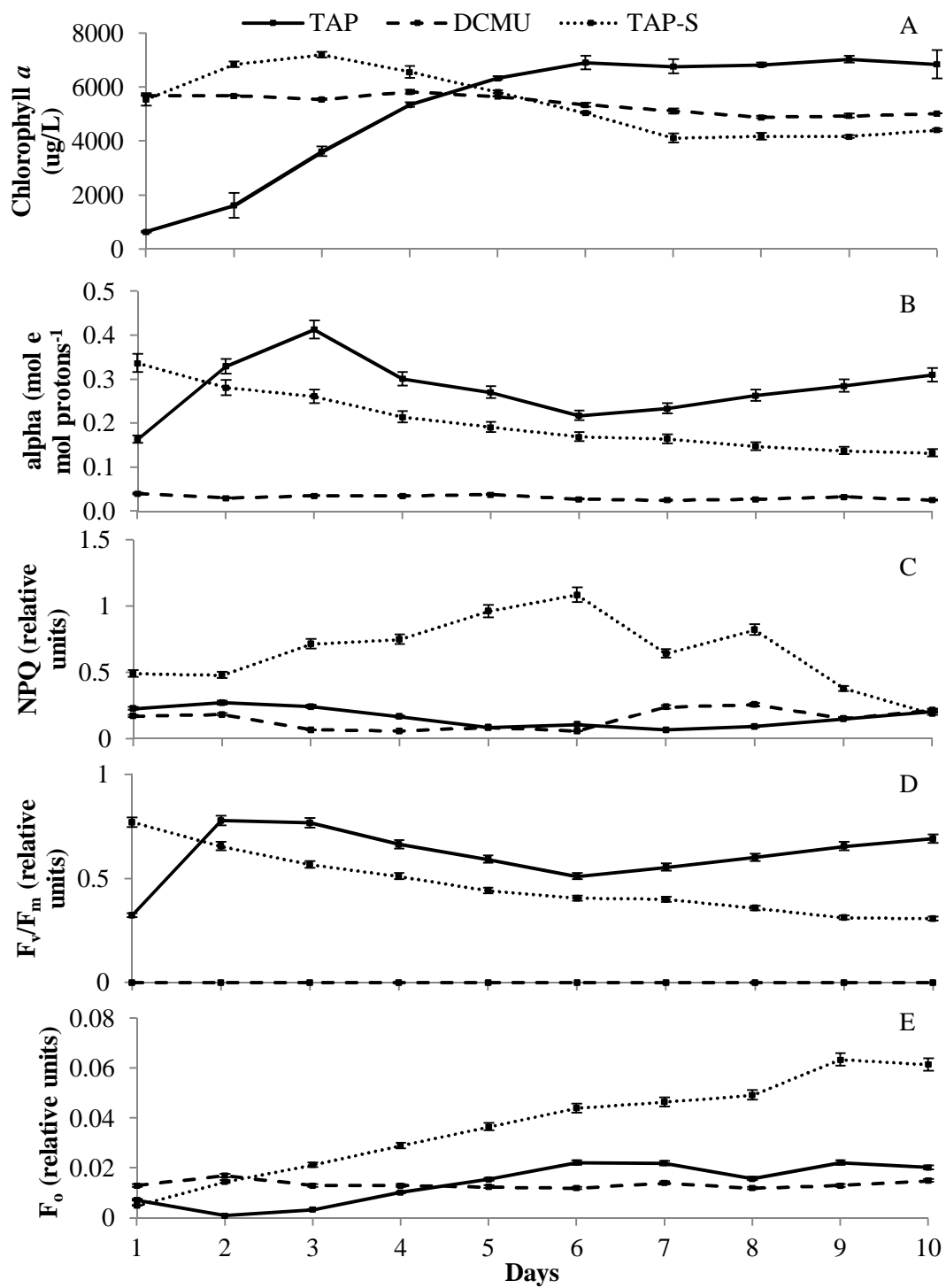
Figure 3.5: Chlorophyll a profiles (A) compared to the PAM Fluorometry parameters α (B), NPQ (C), F_v/F_m (D) and F_o (E) when cells were incubated in TAP media (solid line), TAP-S (dotted line) and TAP+DCMU (dashed line) (values are averages ± standard deviation).

Previous reports would assume PSI to follow suit and be down-regulated as was shown in PSII. This however was not the case. PSI was found to be up-regulated during hydrogen production as depicted by the increase in $rETR_{max}$ and Y(I) values (Fig 3.6). As predicted due to previous research (Scoma et al., 2011), there was a down-regulation of PS II evident by the decreased $rETR_{max}II$ values (Fig 3.6A). During the pre-production phase there was a significant difference (92%) between the TAP-S culture compared to TAP cells shown by the decrease in functioning of PSII due to the damaged D1 protein (Melis and Chen, 2005). The $rETR_{max}II$ values continued to decrease from 63 μmol m^{-2}s^{-1} to 18 μmol m^{-2}s^{-1} during the hydrogen production phase. When compared to cells suspended in DCMU in TAP media, a direct correlation was observed where the $rETR_{max}II$ value decreased from 91.8 μmol m^{-2}s^{-1} to 14.5 μmol m^{-2}s^{-1} over the ten day period. The $rETR_{max}I$ values showed that significant up-regulation of PS I occurred during the hydrogen production phase ($p < 0.05$) (Fig 3.6B). This was evident by the 63% increase in $rETR_{max}I$ measured from day 3 to day 8. Cells without sulphur depletion (control) showed a 39% reduction in $rETR_{max}I$ over the same time period. This is possibly due to the aging culture and no regulation shift at PSI. PSII remained dominant during normal growth conditions.

Further evidence for the up-regulation of photosystem I was observed from the photochemical quantum yield ratio YI: YII (Fig 3.6C). Cells experiencing sulphur depletion showed a significant increase in this ratio by 77% during the hydrogen production phase. A further increase of 62% was recorded in the post H_2 production phase showing the dominance of PS I during sulphur depletion and hence hydrogen production. This showed that P700 is becoming more reduced over time and not limited by the acceptor side. This has a direct correlation to the amount of electrons flowing through PS I and PS II respectively. Cells cultured in TAP media showed an initial decrease in the yield ratio and subsequently remained relatively unchained during the ten day period. Cells exposed to DCMU showed a significant increase in the yield ratio of 57% during the ten day period. As PS II is inhibited with DCMU, PS I electron flow is required to increase to provide adequate ATP for cellular functioning.
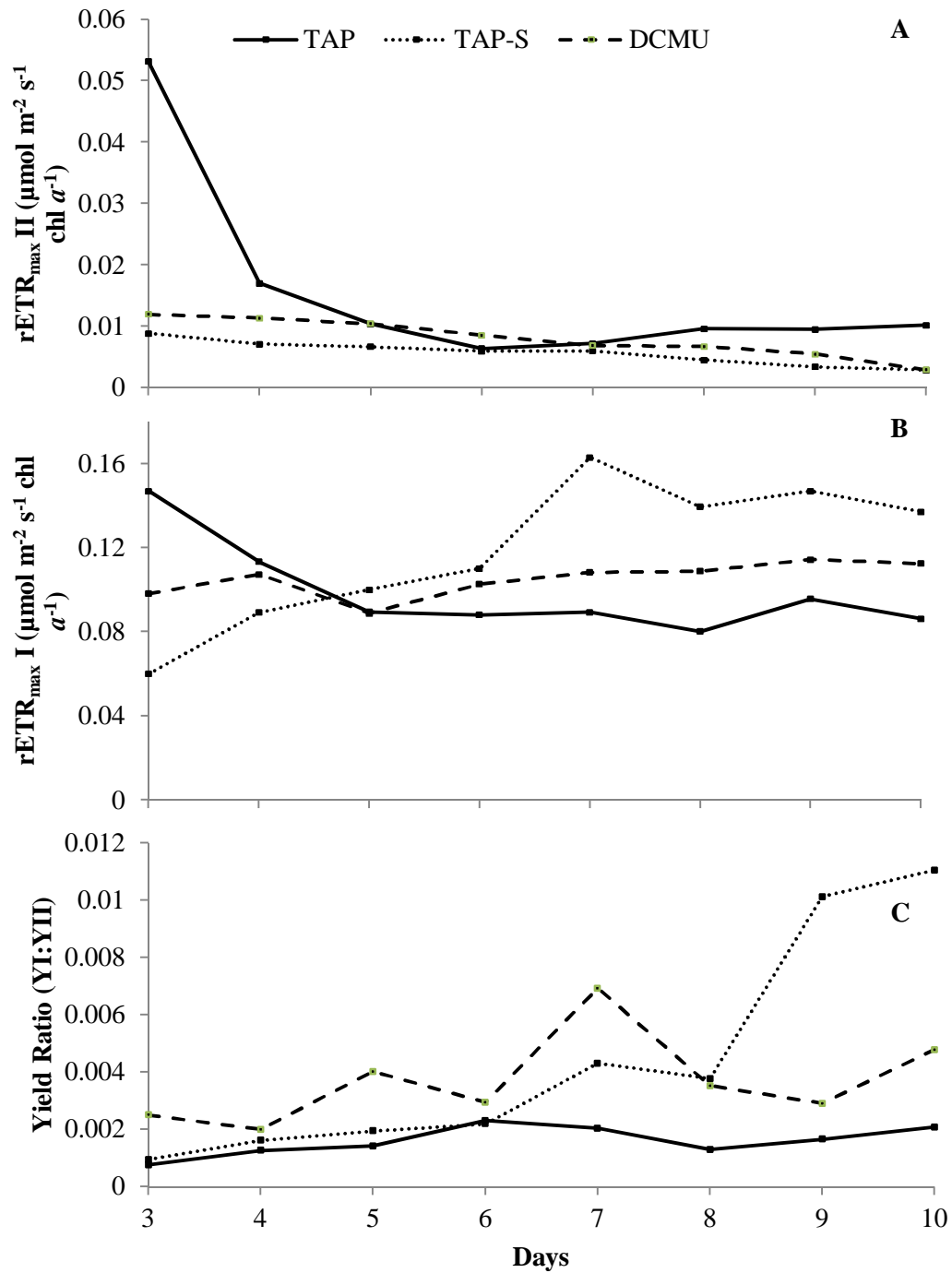
Figure 3.6: Physiological parameters representing PSI rETR$_{max}$II (A), rETR$_{max}$I (B) and the yield ratio YI:YII (C) shown in TAP media (solid line), TAP-S media (dotted line) and TAP+DCMU (dashed line) (values are averages ± standard deviation).

The PAM parameters measured (Y(I):Y(II) and $rETR_{max}I$) gave further indication of the pre H_2, H_2 production and post H_2 production phases as well as the down regulation of PS II (Fig 3.7). When these physiological parameters (Y(I):Y(II) and $rETR_{max}I$) were correlated to actual volumes of hydrogen produced, significant correlations were found (Fig 3.7). A significant direct correlation was shown between $rETR_{max}I$ and the hydrogen evolution values over the ten day period ($r = 0.895$, $p < 0.01$) (Fig 3.7A). A significant direct correlation was also found between the yield ratio YI:YII and the hydrogen produced ($r = 0.912$, $p < 0.05$) (Fig 3.7C). However, the overall photosynthetic efficiency parameters (α value) were found to be indirectly correlated to hydrogen production ($r = -0.917$, $p < 0.01$) (Fig 3.7B). These correlations show that PSI can be considered as a driver of H_2 production. *Cyanobacteria* have been shown to produce photobiological hydrogen (Yeager et al., 2011, Ferreira et al., 2012). A study has shown that *cyanobacteria* have a PSI and a similar structure containing phycobilisomes which is analogous to PSII (Srisangan et al., 2011). This study shows the dominance of PSI during hydrogen production in *Chlamydomonas* which would be a natural process in *cyanobacteria*.
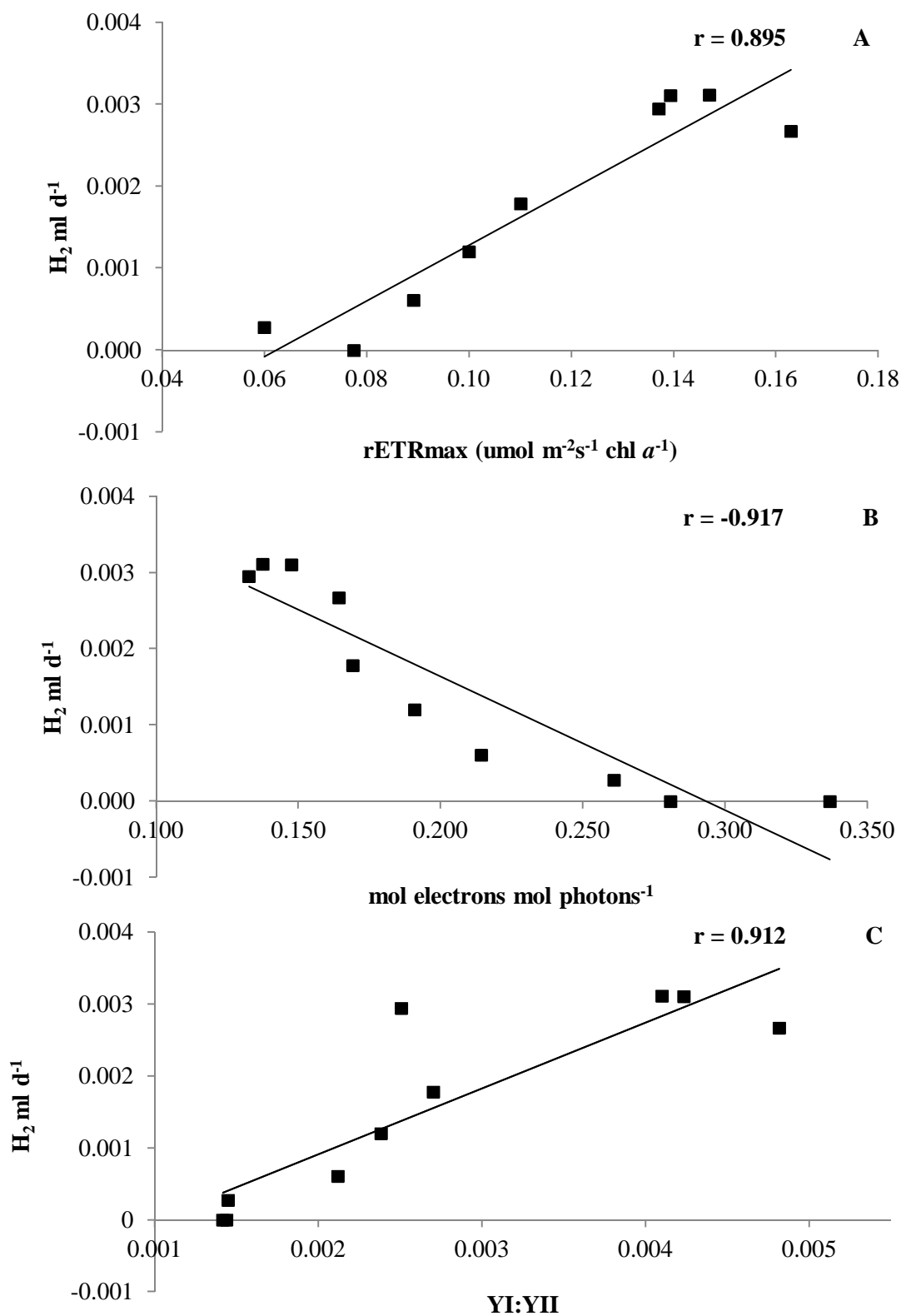
Figure 3.7: Correlations of hydrogen values to the PAM parameters rETR$_{max}$I (A), α (B) and yield ratio YI:YII (C).

No other significant correlations were identified in the PSII PAM parameters when compared to the hydrogen yields. Previous methods of down-regulating PSII from sulphur depletion (Melis et al., 2000) and the use of $NaHSO_3$ as an oxidiser (Ma et al., 2011), combined with methods to up-regulate PSI may prove useful in further improving hydrogen yields and increasing feasibility. Genetic manipulation or genetic up-regulation of PSI upstream compounds such as ferredoxin and the ferredoxin NADP reductase (FNR) may also prove effective in increasing hydrogen production yields.

Table 3.1: Summary of all physiological parameters regulation shifts in TAP-S *Chlamydomonas* cultures compared to the TAP control cultures.

	Pre H_2 Production	H_2 Production	Post H_2 Production
$rETR_{max}$ I	-	↑	↓
$rETR_{max}$ II	↓	↓	↓
α	↓	↓	↓
NPQ	↓	↑	↑
O_2	↑	↓	↑
H_2	-	↑	-
Chl *a*	-	↓	-
YI:YII	-	↑	↑
F_o	↑	↑	↑
F_v/F_m	↓	↓	↓

3.4 Conclusions

The functioning of PSI was found to have a greater electron transport rate than PSII and to be more stable under higher light intensities. PAM Light curves were found to be correlated to P-I curves proving invaluable in rapid physiological measurements pertaining to the application of photosynthesis during hydrogen production. During hydrogen production PSII was down-regulated due to sulphur depletion, however, PSI was found to be up-regulated by an increase of 77% and 66% for the YI: YII yields and $rETR_{max}I$ values respectively. Respiration rates maintained anaerobic conditions despite residual oxygen from PSII. Significant correlations of 91%, and 90% were found throughout the ten day experimental period between the hydrogen yields and YI:YII and $rETR_{max}I$, respectively. The α value showed an inverse correlation coefficient (r = -0.917). A renewed approach of enhancing the activity (genetic or metabolic) of PSI will increase the commercial feasibility of biohydrogen from *Chlamydomonas reinhardtii*.

CHAPTER FOUR

NADPH Fluorescence as an indicator of hydrogen production in the green algae *Chlamydomonas reinhardtii*

Abstract

This study investigated cellular Nicotinamide Adenine Dinucleotide Phosphate (NADPH) fluorescence as a potential indicator of biohydrogen production in *Chlamydomonas reinhardtii* and a *β*-NADPH standard. NADPH fluorescence profiles of cultures grown in TAP-S (Tris-acetate phosphate minus sulphur) media, TAP (Tris-acetate phosphate) media and TAP + 3-(3,4-dichlorophenyl)-1,1-dimethylurea (DCMU) were subsequently compared. Hydrogen production induced from sulphur depletion was found to correlate directly (r = 0.941) with NADPH over the ten day period. The addition of leachate was used to increase hydrogen yields, and subsequently increased the NADPH concentration by 50% - 70%. A direct correlation was observed (r = 0.929) between NADPH and hydrogen when the leachate supplemented media was used. As NADPH is the terminal electron acceptor in the photosynthetic chain, results show that NADPH has a pivotal role in hydrogen production as a carrier molecule. Under sulphur depletion, cellular NADPH fluorescence can be used as an indicator of hydrogen production.

Keywords: Nicotinamide Adenine Dinucleotide Phosphate (NADPH); *Chlamydomonas reinhardtii;* Photobiological Hydrogen; Renewable Energy; Pulse Amplitude Modulated (PAM) Fluorometry;

4.1 Introduction

Hydrogen is envisioned to play a pivotal role as a clean renewable fuel in the hydrogen driven economy of the future (Meherkotay and Das, 2008). Hydrogen can be used as a feedstock for Proton Exchange Membrane Fuel Cells (PEMFC) which are shown to have a high energy efficiency (Guo et al., 2013). Hydrogen causes less to no effect on the environment (Midilli and Dincer, 2008). Hydrogen has shown to have attractive characteristics during its use with regard to exergetic performance (Rakopoulos et al., 2008). Hydrogen cannot be depleted and if used carefully it can provide a reliable and sustainable energy source (Midilli and Dincer, 2008). Microalgae have shown to be a sustainable source of hydrogen and numerous strains have been found to produce hydrogen such as cyanobacteria, *Scenedesmus obliquus* (Florin et al., 2001) and *Chlamydomonas reinhardtii* (McKinlay and Harwood, 2010).

Chlamydomonas is one of the best reference organisms for studying algal biology, physiology and photosynthesis (Dent et al., 2001). This is due to the fact that its genome has retained genes from the last common ancestor to both the plant and animal lineages (Merchant et al., 2007). It can be grown into very high cell densities in a few days using a simple chemical defined growth medium. It has a single large cup-shaped chloroplast that is biochemically and structurally similar to that of higher vascular plants (Merchant et al., 2007). A unique attribute pertaining to *Chlamydomonas* is its ability to be cultured heterotrophically (in the dark using acetate), autotrophically (using CO_2 and light) as well as mixotrophically (using acetate in the light) allowing for various studies under these conditions (Blaby-Haas and Merchant, 2012) . *Chlamydomonas* has been found to shift metabolically when under these specific growth conditions altering its photosynthetic functioning.

Under normal growth conditions (oxygenic photosynthesis) Adenosine Triphosphate (ATP) and Nicotinamide Adenine Dinucleotide Phosphate (NADPH) are produced for the fixation of CO_2 and the subsequent dark metabolic reactions. This is driven by the photosynthetic apparatus present within the thylakoid membranes. The photosynthetic apparatus comprises of two photosystems namely photosystem one (PSI) and photosystem two (PSII). PSII catalyses the first step of the electron transport which is the solar driven water oxidation. Here water is broken into its components of 2 electrons, 2 protons and oxygen. PSI catalyses the final step of photosynthesis which is the oxidation of plastocyanin in the thylakoid lumen

and the reduction of ferredoxin in the chloroplast stroma. The photosystems are interconnected by cytochrome b_6f complex via two diffusible redox carriers plastoquinone and plastocyanin. $NADP^+$ is the terminal acceptor of the electron where it is converted into NADPH as an energised molecule (Sakurai et al., 2013). NADPH is used to provide H atoms for the formation of glucose, while ATP provides the energy to do this. Under sulphur depleted conditions when *Chlamydomonas* produces hydrogen specific changes in the photosynthetic pathway take place (Gaffron and Rubin, 1942). Within 24 hours of sulphur depletion, water oxidation and oxygen production decline below the respiration level resulting in anaerobic conditions (Ghirardi, 2006). Under these conditions electrons are driven via reduced ferredoxin, to the FeFe-hydrogenase enzyme generating photobiological H_2 (Florin et al., 2001). The use of a landfill leachate supplemented media has shown to further increase the photobiological hydrogen yield possibly using the same up-regulated mechanism (White et al., 2013). Monitoring the change in intercellular NADPH fluorescence during H_2 synthesis may reflect the quantity of hydrogen gas produced in a closed reactor.

Fluorescence provides an extremely sensitive tool for examining energy metabolism in photosynthetic cells (Oxborough et al., 2000). The DUAL-PAM-100 fluorometer possesses both the properties of a Pulse Amplitude Modulated (PAM) chlorophyll fluorometer with the addition of a dual wavelength absorbance spectrometer. The DUAL-PAM-100 (Walz, Germany) has a NADPH module that is fitted with a UV-A Power LED. It has a photomultiplier to detect emissions in the blue green range of 420 to 580nm. It has an excitation spectrum at approximately 340nm and an emission peak at around 465nm (Schreiber and Klughammer, 2009). This module detects light induced changes of NADPH fluorescence in suspensions of isolated chloroplasts, algae and cyanobacteria (Schreiber and Klughammer, 2009). The DUAL-PAM-100 software allows for simultaneous measurements of chlorophyll and NADPH fluorescence. Measuring NADPH fluorescence has previously been shown to be complicated due a number of factors; the amplitude of NADPH fluorescence is 2000 times smaller than that of chlorophyll, numerous cellular components (cellulose and flavins) increase the background signal and NADPH accumulates at very low light intensities making the use of high measuring light intensities problematic (Schreiber and Klughammer, 2009). NADPH fluorescence changes provide information on the electron transport at the acceptor side of Photosystem I (PSI). Under normal conditions NADPH is the terminal electron acceptor and under hydrogen producing conditions electrons are driven to Fe-hydrogenase.

This study therefore aims to investigate the use of NADPH fluorescence to elucidate correlations between NADPH concentrations and hydrogen production in *Chlamydomonas reinhardtii.*

4.2 Material and methods

4.2.1 PAM Settings

Non invasive fluorescence measurements NADPH Florescence were obtained using a DUAL-PAM 100 Chlorophyll Fluorometer (Heinz Walz Gmbh, Effeltrich, Germany). This unit was equipped with a NADPH/9-AA emitter-detector module (DUAL-ENADPH). The system was stabilised using the Blue F standard (Heinz Walz Gmbh, Effeltrich, Germany) and NADPH standard compound using the NADPH programme script (Table 4.1). Fluo+NADPH settings were used for all further experiments.

4.2.2 NADPH Calibration

A diluted ethanolic solution of Lumogen F Violet, commonly known as Blue F Standard was used to stabilise the NADPH detector-emitter system. This compound emits blue fluorescence upon 365 nm excitation as an analogy to NADPH fluorescence. The coarse and fine amplification were adjusted to align the background reading to 0. Biological samples can then be used to determine the amplification readings required to obtain valid readings. Figure 4.1 depicts a general graph from the programme Fluo and NADPH on the DUAL-PAM module using the control *Chlamydomonas* culture. The profile runs for a duration of 2 minutes and 30 seconds where the measuring light is switched on after 1 minute and off again after two minutes. At the onset of actinic light, the NADPH fluorescence increases. The chlorophyll *a* fluorescence peaks at the onset of actinic light and then decreases sharply as the photo-protective mechanism is activated (Jahns P et al., 2000). Fluorescence then maintains a steady state. After the actinic light is switched off, NADPH fluorescence returns to initial value and the chlorophyll *a* starts to decrease until initial value is reached. The calibration curve used β-NADPH (Sigma-Aldrich) to correlate fluorescence voltage to concentration. Different concentrations of β-NADPH were prepared in dH_2O ranging from 0 to 5μmol in 0.5μmol increments. A volume of 3 ml aliquots were placed in quartz cuvettes (10 x 10 x 40 cm) and inserted into the PAM fluorometer. Readings were made in triplicate.

Table 4.1: NADPH Programme Script used to monitor NADPH Fluorescence and chlorophyll *a* Fluorescence

NADPH Programme Script
P ML Off
Open User settings Walz_NADPH
Measure Mode = Fluo + P700
Analysis Mode = Fast Acquisition
Recording Mode = Trig Run
F ML-Int = 10
F ML On
Damping Ch1 = 1ms (High)
P ML-Int = 20
P ML On
Open Slow Kin. Tri File testNADPH
Visible Page= Slow Kinetics
Slow Kinetics On
Slow Kinetics Average Points 256
Comment = Fluo+NADPH.prg. Slow Kin based on Trig Run
Paste to Slow Chart Comment Line
Wait(s) = 130
Slow Kinetics Auto Scaling Left
Slow Kinetics Auto Scaling Right
Wait(s) = 50
Target Averages = 10
Fast Kin. Averaging On
Read with Start Cond On
Open Fast Kin Trig File testNADPH
Fast Kinetics Average Points = 256
Visible Page = Fast Kinetics
Clock Mode = Sat. Pulse
Clock Timer = 1 min
F ML On
Clock On
Comment = Fluo+NADPH.prg, Fast Kin based on testNADPH
Paste for Fast Chart Comment Line
Wait(s) = 40
Fast Kinetics Auto Scaling Left
Fast Kinetics Auto scaling Right

4.2.3 Protocol Development

Chlamydomonas reinhardtii CC125 cells were grown until late exponential phase in Tris-acetate-phosphate (TAP) media (pH 7.0) under 200μmol m^{-2}s^{-1} in a 12:12 light: dark cycle. Three millilitre samples were taken and centrifuged and resuspended in fresh TAP media and distilled water. Samples were also taken directly from initial bottle for measurement. The NADPH programme was used as previously described.

4.2.4 Culture Conditions

Chlamydomonas reinhardtii CC125 cells were grown until late exponential phase in Tris-acetate-phosphate (TAP) media (pH 7.0) under 200 μmol m^{-2}s^{-1} in a 12:12 light: dark cycle. Cells were harvested and centrifuged at 3000rpm for 15 minutes (Hermle, Germany) before being washed three times in TAP-S media. Cells were then suspended in1L culture bottles (Schott, Duran) with TAP media at a concentration of 644.42 $\pm$ 36.78 chlorophyll *a* μg/L. Cells were also suspended in duplicate in TAP minus sulphur (TAP-S) in modified Schott bottles with 3 sealed ports at a concentration of 5543.11 $\pm$ 228 chlorophyll a μg/L and in TAP media with the addition of DCMU at a concentration of 5683.05 $\pm$ 27.66 chlorophyll *a* μg/L. The bottles were then placed on magnetic stirrers and incubated at a light intensity of 200 μmol m^{-2}s^{-1} at a light cycle of 12:12 light: dark. Experiments were repeated twice for validation purposes and all physiological measurements were conducted in triplicate.

4.2.5 Leachate supplemented media

Chlamydomonas reinhardtii CC125 cells were grown until late exponential phase in Tris-acetate-phosphate (TAP) media with 16% leachate (pH 7.0) under 100μmol m^{-2}s^{-1} in a 12:12 light : dark cycle (White et al., 2013). Leachate has been shown to increase hydrogen yields and may therefore increase NADPH concentrations (White et al., 2013). Cells were harvested and centrifuged at 3000rpm for 15 minutes before being washed three times in TAP-S media. Cells were then resuspended in TAP minus sulphur (TAP-S) media in duplicate 1L modified Schott (Schott, Duran) bottle with 3 sealed ports at a concentration of 5265.95 $\pm$ 126.38 chlorophyll *a* μg/L. These bottles were then placed on magnetic stirrers and incubated at a light intensity of 100 μmol m^{-2}s^{-1} at a light cycle of 12:12 light: dark and a

temperature of $23 \pm 1°C$. Hydrogen was collected and NADPH fluorescence was conducted as previously discussed.

4.2.6   Chlorophyll *a* determination

Microalgal biomass was quantified by chlorophyll *a* (chl *a*) fluorescence, using a Trilogy Fluorometer (Turner Designs, California). Chlorophyll *a* from microalgal samples (10ml) was extracted in 90 % acetone at 4 ℃ for 24 hours (Parsons et al., 1984). Chlorophyll *a* standard (Sigma) was used to calibrate the Trilogy fluorometer.

4.2.7   Hydrogen Evolution measurements

Hydrogen was collected from the sealed modified Schott bottle by the upward displacement of water in a 50ml burette (Laurinavichene et al., 2002). Measurements were recorded daily. The hydrogen gas was collected in a Hamilton gas-tight syringe and manually injected into a gas chromatograph (Shimadzu GC 2010, Shimadzu, North America) equipped with a thermal conductivity detector and a Restek Molecular Sieve 5A column (30m*0.53mm*50μm). The oven was set at a temperature of 60°C. The carrier gas used was argon with a linear velocity of 110 cm/s and the injection volume was 0.5 ml.

4.2.8   Statistics

Statistical comparisons were performed using SPSS version 11.5.1 for Windows. All values were logarithmically ($\log_{10}$) normalised to meet the requirements for parametric statistical tests. One way analyses of variance (ANOVA) were used to test for differences in data ($p < 0.05$). Pearson's bivariate correlation was used to determine the relationship between raw β-NADPH and NADPH Fluorescence and well as to correlate NADPH concentrations to hydrogen values.

4.3 Results and Discussion

The DUAL-PAM Fluorometer was setup and calibrated to measure NADPH fluorescence (Fig 4.1). The effects of background noise and autofluorescence due to processing, media and excreted substances were assessed in a series of duplicated runs using different processing techniques (Fig 4.2). *Chlamydomonas* cells were analysed using the Fluo+NADPH programme after being centrifuged and then resuspended in TAP media or distilled water. It has been recommended to centrifuge cells and resuspend in fresh media, particular when media with soil extract is used as it displays strong fluorescence at 365nm excitation (Schreiber and Klughammer, 2009). The NADPH script programme was run using pure TAP media. No significant change in the background noise was evident upon measuring light activation. When cells were centrifuged and resuspended in fresh TAP media (Fig 4.2B), an increase of 9% was evident in the chlorophyll fluorescence values as compared to the control (Fig 4.2A). An increase in stress was evident by this fluorescence increase as less energy is being channelled into the electron transport chain and a greater amount of this energy is being released as fluorescence. When cells were resuspended in dH_2O, a 12% decrease in fluorescence was observed (Fig 4.2C). This shows more energy is required to maintain homeostasis with the lack of nutrients. Centrifuging also negatively affects the chlorophyll fluorescence due to the mechanical stress. This effect can however be mitigated by allowing an acclimation period before samples are placed in the fluorometer. The NADPH fluorescence showed a significant reduction of 50% after centrifuging and resuspending in both fresh TAP and dH_2O (Fig 4.2). Based on the lack of autofluorescence and particulate matter from TAP media and the negative effect of centrifuging, cells cultured in TAP media don't require further treatment before NADPH fluorescence can be measured.
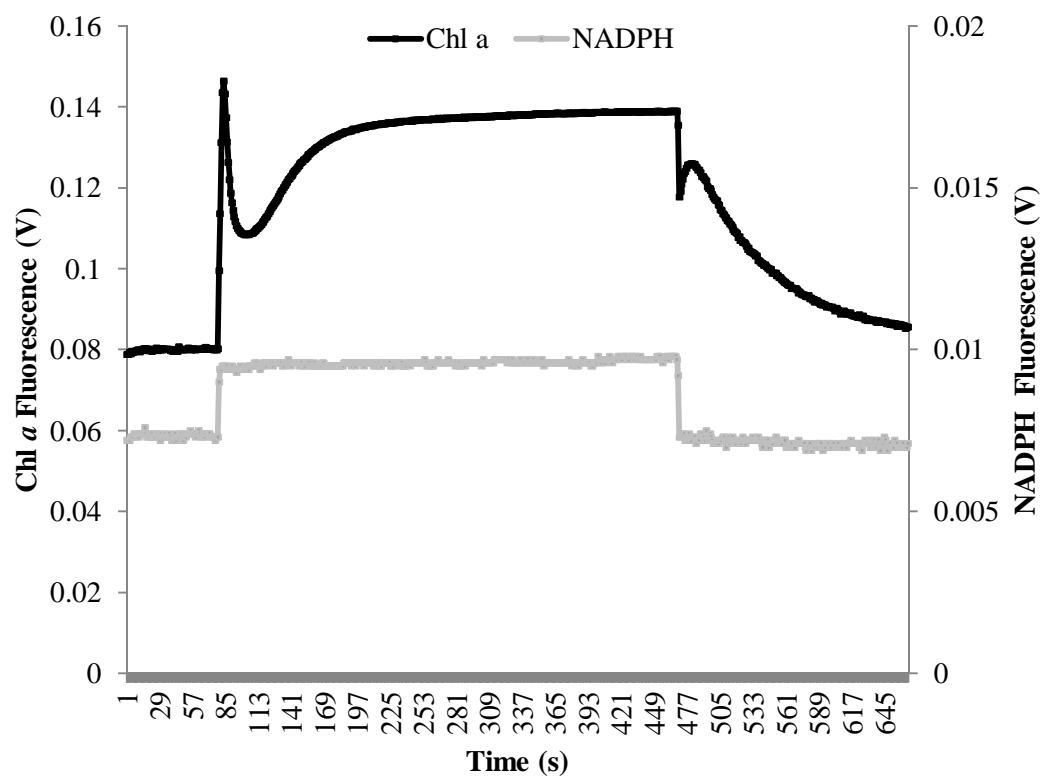
Figure 4.1: NADPH fluorescence (black) and chlorophyll fluorescence (grey) based on voltages in a control *Chlamydomonas* culture cultured in TAP media in the exponential growth phase (Values are averages of n = 256 data points).
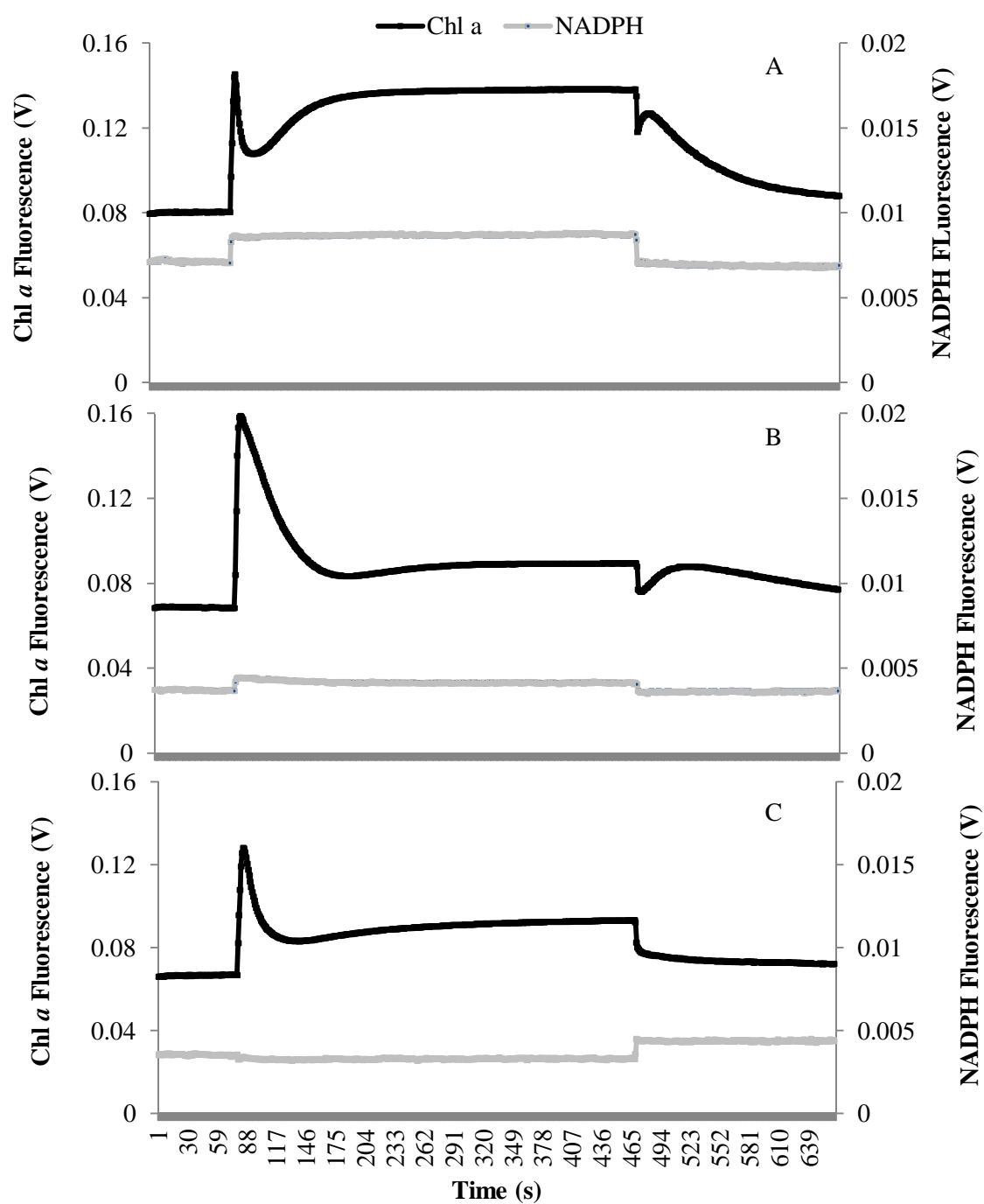
Figure 4.2: Chlorophyll fluorescence and NADPH fluorescence from *Chlamydomonas* cells in exponential phase in TAP media (A), Cells centrifuged and resuspended in fresh TAP media (B) and cells centrifuged and resuspended in dH₂0 (C) (Values are averages of n = 296 data points).

A calibration curve was generated using β-NADPH (Fig 4.3) to quantify the NADPH fluorescence voltage in terms of μmols of NADPH. When NADPH concentrations ranging from 0 μmol to 5 μmol were assessed, fluorescence voltages were found to range between 0 V and 0.1191 V. These values were found to correlate directly (r = 0.973, p < 0.05). An equation (y = 0.0223x) was generated to convert all NADPH fluorescence voltages into a NADPH concentration. The resulting model will be used to convert NADPH fluorescence into μmols throughout this study.
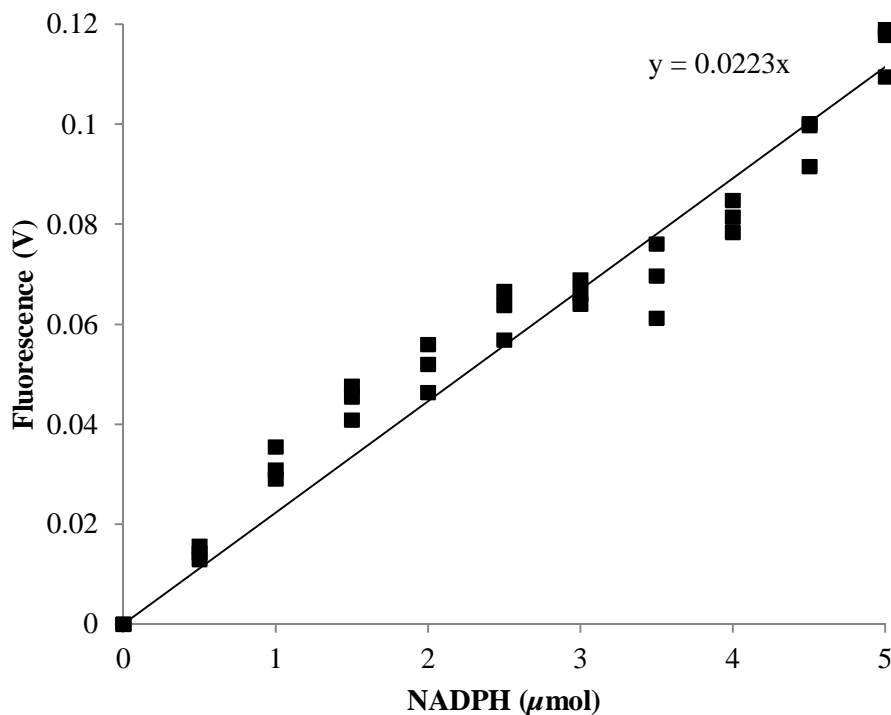
Figure 4.3: Calibration curve of NADPH at various known β-NADPH concentrations against fluorescence voltage from NADPH module.

When NADPH concentrations were analysed against chlorophyll *a* values (Fig 4.4), it was found that in the control culture (TAP), NADPH concentrations decreased significantly (p < 0.05) from 7.55×10^{-4} μmol to 1.16×10^{-4} μmol (84%) during the exponential growth phase. NADPH concentrations showed no significant difference during the stationary phase with values ranging between 3.41×10^{-5} μmol and 5.87×10^{-5} μmol. The initial high values recorded in the control culture were due to the inoculum being in exponential growth phase and a low cell density allowing for minimal shading. Under oxygenic photosynthesis, the photosynthetic chain can function in two modes. Linear electron flow produces ATP and NADPH in a ratio of 3:2 and cyclic electron flow which only produces ATP (Alric et al.,

2010). ATP is generally used for cellular division and carbon assimilation occurring under normal growth conditions such as in TAP media. However, in TAP-S (Fig 4.4b) there was a significant increase ($p < 0.05$) in NADPH concentration from 5.11 $x10^{-5}$ μmol to 1.86 $x10^{-4}$ μmol. During this linear electron flow, the hydrogen production phase (day 3-8) there was a 73 % increase in NADPH. Subsequently, the NADPH concentration decreased from 1.86 $x10^{-4}$ μmol to 1.53 $x10^{-4}$ μmol (18%) in the post hydrogen production phase (day 9-10), inferring a shift to cyclic electron flow through PS II. When DCMU was used to induce the non functionality of PS II (in TAP) (Fig 4.4C), a significant increase ($p < 0.05$) in the NADPH concentration was observed from 5.29 $x10^{-5}$ μmol to 2.67 x 10^{-4} μmol (80%). Throughout this 10 day period, a decrease in biomass was evident as ATP synthesis decreased during this linear electron flow.

It is well known that TAP-S media induces hydrogen production in *Chlamydomonas* (Ghirardi, 2006, Tolstygina et al., 2009, McKinlay and Harwood, 2010), however, DCMU is also known to induce hydrogen production by disabling PS II (Fouchard et al., 2005, Oncel, 2013). The corresponding increase in NADPH in both TAP-S (Fig 4.4B) and TAP + DCMU (Fig 4.4C) shows that NAPDH increases during hydrogen production. NADPH is known to carry H^+ to synthesise glucose and other compounds. ATP can be produced without net NADPH generation through cyclic electron flow (CEF) around PSI (Finazzi, 2005). It has been found that an increase in CEF induces an increase in NADPH hydrogenase compounds (Ma and Mi, 2008). CEF may therefore be directly related to hydrogen production, explaining the source of electrons for hydrogen production. NADPH may therefore acts as a carrier molecule during hydrogen production.
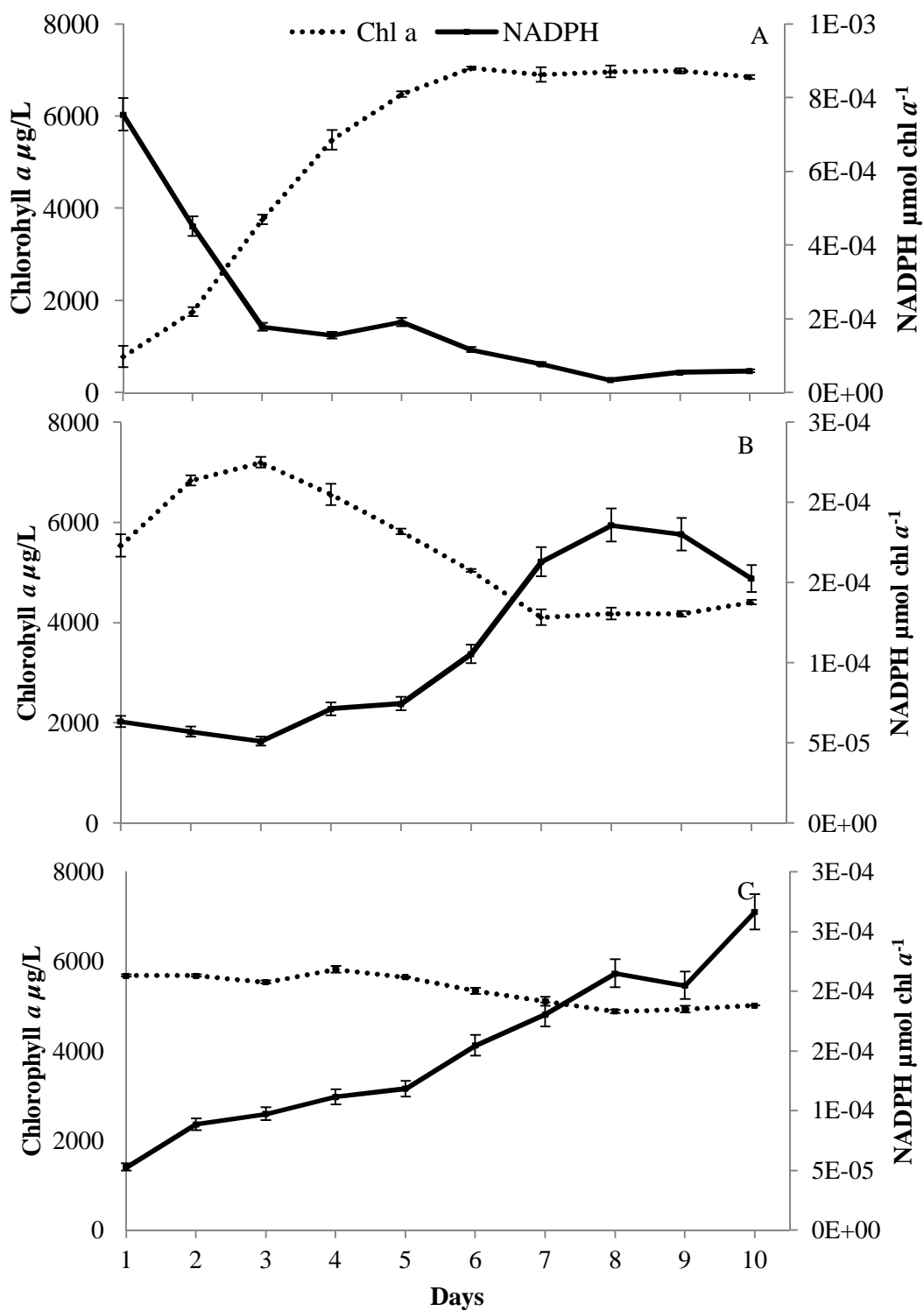
Figure 4.4: NADPH concentration (μmol chl a^{-1}) compared to chlorophyll a concentration (μg/L). *Chlamydomonas* cultured in TAP media (A), in TAP-S media (B) and in TAP with the addition of DCMU (C) compared to the respective chlorophyll a values (Values are averages ± SD).

Maximum chlorophyll fluorescence voltages were recorded on a daily basis (Fig 4.5). In the control culture (TAP) the Fluo was found to decrease initially and then maintained a stable fluorescence value of approximately 2×10^{-5} V. The chlorophyll fluorescence voltages in TAP-S cultures show that over time the maximum fluorescence increases significantly from 1.77×10^{-5} V to 5.20×10^{-5} V. Due to sulphur depletion, the partial and reversible inhibition of photosystem II takes place (Kosourov et al., 2002). Electrons are therefore unable to flow into the electron transport chain and are emitted as thermal energy and fluorescence as seen in Fig 4.5. Cultures in TAP + DCMU decreased in chlorophyll fluorescence by 29% over five days where it increased by 40% by day ten. This increase is due to the inactivation of photosystem II and the subsequent increase in thermal energy and emitted fluorescence. In other studies this rise in fluorescence has been found to reflect the gradual increase in the reduction state of the plastoquinone pool (Mus et al., 2005). These extra reductants can reflect increased cyclic electron transport or an accumulation of NADPH in the chloroplast (Mathews and Wang, 2009). NADPH has been thought to accumulate as it is not being used for anabolic processes due to the down-regulation caused by sulphur depletion (Cardol et al., 2011). This confirms the corresponding increase in NADPH and chlorophyll fluorescence during hydrogen production.
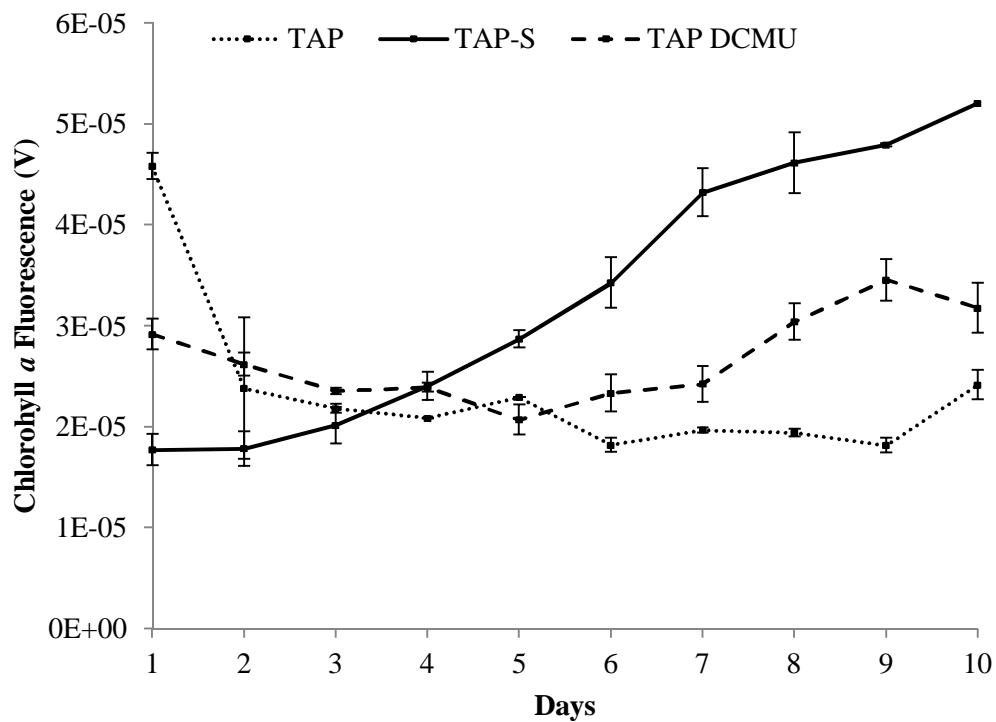
Figure 4.5: Chlorophyll Fluorescence voltages depicting maximum fluorescence over the 10 day period (Values are averages ± SD).

A significant direct correlation (r = 0.941, p < 0.01) was found between collected biohydrogen and NADPH concentration for the ten day experimental period (Fig 4.6). This shows that NADPH has an active role as a carrier molecule during the hydrogen production process.
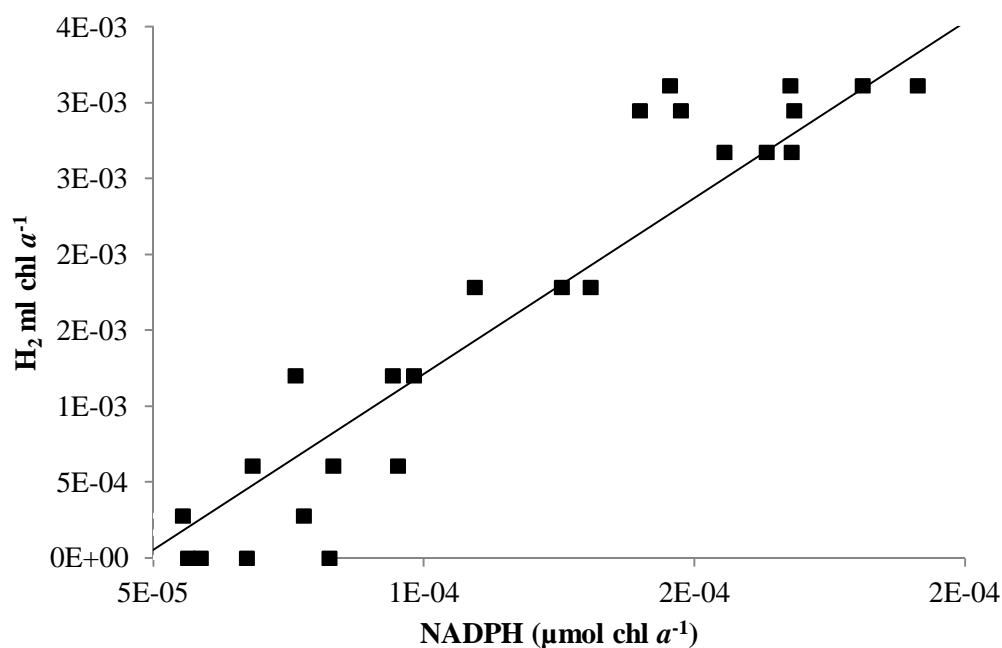
Figure 4.6: Correlation of cumulative hydrogen production vs. NADPH concentration in *Chlamydomonas* cultured in TAP-S media for duration of 10 days.

Chlamydomonas cells were cultured in 16% leachate prior to being induced to produce hydrogen (White et al., 2013). This increased the hydrogen yield by 37%. The addition of leachate initially doubled the amount of NADPH present from 6.34×10^{-5} μmol to 1.23×10^{-4} μmol (Fig 4.7). The greatest increase was evident during the hydrogen production phase (days 2-9), having a maximum increase of 70% compared to cells cultured without leachate The increase in NADPH is probably due to the increase in hydrogen production. Because NADPH was found to be directly correlated with hydrogen, a proportional increase in NADPH would be expected from higher hydrogen yields.
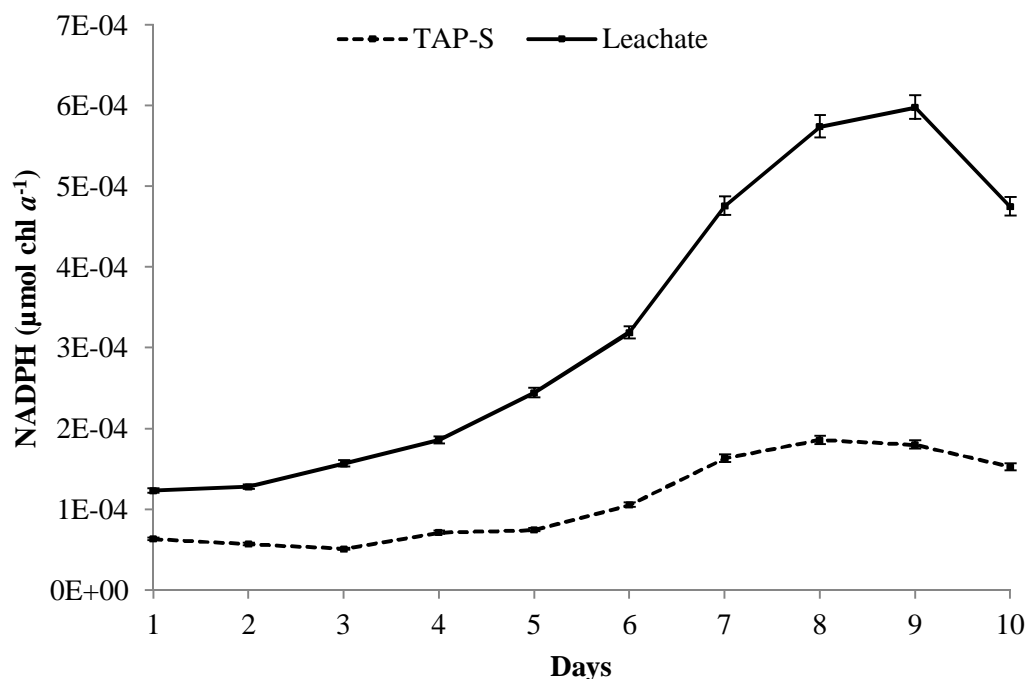
Figure 4.7: NADPH concentrations (μmol chl a^{-1}) in *Chlamydomonas* cells cultured in TAP + 16% leachate and induced to produce hydrogen in TAP-S (solid line) and cells cultured in TAP and induced to produce hydrogen in TAP-S (dotted line) (values are averages ± SD).

During the same time period maximum chlorophyll *a* fluorescence was found to be significantly reduced by between 50 - 70% (Fig 4.8). This shows less energy was emitted as fluorescence and more was channelled along the electron transport chain. This should result in a greater hydrogen yield which has been previously shown (White et al., 2013).A direct correlation ($r = 0.929$, $p < 0.01$) between NADPH concentration and hydrogen was found in cells initially cultured with 16% leachate (Fig 4.9). The corresponding increase in NADPH in both TAP-S and cells with leachate shows that NADPH must act as a carrier molecule during the hydrogen production process (Cardol et al., 2011).
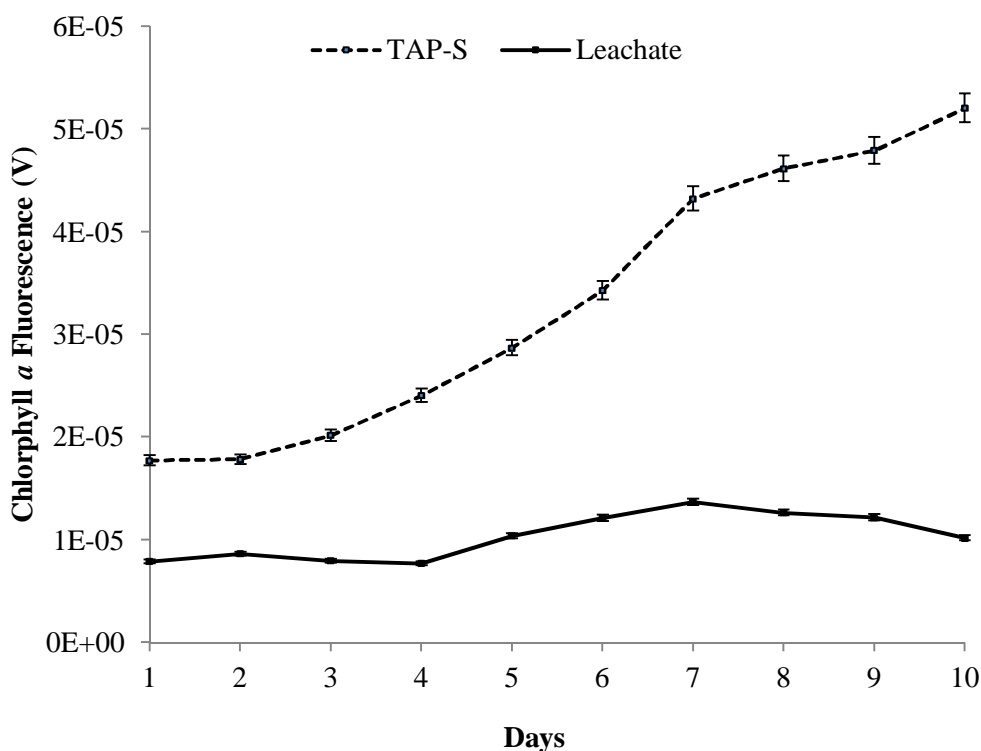
Figure 4.8: Chlorophyll Fluorescence voltages depicting maximum fluorescence over the 10 day period in cells cultured in TAP+16% leachate (solid line) and cells cultured in TAP (dotted line) (Values are averages ± SD).

It has been thought that the production of hydrogen is an effective way of releasing excess reductants from the cell which were generated under anaerobic conditions (Kosourov et al., 2007, Cardol et al., 2011). These reductants are provided to PSI either through the dicarboxylic acid shuttle or the NADPH-plastoquinone oxido-reductase enzyme (Mus et al., 2007, Mignolet et al., 2012). In this pathway NADPH acts as a carrier molecule which will be up-regulated during hydrogen production either on the acceptor side of PSI (Kosourov et al., 2007), or on the acceptor side of the FeFe-hydrogenase enzyme via ferredoxin (Bukhov et al., 2001, Smith et al., 2012, Sakurai et al., 2013). NADPH should be up-regulated during hydrogen production irrespective which pathway is used, or if both are active.
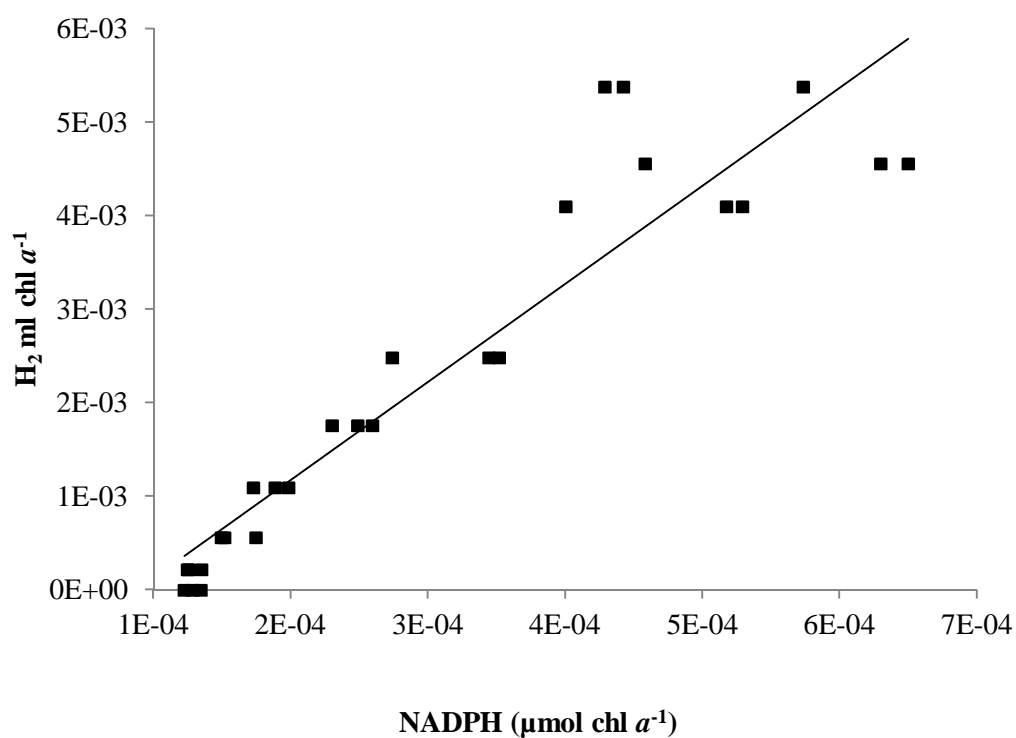
Figure 4.9: Correlation of cumulative hydrogen production vs. NADPH concentration in *Chlamydomonas* cultured in TAP+16 % leachate and subsequently TAP-S media for hydrogen induction.

4.4 Conclusions

NADPH concentrations were found to correlate directly (r = 0.941) with hydrogen production induced by sulphur depletion in *Chlamydomonas reinhardtii*. Increasing the hydrogen yields by 37% using leachate resulted in an increase in NADPH values of 50-70%. NADPH values were also shown to correlate directly (r = 0.929) with hydrogen when the leachate supplemented media was used. The correlation of NADPH to hydrogen provides evidence that NADPH has a pivotal role as a carrier molecule during hydrogen production. This may either take place via the NADPH-plastoquinone oxido-reductase enzyme before PSI or via ferredoxin before FeFe-hydrogenase. NADPH fluorescence was calibrated using *β*-NADPH to allow for conversion of raw fluorescence to concentration using a Dual PAM fluorometer. NADPH was shown to be a reliable indicator of hydrogen production from *Chlamydomonas*. Future studies will investigate up-regulating NADPH in an attempt to increase hydrogen yields and process feasibility.

CHAPTER FIVE

Modular Pilot Scale Biohydrogen Bioprocessing System

Abstract

This study investigated the conceptual design and process of a Modular Pilot Scale Biohydrogen Processing Plant based on laboratory scale data (Thesis chapters 2-4). A two-phase modular system was designed where in phase 1 *Chlamydomonas* will be produced continuously in an 86 m^3 reactor at a concentration of 2.5g/L. The biomass will be harvested and cells induced to produce hydrogen gas in a 72 m^3 modular reactor system during phase 2. The reactors will contain specialized monitoring probes to record physico-chemical and physiological parameters, using an YSI multi probe and a Pulse Amplitude Modulated Fluorometer. These probes connect to an online SCADA system for accurate on/off-site monitoring. Total extrapolated hydrogen yield was predicted to reach ±5584.77 L per day produced by the cycling and off-setting of the 5 modules. A 300 W hydrogen fuel cell requiring 5148 L gas to operate for 22 hours per day will be used to produce electricity to be stored in 43 V NiMH batteries. Advances in the technology of system components will increase the process feasibility producing a hydrogen economy for the future.

Key words: Pilot scale; Biohydrogen, Bioprocessing; *Chlamydomonas reinhardtii*, Hydrogen Fuel Cell

5.1 Introduction

Depleting sources of fossil fuels, increasing greenhouse gas emissions coupled with a booming global population paints a bleak image of planet earth and its future energy and survival of its species. The increasing demand for energy has become a global challenge for the continuation of our modern living conditions. Science, engineering and technology have now focused on alternative renewable energy sources reducing further damage to the environment. These energy sources include hydrogen which is an ideal energy vector and yields pure water as an end-product (Show et al., 2012). Hydrogen gas has been proposed as the ultimate transport fuel for vehicles and vessels and enables the use of highly efficient fuel cells to convert chemical energy to electricity (Forsberg, 2007). Current technology for hydrogen production utilizes fossil fuels, thermochemical processes or electrolysis of water and methane steam reformation (Levin et al., 2004). Hydrogen has the potential to be produced via biological means (Laurinavichene et al., 2006, Oncel and Sukan, 2011). Biologically produced hydrogen technologies include direct biophotolysis, indirect biophotolysis, photo fermentation, dark fermentation and then integrated systems incorporating both fermentation and photosynthetic approaches (Oncel and Sukan, 2011, Ferreira et al., 2013a, Oncel and Sabankay, 2012). Biohydrogen has attracted global attention by many companies such as Ford, Opel, Honda and Toyota as it may become a continuous, low cost and renewable source of clean energy (Daimler et al., 2009, Show et al., 2012).

Microalgae, as a photosynthetic organism with high light conversion efficiencies, have shown great potential to produce hydrogen through biophotolysis(Rosner and Wagner, 2012). The biophotolysis of water, normally carried out by microalgae (*Chlamydomonas, Scenedesmus, Chlorella* (Gaffron and Rubin, 1942, Oncel and Sukan, 2011, Florin et al., 2001)) and *Cyanobacteria* (Srisangan et al., 2011), is the most desirable route as only water and light are utilised (Kruse et al., 2005). *Chlamydomonas* is induced to produce hydrogen through sulphur depletion. Within 24 hours of sulphur depletion, water oxidation and subsequent oxygen production decline below the respiration level resulting in anaerobic conditions (Ghirardi, 2006) . Under these conditions electrons are driven via reduced ferredoxin, to the FeFe-hydrogenase enzyme generating photobiological H_2 (Florin et al., 2001).

Persistent problems with this route have been identified such as inhibition of hydrogenase by oxygen and low photochemical efficiency (Oh et al., 2011). Due to the intricate regulatory

network of physiological processes in *Chlamydomonas*, identifying the optimal production strategy and design is impossible without understanding the complex interplay of all the cellular processes (Rupprecht, 2009). The interactive nature of culture parameters (nutrients, temperature, pH, oxygen, mixing and light) also makes the design of a photobioreactor a complex procedure (Oncel and Sabankay, 2012, Fouchard et al., 2008). Bottlenecks in this process are the scale up and the design of photo bioreactors applicable to commercial scale biohydrogen production and low hydrogen yields (Pulz, 2001, Levin et al., 2004, Rashid et al., 2013). Large scale production has also found challenges relating to gas exchange, light delivery, land and water availability as well as the harvesting procedures (Christenson and Sims, 2011).

Research into the use of *Chlamydomonas reinhardtii* has tackled these problems including hydrogenase inhibition (Ma and Mi, 2008, Smith et al., 2012, Sybirna et al., 2013), metabolic engineering (Mathews and Wang, 2009, Oh et al., 2011), genetic engineering strategies (Srisangan et al., 2011), and further understanding of the physiological changes during hydrogen production (Chochois et al., 2010, Schottler et al., 2011, Hoshino et al., 2012). Improved design structure in large scaled up systems has also assisted in improving processing feasibility. Continued research into the field has resulted in increasing hydrogen yields and decreasing processing costs allowing for the large scale production of biohydrogen from *Chlamydomonas* (Melis, 2007).

The key to large scale production is to have a two stage system where biomass cultivation is maximised in the first stage and then photosystem II is down-regulated and photosystem I is up-regulated in the second stage (Chapter 3). This allows for optimum growth conditions to be utilised for maximum biomass production, followed by conditions conducive to optimise hydrogen synthesis.

With the rapid evolution of technology, each component of a large scale plant is constantly being researched and improved. This includes research from increasing algal growth to optimising fuel cell efficiency (Hassan et al., 2014) to improving hydrogen storage abilities. Previous studies have shown the use of landfill leachate to increase *Chlamydomonas* biomass production (White et al., 2013). This concept can be incorporated into reactor designs that will increase yields to a greater extent than what was previously thought. Research into understanding the different functionality of photosystem I and photosystem II has altered reactor designs to maximise on the dominant role of PS I during hydrogen

production (Chapter 3). New indicators of hydrogen production have been developed making the monitoring and measuring of hydrogen synthesis easier and more reliant (Chapter 4). This research and continued research continually improve the feasibility of biohydrogen production and make biohydrogen gas the fuel of the future.

The aim of this study is to conceptualise a design for a two stage pilot-scale automated biohydrogen production facility using *Chlamydomonas reinhardtii*.

5.2 Design

5.2.1 Location

Municipal landfills generally have large land available for waste, which would be a suitable location for the construction of a pilot scale biohydrogen plant. The nutrient rich leachate would be readily available onsite, reducing leachate transportation costs. The subtropical climatic conditions in Durban, KwaZulu Natal, South Africa are favourable for microalgal cultivation having adequate PAR and appropriate ambient temperatures. This adequate PAR refers to light levels capable of allowing for maximum electron transport rate, (i.e. on average above 500 μmol m^{-2}s^{-1}.

5.2.2 Biohydrogen Processing System Design

This system will produce enough hydrogen gas to provide a continuous 300 W supply of energy. The pilot scale biohydrogen production plant will be comprised of a two phase system (Fig 5.1). Phase 1 will consist of a continuous growth reactor used to produce *Chlamydomonas* biomass (Fig 5.1A). Automated harvesting and washing will remove extracellular sulphur (Fig 5.1B). In phase 2, an anaerobic environment conducive to hydrogen production from *Chlamydomonas* will be created (Fig 5.1C). This hydrogen will be collected and dehumidified prior to being compressed into storage tanks for use. These cylinders will be connected to a 300 W Fuel Cell stack which will provide renewable electricity with only water as the by-product (Fig 5.1D).
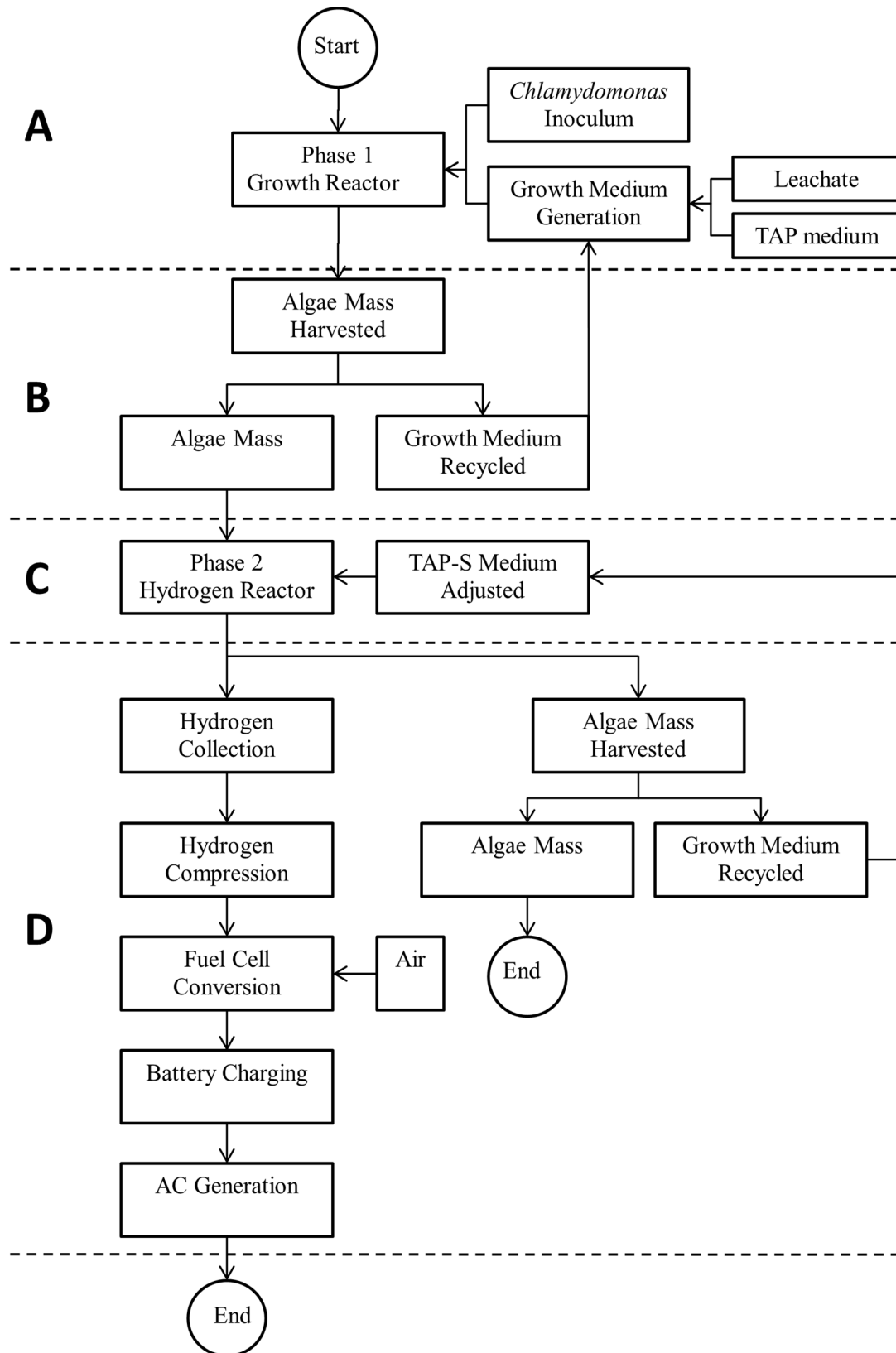
Figure 5.1: System Design of the Modular Pilot Scale Biohydrogen Processing Plant

5.2.3 Continuous *Chlamydomonas* Growth Reactor Design (Phase 1)

Phase 1 of the design will be the continuous microalgal production reactor (Fig 5.2). This system will consist of 90 tanks using the specifications in Table 5.1. *Chlamydomonas* will be cultured on a continuous basis providing biomass daily. This system will use TAP media supplemented with landfill leachate as previously described . The microalgae concentration will be kept at 2.5 g/L.

Table 5.1: Specifications for the Modular *Chlamydomonas* Growth Reactor (Phase 1)

Parameter		Specification
Tank	Radius (m)	0.35
	Length (m)	2.5
	Volume (m^3)	0.962
	Biomass per litre (g)	2.5
	Biomass per tank (kg)	2.41
	Leachate per tank (L)	153.94
Total		
	Volume (m^3)	86.59
	Leachate (m^3)	13.85
	Biomass (kg)	216.9

Figure 5.2: Continuous *Chlamydomonas* Growth Reactor

5.2.3.1 Lighting

The photobioreactor will have a dual light source consisting of natural sunlight and an internal light supply from blue Light Emitting Diodes (LED) (Fig 5.2). LED technology has advantages of being highly efficient and reliable having a long lifetime and very low power consumption (Fu et al., 2012). The internal light source will be adjustable to produce optimum light levels depending on culture turbidity and ambient sunlight (unfavourable weather conditions) (Giannelli and Torzillo, 2012).

5.2.3.2 Aeration

A high pressure air pump will provide vertical aeration from the reactor base to 1) increase CO_2, 2) allow for mixing of the microalgae to prevent settling of cells and 3) remove attached biomass from the central internal LED light source (Fig 5.2). This air pump will have the option of adding pressurised CO_2 gas to increase biomass. Flue gas may also be used as a supplemented carbon source. These however will be on an add-on basis and not included in this initial photobioreactor design.

5.2.3.3 Probes for Online Monitoring

Probes used in the continuous cultivation photobioreactor will include the following:

- A YSI Legacy water Quality Data Logger (YSI, USA) where the specifications can be seen in Table 5.2

- Pulse Amplitude Modulated (PAM) Fluorometry to monitor electron flow in both photosystem I and II where the specifications can be seen in Table 5.3.

These systems will be connected to the online SCADA system for continuous monitoring.

Table 5.2: Performance Specification of the YSI Legacy Data Logger

Parameter	Range	Resolution	Accuracy
Dissolved Oxygen	0 – 50 mg/L	0.01mg/L	0.2mg/L
Conductivity	0 – 100 mS/cm	0.1 mS/cm	0.5% of reading
Temperature	-5°C – 50 °C	0.01 °C	0.15 °C
pH	0 – 14 units	0.01 units	0.2 units
Salinity	0 – 70 ppt	0.01 ppt	0.1 ppt
Chlorine	0 – 3 mg/L	0.01 mg/L	0.05mg/L
Nitrate	0 – 200 mg/L-N	0.1 mg/L-N	2mg/L
Ammonium	0 – 200 mg/L-N	0.1 mg/L-N	2mg/L
Chloride	0 – 1000 mg/L	0.1 mg/L	5 mg/L
Turbidity	0 – 1000 NTU	0.1 NTU	0.3 NTU
Chlorophyll	0 – 400 μg/L	0.1 μg/L	1 μg/L
Cyanobacteria	0 – 280 000 cells/mL	220 cells/mL	-
PAR	400 – 700 nm	±5 %	-

Table 5.3: Pulse Amplitude Modulated (PAM) Fluorometer Specifications

Pulse Amplitude Modulated (PAM) Fluorometer Specifications	
Version	Dual-PAM 100
Communication	PC Interface with USB 1.0 and 2.0
User Interface	Windows with Dual PAM software
Power and Control Unit	DUAL-C
Micro controller	2x AVR-RISC (8MHz)
Power Supply	Rechargeable Lead Acid battery 12V 2Ah
Power Consumption	Basic Operation 160 mA
Dimensions	31 x 16 x 33.5 cm
Weight	20 kg
Measuring Head with Emitter DUAL-E	Measuring Light (P700) P700 dual wavelength emitter Sample wavelength 830 nm Reference wavelength 870 nm Actinic Light Far-red LED lamp 720 nm Chip on board LED array 635 nm Max 2000 μmol m^{-2} s^{-1} PAR. Saturating light max 200 000 μmol m^{-2} s^{-1} PAR. Adjustable 5-50μs
Measuring Head with Detector DUAL-DB (Blue) or DUAL-DR (Red)	Measuring Light (Fluo) Fluorescence emitter 460 (DUAL-DB) Fluorescence emitter 620 (DUAL-DR) Actinic Light Blue LED lamp: 460 nm for continuous actinic illumination Maximal 700 μmol m^{-2} s^{-1} PAR. Chip-on-board LED array 635 nm Signal detection PIN photodiode with special pulse

	preamplifier for measuring P700 and fluorescence changes with maximal time resolution of 30 μs.
Computer Requirements	1 free USB socket
	500 or more MB RAM
	Windows XP or Vista

5.2.4   Hydrogen Production Reactor (Phase 2)

Phase 2 will consist of the Hydrogen Production Reactor System (Fig 5.3). This will consist of 75 tanks within 5 modules according to the specifications set out in Table 5.2. Harvested algae will be added to Phase 2 at a concentration of 3g/L (data obtained from chapter 2). Hydrogen will be produced in a batch system every 10 days. Two days will consist of harvesting, inoculating tanks and allowing for anaerobic phase to be reached. Hydrogen will then be produced for the remaining eight days. Hydrogen yields were calculated on 565ml of gas produced per litre for a batch system using sulphur depletion (Kosourov et al., 2012). As leachate has been found to increase hydrogen yields by 37% (White et al., 2013), this value was increased to an extrapolated value of 774 ml per litre and used as the hydrogen yield for projected calculations.

Table 5.4: The specifications for the Hydrogen Production Plant (Phase 2)

Modular Design of Hydrogen Production Plant	
Parameter	**Specification**
Tank	
Radius (m)	0.35
Length (m)	2.5
Volume (m^3)	0.962
Biomass per litre (g)	3
Biomass per tank (kg)	2.89
Hydrogen per day per litre (mL)	96.75
Hydrogen per day per tank (L)	93.08
Hydrogen per 10 day 10 day batch (L)	774.72
Module	
Tanks per module	15
Volume per module (m^3)	14.43
Hydrogen per day per module (L)	1396.19
Hydrogen per module per 10 day batch (L)	11169.54
Total	
Total number of tanks	75
Number of modules	5
Total Volume (m^3)	72.158
Total Biomass (kg)	216.48
Total Hydrogen per day (L)	6980.965
Total Hydrogen per 10 day batch (L)	55847.72
Continual Hydrogen production (L)	5584.771

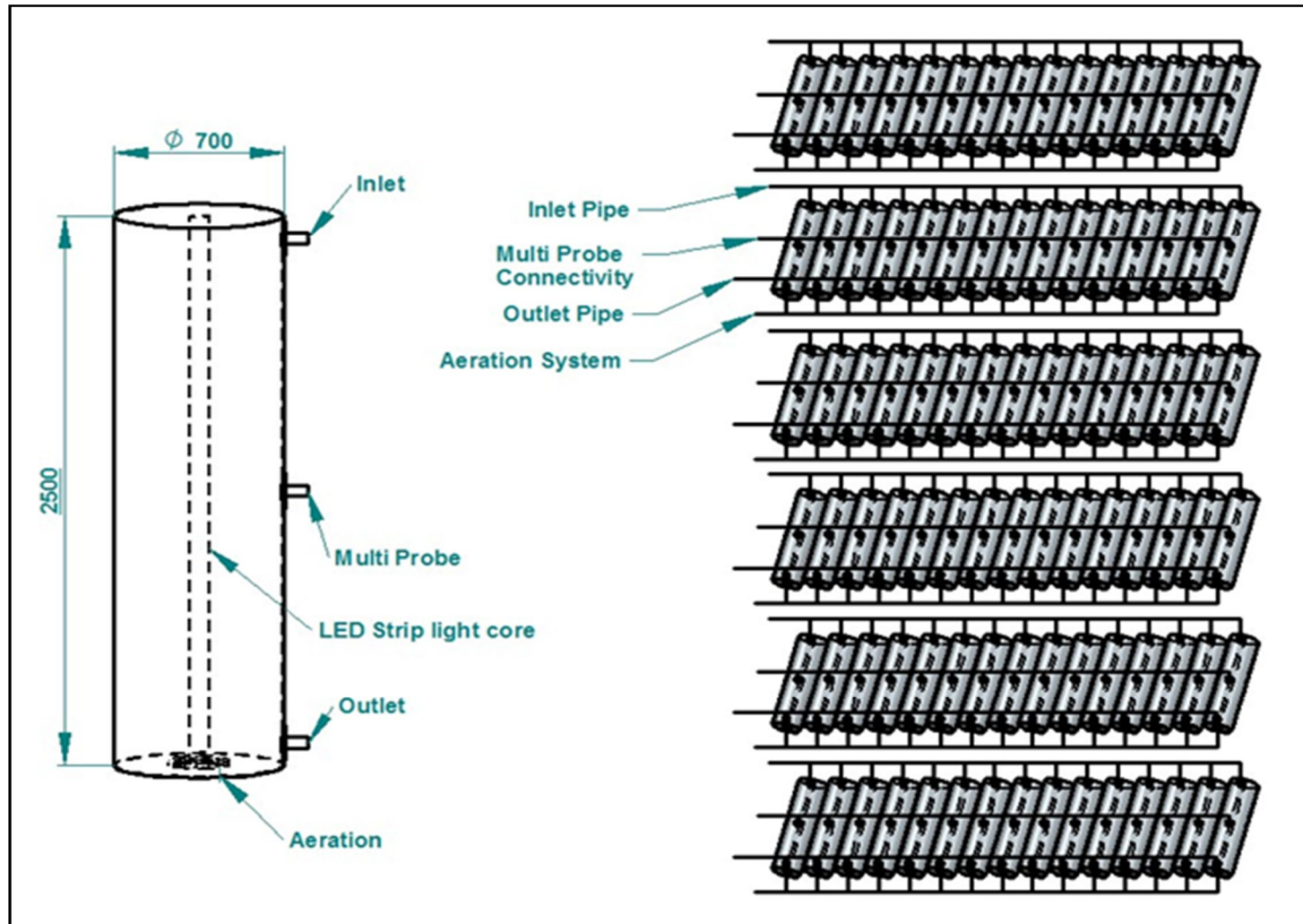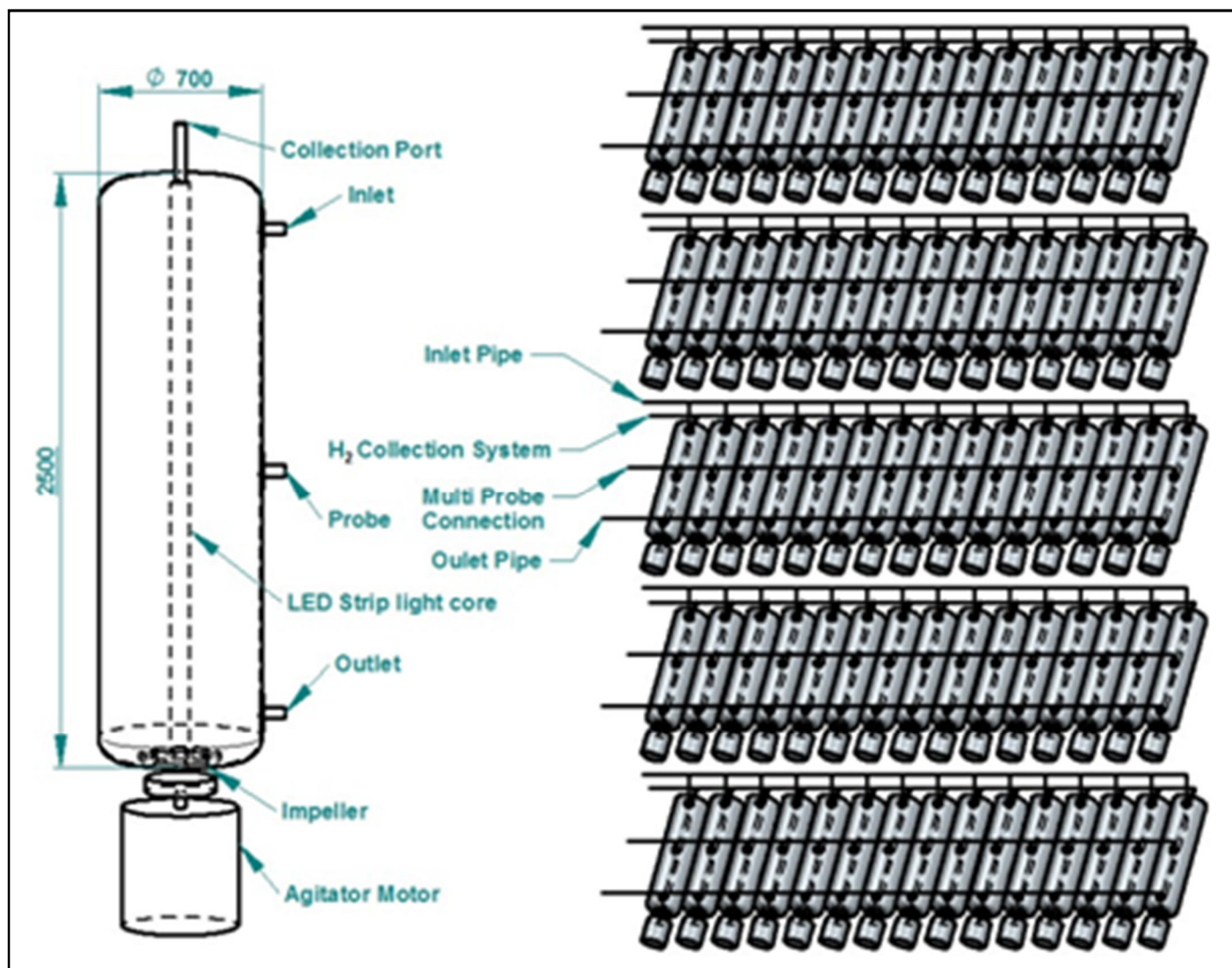**Figure 5.3: Biohydrogen Production Reactor**

5.2.4.1 Lighting

The photobioreactor will have a dual light source consisting of natural sunlight (~ 2000 μmol m^{-2}s^{-1}) and an internal light supply from blue Light Emitting Diodes (LED) (Fig 5.3). The internal source will be adjustable to produce optimum light levels depending on culture turbidity and ambient sunlight (in case of unfavourable weather conditions) (Giannelli and Torzillo, 2012).

5.2.4.2 Mixing

The mixing speed is regulated electronically to create conditions conducive to hydrogen production in an anaerobic environment. For this purpose an impeller with an agitator motor will be used to mix the microalgae, allowing adequate PAR to reach the microalgae and to prevent settling (Fig 5.3).

5.2.4.3 Probes for Online Monitoring

Probes used in the continuous cultivation photobioreactor will include the following:
- A YSI Legacy Water Quality Data Logger (YSI, USA) where the specifications can be seen in Table 5.2
- Pulse Amplitude Modulated (PAM) Fluorometry to monitor electron flow in both photosystem I and II where the specifications can be seen in Table 5.3
- A hydrogen meter (specifications in Table 5.5)

These systems will be connected to the online SCADA system for continuous monitoring.

Table 5.5: Horiba Scientific Hydrogen Meter Specifications

Parameters	Values
Manufacturer	Horiba Scientific
Model Type	EMGA – 921 Hydrogen analyser
Measurement range	0 – 0.25%
Sensitivity	0.001 ppm
Sample weight	1.0 ± 0.1 g
Detector	Thermal conductivity detector

5.2.5   Hydrogen Collection System

Teflon tubing will be used to collect the hydrogen gas from each individual reactor and transport it to the main collection chamber. Teflon tubing is the preferred tubing as it has the lowest gas permeability when compared to conventional polytetrafluoroethylene (PTFE) tubing. Teflon has a value of 220 000 cB compared to 980 cB of PTFE. (cB = centriBarrer = 10^{-8} cm^3 H$_2$ cm^2 cm^{-3}s^{-1} mmHg^{-1}).The gas will be temporarily stored until it can be compressed. The hydrogen compression system will be a Pressure Products Industries (PPI) diaphragm compressor that is fully installed as a complete system. This includes the compressor, control panel, transformers, motor and switches, safety discharge switches, pressure gauges and a fully controllable programmed PLC system. Specifications of the compressor can be seen in Table 5.6.

Table 5.6: PPI Hydrogen Compression System Specifications

Parameters	Values
Manufacturer	PPI
System Type	Diaphragm compressor 4000
Number of stages	1
Max Discharge pressure	103.5 mPa
Max Displacement at 400rpm	85 m^3 / hr
Standard Drive	7.5 kw
Corrosion resistance	300 series stainless steel
Control unit	PLC

5.2.6   Harvesting Procedure

The harvesting of microalgal biomass will be an automated procedure using the Evodos Type 25 settling system (Evodos, Netherlands). This model has a maximum flow rate of 4000 L per hour positioning it in the midrange of available dewatering systems. This system uses Evodos Spiral Plate Technology allowing for high separation effectiveness with a minimal energy demand (Fig 5.4). This highly effective settling process uses only 3000 G's resulting in a low energy demand on the system. Harvested cells are in a paste form containing only 2% water and have been found to be generally free of bacteria and free of cellular damage.

Once harvesting is initiated on the SCADA system control unit, the pump will feed fluid into the cylindrical drum where it is accelerated to 3000 G. The solids will settle into the Spiral Plate Technology vanes. The remaining liquid is removed and stored for reuse. When enough solids have formed in the drum vanes the discharge process will initiate. Here the drum shell is lifted freeing the vanes. The rotor is run at 800 rpm swinging off the algae paste onto the splash screen where it is collected on a conveyor. After the discharge cycle the drum shell is returned to its working position and the unit will start a new run. If the continuous growing system was harvested, the algae paste will be subjected to a washing cycle (mixed with water and harvested again to remove sulphur) before been used for hydrogen production. If the hydrogen reactors were harvested, the resulting biomass will be sold as a fertilizer. All control parameters can be controlled from the main control system of the Microalgae Production System (Fig 5.1).

Figure 5.4: Evodos Algal dewatering system depicting (clockwise) the type 25 unit, the spiral technology plate with the algae paste and harvested algae paste with a 20% liquid content
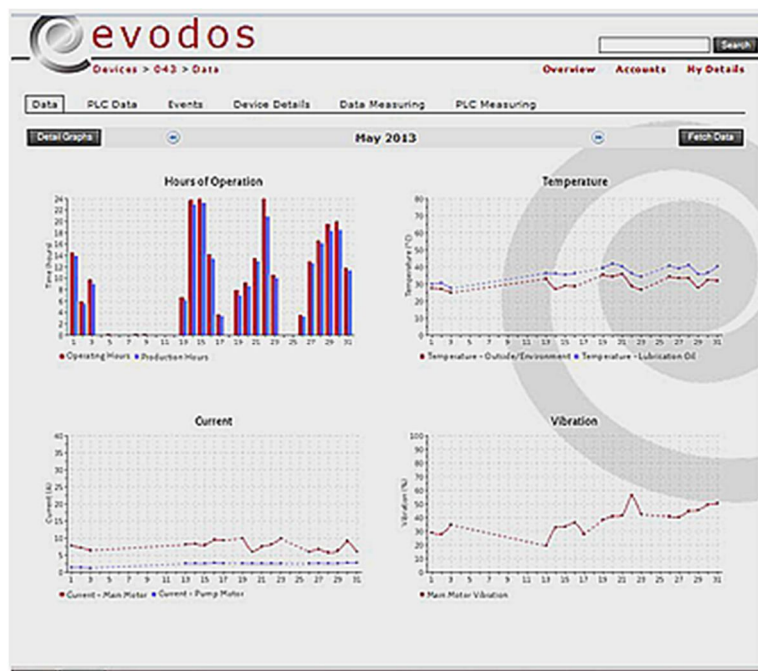
Figure 5.5: Monitoring system of the Evodos Type 25 Dewatering system will be available to monitor from the main control application for the entire Biohydrogen Production System.

Table 5.7: Evodos Type 25 Harvester Specifications

Evodos Type 25 Harvester Specifications	
Type of Setup	Evodos 25
Operating Capacity	250 – 4000 L/hr
Volume Solids per cycle	15 Litres
Maximum Discharges per hour	5
Dimensions	2,179 m x 1,203 m x 1,206 m
Weight	1600 kg
Maximum Fluid Temperature	95°C (add on accessory)
Normal Fluid Temperature	5°C – 45°C
Water Requirements	Fresh water or Sea water
PLC	Siemens PLC

5.2.7   Online SCADA system

In order to automate the algal photobioreactor and minimise human intervention, there is a need to develop a SCADA system to monitor the plant. Supervisory Control and Data Acquisition (SCADA) systems are widely used in industry for supervisory control of industrial processes (Ozdemir and Karacor, 2006). These systems generally use personal computers or notebooks to track data and present the information in a display type interface. This type of interface will be used to monitor the photobioreactor operational parameters. Wireless communication will be used between a mobile phone and the SCADA server will be used allowing for off-site parameter modification, reducing costs and increasing productivity (Ozdemir and Karacor, 2006). General Packet Radio Service (GPRS) and Wireless Application Protocol (WAP) will be used to wirelessly transmit the real-time data (Ozdemir and Karacor, 2006). The SCADA system will be user friendly and easily able to integrate with additional devices for the photobioreactor.

A PLC (Programmable Logic Controller) will be used for the internal storage of instructions for implementing the functions such as logic, sequencing, timing, counting and arithmetic to control the various photobioreactor through digital and analog input/output modules (Morsi and El-Din, 2013). Information will be collected via a Remote Terminal Unit (RTU), PLC

and Intelligent Electronic Devices (IED) and transferring it back to the central site where analysis will be carried out and information displayed on the operator screens.

5.2.8   Hydrogen Storage

Due to the low volumetric energy density compared to fossil fuels, the storage of hydrogen gas proves to be a challenge (Di Profio et al., 2009). There are three methods in which hydrogen gas can be stored effectively namely; cryogenic liquid hydrogen, compressed hydrogen gas and metal hydride absorption (Ananthachar and Duffy, 2005, Aceves et al., 2006). Compressed gas has become a viable technology due to the improvements in high tensile strength composite fibres used in tank design and low infrastructure impact (Zhevago et al., 2010). Hydrogen gas can be stored at high pressures (10 000 psi) and research is increasing this even further to currently 29 000 psi (Aceves et al., 2006). Research has shown that 12.3 m^3 is required to store 1kg of hydrogen at standard temperature and pressure. Compressing to 350 bars decreases storage volume by 99.6% (Hosseini et al., 2012). It is for this reason that the hydrogen produced from Phase 2 will be compressed and stored in gas cylinders before being connected to the Fuel Cell.

5.2.9   Hydrogen Fuel Cell for Electricity Generation

Compared with other fuel cells types, Polymer Electrolyte Membrane (PEM) fuel cells have shown promising results with advantages such as low temperature, high power density, fast response and zero greenhouse gas emissions (Li et al., 2009). With the cost decrease of commercially produced hydrogen and advances in technology, PEM fuel cells show the most optimistic prospect for moving into large scale production and commercialization (Hou et al., 2014, da Fonseca et al., 2014). It is for this purpose that an H-series (PEM) fuel cell stack designed by Horizon (Horizon Fuel Cell Technologies, Singapore) will be used (Table 5.8). This is an efficient, reliable system that is lightweight and air-cooled and self-humidified. The system will have a power rating of 300W and be able to provide a voltage of 43V with a corresponding 7A current. The fuel cell will use dehumidified pure hydrogen gas with air. A flow rate of 3.9l/min of hydrogen gas is required to maintain maximum power. The H-300 PEM Fuel Cell system includes all connections and tubing, the electronic valves and control box, stack with blower, fuel cell switch and the SCU switch.

Table 5.8: Fuel Cell Specifications for the 300W PEM fuel cell stack from Horizon

Fuel Cell Specifications	
Type of Fuel Cell	PEM
Number of Cells	72
Power Rating	300 W
Performance	43V @ 7A
Hydrogen Supply Valve Voltage	12V
Purging Valve Voltage	12V
Blower Voltage	12V
Reactants	Hydrogen and Air
External Temperature	5-35°C
Maximum Stack Temperature	65°C
Composition	99.999% Dry Hydrogen
Humidification	Self humidified
Cooling	Air (integrated fan cooling)
Weight (with fan and casing)	2kg
Dimensions	32.4cm x 10.9 cm x 9.4 cm
Hydrogen Flow Rate	3.9 l/min of hydrogen gas
Start up Time	Immediate
Low Voltage Shut Down	36V
Over Current Shut Down	12A
Over Temperature Shut Down	65°C

5.2.10 Energy Storage

The resulting electricity derived from the fuel cell will be stored in 43V batteries for use later on. These batteries can then be used with the addition of a Direct Current (DC) to Alternating Current (AC) converter as well as a step up transformer to produce 220V electricity for household use.

Table 5.9: Battery Specifications

Parameter	Value
Manufacturer	AA Power Corp USA
Voltage	43.2 V
Amperage	20 Ah
Battery type	NiMH M battery Pack
Wiring	12.0" open end wire
Maximum Discharge Rate	4A
Dimensions	527 x 115 x 93 mm
Weight	14.3 kg
Protection	65°C thermostat
Heat shrink Capacity	864Wh

5.3 Operational Parameters

The continuous Growth Reactor will produce biomass on a continual basis as supposed to a batch system. The microalgae will remain in the logarithmic growth phase producing on average 927.20 ± 6.9 μg chl a $L^{-1}d^{-1}$ (White et al., 2013). TAP growth media supplemented with leachate will be used. All growth parameters will be monitored on a continual basis as they influence the overall productivity of the bioprocessing system.

Temperature has been widely reported to influence cellular physiological processes such as photosynthesis, respiration and nutrient assimilation because enzymes in these processes are dependent on optimum temperatures. Both, in the growth reactor and hydrogen producing reactor, temperature probes will provide online data to manage optimum cellular functioning. Ambient air temperatures (23 - 28 °C) and solar radiation will maintain reactor temperatures. When reactor temperatures rise above optimum, automatic switches activate a water sprinkler that sprays recycled water over the reactors to reduce the solar heating effect.

PAR (400-700 nm) levels will be monitored using multiple LI-COR LI-190 (LI-COR, USA) underwater spherical quantum sensors. The PAR diffuse attenuation coefficient (Kd) within the reactor will be determined according to the model: $Kd = \ln (I_{z2}/I_{z1})/z2\text{-}z1$ (Kirk, 2003). The internal LED lighting will compensate for attenuated light within the reactor.

Automated logical control will maintain optimum light environments for maximum growth and biomass yield.

Chlorophyll *a* concentrations are the best indicator of biomass which will be monitored by online chlorophyll probes pre-calibrated at lab scale with known concentrations of pure chl *a* extracts *Anacystis nidulans*. Data from this probe is analysed by the automated logical control system to determine growth rate which will be extrapolated to graphically identify the logarithmic, stationary and lag phases. Data from this probe will also indicate when to harvest and to maintain biomass levels at ± 2.5 g/L.

Ammonia, nitrite and nitrate levels will be monitored as this level directly correlates with biomass production. The addition of leachate will increase ammonia levels and therefore needs to be maintained within threshold levels. Monod's kinetic model is widely utilized to identify the limiting nutrient. According to the hyperbolic function ($u = \hat{U}$ [S/Ks+S]), where u = specific growth rate per day, $\hat{U}$ = maximum specific growth rate, S = nutrient concentration (mg/l) and Ks = half saturation coefficient (mg/l) which is the concentration at $u = \hat{U}/2$. Total N assimilation $= NH^3 + NO^{3-} + NO^{2-}$, and total P $= PO^{4+}$.

In the continuous growth reactor, the dissolved oxygen probe will be used to monitor photosynthesis and hence biomass production as oxygen is required for structural and metabolic processes. Dissolved oxygen readings will be compared to electron transport rates to confirm optimum photosynthesis to provide maximum biomass. It will also be used to confirm anaerobic phase in the hydrogen reactor with negligible oxygen readings.

An optimised pH value is crucial to microalgal growth due to the sensitivity of enzymes to pH. It is for this reason that the pH needs to be monitored and corrected to maintain optimum parameters. Landfill leachate generally has an alkaline nature and the continuous addition will alter the pH forming a basic pH. The addition of a weak acid will be able to control the basic nature of the leachate and maintain growth conditions conducive to cell division and growth.

The turbidity recordings will be used to assess the particulate nature of the biomass and when used in conjunction with the PAR sensor, assist in adjusting the light intensity to optimum levels. The turbidity recordings can also be used in conjunction with the chlorophyll a readings to assess growth.

Chlamydomonas reinhardtii is a fresh water microalgae that is sensitive to increases in salinity levels. The salinity probe will be used to maintain a salinity level conducive to optimum growth. The media components of TAP media uses chloride ions and the continuous nature of Phase 1 may allow for the accumulation of these salts. Leachate was also found to be rich in chloride ions thereby having the potential to affect the salinity. Fresh water can be used to dilute the salt to return the salinity to levels appropriate for *Chlamydomonas* cultivation.

The parameters obtained from PAM Fluorometry will be used for various purposes. In the growth reactor the electron transport rates will be used to monitor photosynthesis and maintain increased levels and therefore growth. It will be used in conjunction with the dissolved oxygen meter to confirm oxygen production and correlated electron transport. The maximum quantum efficiency values will be utilised to measure nutrient stress. Non photochemical quenching (NPQ) will be used to determine the amount of light that is being quenched and not used for photosynthesis, alluding to PAR levels that are too high. Rapid Light Curves will be used to find the PAR intensity that corresponds to the maximum electron transport rate. The use of PAM Fluorometry in the hydrogen reactor will be utilized to ensure a down-regulated PS II and to monitor up-regulation in PS I. Rapid light curves will be used to apply a light intensity conducive to PS I stimulation for increased hydrogen yields.

Biomass will be harvested every alternate day according to Fig 5.6. The calendar shows a 2 month process simulating the harvesting processing. This will allow for algae in the logarithmic growth phase to be harvested within a day and re-inoculated into the hydrogen production reactors. In this manner the algae paste will be exposed to minimal stress.

Sun	Mon	Tues	Wed	Thur	Fri	Sat
1	2	3	4	5	6	7
8	9	10	11	12	13	14
	Biomass	Module 1	Biomass	Module 2	Biomass	Module 3
15	16	17	18	19	20	21
Biomass	Module 4	Biomass	Module 5	Biomass	Module 1	Biomass
22	23	24	25	26	27	28
Module 2	Biomass	Module 3	Biomass	Module 4	Biomass	Module 5
29	30	31	1	2	3	4
Biomass	Module 1	Biomass	Module 2	Biomass	Module 3	Biomass
5	6	7	8	9	10	11
Module 4	Biomass	Module 5	Biomass	Module 1	Biomass	Module 2
12	13	14	15	16	17	18
Biomass	Module 3	Biomass	Module 4	Biomass	Module 5	Biomass
19	20	21	22	23	24	25
Module 1	Biomass	Module 2	Biomass	Module 3	Biomass	Module 4
26	27	28	29	30		
Biomass	Module 5	Biomass	Module 1	Biomass		

Figure 5.6: Calendar of daily harvesting processes, alternating between Biomass harvesting and Module harvesting

The harvesting of the biomass tanks will take place for 4.5 hours at 4000L per hour. This will dewater 18 m^3 of water and produce ± 45 kg algae from a concentration of ± 2.5 g/L (Table 5.10). The algal paste will then get mixed with 1 m^3 of water in a 1.5m^3 drum with a high pressure air pump aerating the mixture. This will resuspend the biomass and to remove residual sulphur. The biomass will then be dewatered and the process will be repeated twice. After the final dewatering process, the algae slurry or cake will get transferred into the TAP-S media at a concentration of 3g/L to induce the production of biohydrogen.

Table 5.10: Harvesting Parameter for Phase 1 and Phase 2 of the Biohydrogen Pilot Scale Processing Plant

	Phase 1 - Biomass	Phase 2 - Biohydrogen
Duration (hr)	4.5 + 1	4
Volume (m^3/hr)	4	4
Volume dewatered (m^3)	18	14.43
Sulphur Rinsing (m^3)	1 (x2)	-
Concentration (g/L)	2.5	3
Biomass (kg)	45	43

The biohydrogen plant will work in a batch system with modular cycling. Each module will be offset by two days. This will allow for continual hydrogen production from 4 modules at any given time and one module will either be in aerobic phase or will be undergoing harvesting as shown in Fig 5.7. This depicts the hydrogen production processing parameters for the five modules over a two month period. The red blocks represent when hydrogen will be produced, the grey blocks show harvesting and the green blocks show the aerobic phase. After the ten day cycle, the tanks will be harvested to produce dewatered algae paste. This paste will then be sold for further processing. The price of algae ranges from $1- $4 or R10-R40 per kg. If an average is taken the produced biomass can be sold for R25 per kg.

Figure 5.7 — The modular cycling of the Biohydrogen Phase 2 Plant.

Legend: A = Aerobic Phase (green), R = Hydrogen Production (red), H = Harvesting (grey), blank = no activity.

Month 1

Day	Module 1	Module 2	Module 3	Module 4	Module 5
1	A				
2	R				
3	R	A			
4	R	R			
5	R	R	A		
6	R	R	R		
7	R	R	R	A	
8	R	R	R	R	
9	R	R	R	R	A
10	H	R	R	R	R
11	A	R	R	R	R
12	R	H	R	R	R
13	R	A	R	R	R
14	R	R	H	R	R
15	R	R	A	R	R
16	R	R	R	H	R
17	R	R	R	A	R
18	R	R	R	R	H
19	R	R	R	R	A
20	H	R	R	R	R
21	A	R	R	R	R
22	R	H	R	R	R
23	R	A	R	R	R
24	R	R	H	R	R
25	R	R	A	R	R
26	R	R	R	H	R
27	R	R	R	A	R
28	R	R	R	R	H
29	R	R	R	R	A
30	H	R	R	R	R
31	A	R	R	R	R

Month 2

Day	Module 1	Module 2	Module 3	Module 4	Module 5
1	R	H	R	R	R
2	R	A	R	R	R
3	R	R	H	R	R
4	R	R	A	R	R
5	R	R	R	H	R
6	R	R	R	A	R
7	R	R	R	R	H
8	R	R	R	R	A
9	H	R	R	R	R
10	A	R	R	R	R
11	R	H	R	R	R
12	R	A	R	R	R
13	R	R	H	R	R
14	R	R	A	R	R
15	R	R	R	H	R
16	R	R	R	A	R
17	R	R	R	R	H
18	R	R	R	R	A
19	H	R	R	R	R
20	A	R	R	R	R
21	R	H	R	R	R
22	R	A	R	R	R
23	R	R	H	R	R
24	R	R	A	R	R
25	R	R	R	H	R
26	R	R	R	A	R
27	R	R	R	R	H
28	R	R	R	R	A
29	H	R	R	R	R
30	A	R	R	R	R

Red — Hydrogen Production
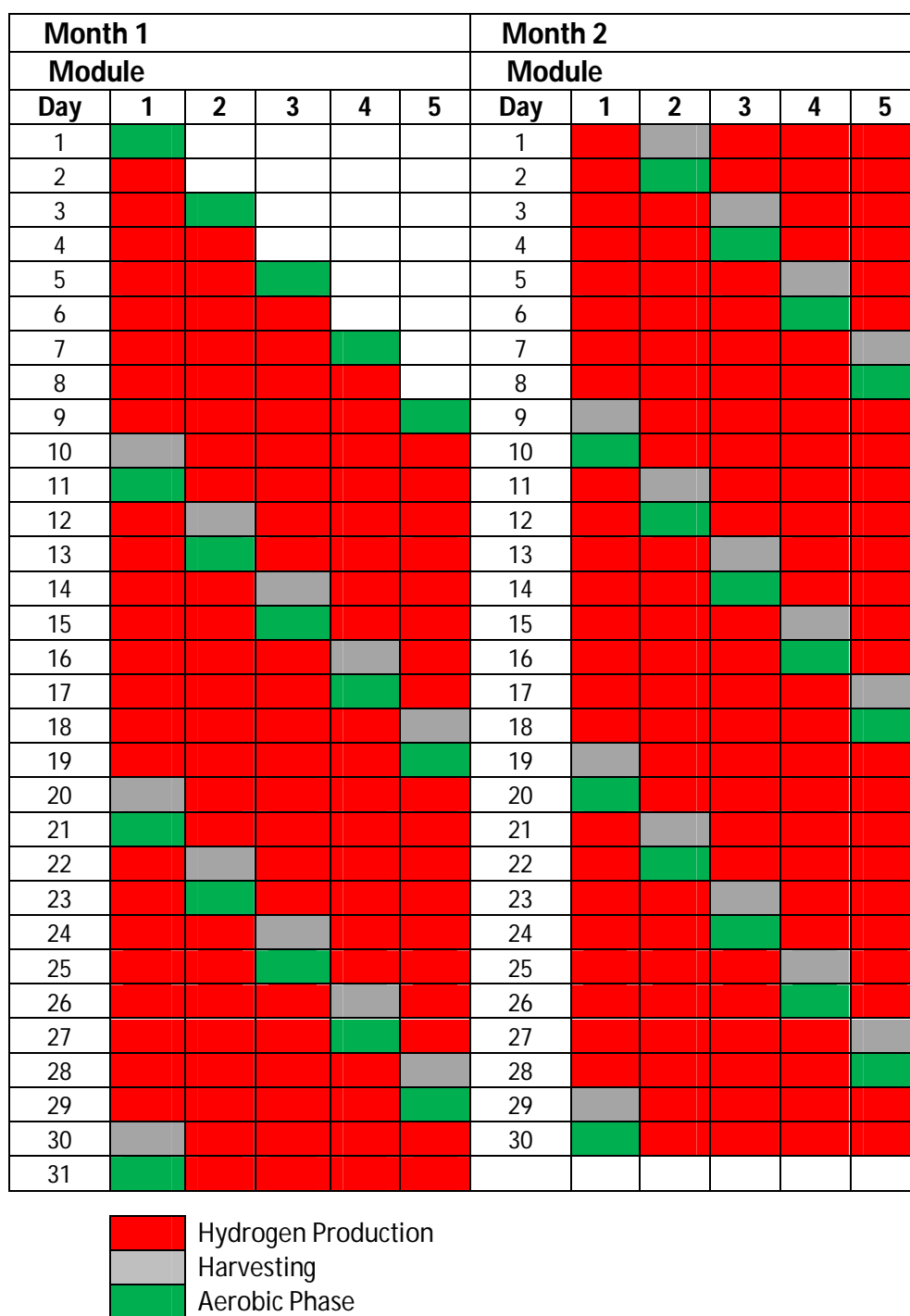Grey — Harvesting
Green — Aerobic Phase

Figure 5.7: The modular cycling of the Biohydrogen Phase 2 Plant. Each module starts from the Aerobic Phase (green block) for a day followed by 8 days of hydrogen production (red block) followed by harvesting of the module (grey block). Each module is offset by two days to allow for continuous hydrogen production.

Phase 2 will be continually monitored using the multi-probe as mentioned previously. All parameters mentions in Phase 1 will be monitored. In addition, the hydrogen levels will be monitored and recorded. This will ensure phase 2 is functioning optimally. Chapter 3 showed that PS I is up-regulated during hydrogen production and it is well known that PSII is down-regulated. The PAM PSI and PSII electron transport rates will be monitored to ensure the correct physiological changes are taking place. The lower PSII electron transport rates in conjunction with negligible oxygen measurements from the YSI probe will confirm anaerobic conditions. Up-regulated PSI electron transport rates will confirm that hydrogen is being produced. Adjustments in the physico-chemical parameters (especially PAR intensities) will allow for PS I ETR optimization and increased hydrogen yields. The yield ratio (YI: YII) will also be monitored and correlated to hydrogen yields from phase 2 providing another method to monitor and maintain indicators directly correlated with hydrogen synthesis.

Since NADPH concentrations were found to significantly correlate with hydrogen levels and increase when hydrogen levels increased (Chapter 4), NADPH levels will be constantly monitored in the hydrogen reactor. This will allow for unique optimal real time monitoring of hydrogen production in the large reactors. Fluctuations in hydrogen yields will be pre-empted due to NADPH concentration fluctuations and lower total hydrogen can be prevented as actions can be taken to prevent lower yields.

Taking into account the cyclical hydrogen production, four modules producing hydrogen will result in 5584.771 L of hydrogen on a continual basis. The 300W fuel cell requires 3.9L/min of hydrogen. Therefore when calculating the amount of hydrogen required for operation, it can be seen that the Fuel Cell will operate continually for 22hr a day (Fig 5.8). This will allow for 436.77 L surplus per day. This surplus will be compressed and stored in cylinders. This surplus will act as a buffer when optimal yields are not reached per day. This may be due to cooler weather conditions (winter) or cloudy days and insufficient PAR resulting in maximal production yields not being reached.

It will take a production time of eight days before the Fuel Cell can be switched on and electricity can be generated (Fig 5.8). The Fuel Cell can then be operated for 22 hours per day (Table 5.11) and the produced electricity will be stored in 43V batteries for further use in the specific application that is required.

Table 5.11: Hydrogen required for operating the 300W Fuel Cell for varying time periods

Application	Hydrogen required (L)
Actual Hydrogen produced	5584.771
20 hour Fuel Cell	4680
22 hour Fuel Cell	5148
24 hour Fuel Cell	5616
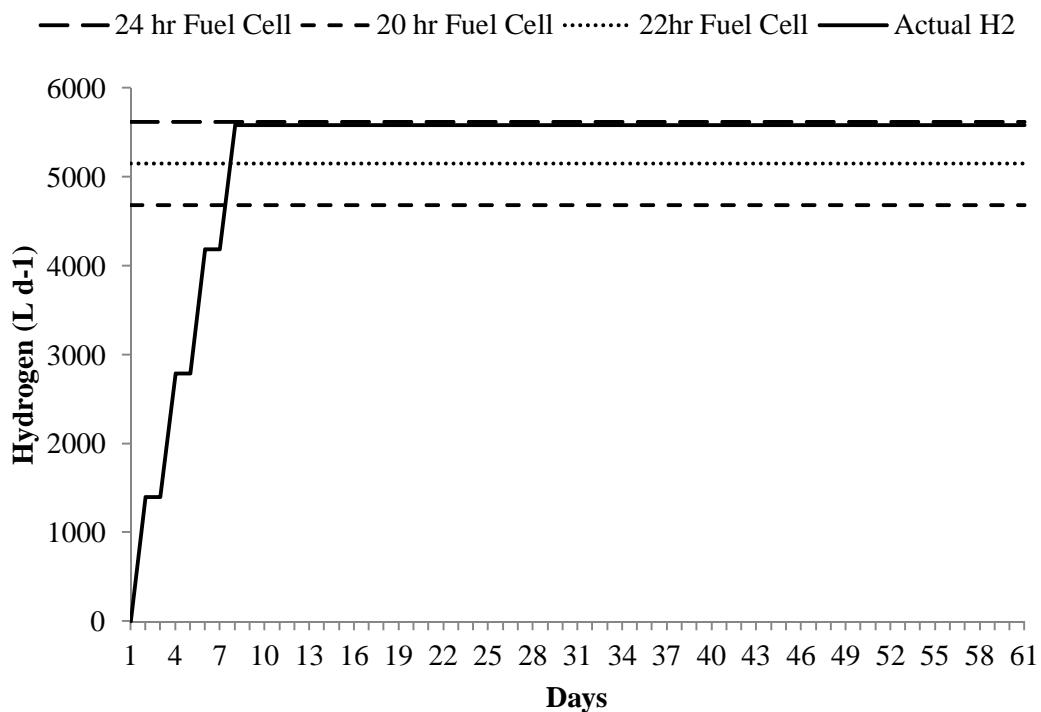
Figure 5.8: Actual Hydrogen produced on a daily basis (black line) compared to specifications required to use the 300W Fuel Cell for 20 hours (dashed line), 22 hours (dotted line), or 24 hours (long dashed line).

The projected yields from the modular biohydrogen production plant show results expected from a pilot scale type system. Assuming the biohydrogen production plant operates continually for a year, taking into account 30 days for maintenance per module, 33 cycles of ten days each will take place. This will produce approximately 7.236 tons of biomass and

1870 kL of hydrogen gas. This will allow for the production of 2212 kWh of power to be produced by a 300W fuel cell stack (Table 5.12).

Table 5.12: Annual yields expected from the Modular Biohydrogen Pilot Scale Processing Plant

Parameter	Annual Production
Biomass (t)	7, 236
Hydrogen (kL)	1870, 899
Carbon captured (t)	13, 024
Leachate used (t)	5.156
Biomass sales (@ R25 per kg (Norsker et al., 2011))	R 180 900
Power produced (KWh)	2211

5.4   Conclusions:

A Two Phase Modular Biohydrogen production system was designed to produce continual hydrogen. Operational processing parameters were also designed to optimize the plant and ensure it is running at maximum capacity. Unique features included the use of leachate to increase biomass and subsequent hydrogen yields.   The incorporation of an online monitoring device using PAM Fluorometry and readily available multi-probes allowing for offsite wireless data acquisition using a SCADA system was also used. Phase 1 consisted of an 86 m^3 reactor capable of producing 216 kg of continually available algae. Phase 2 consisted of a 72 m^3 reactor capable of producing 5584 L of hydrogen per day. This allowed for a 300W fuel cell to operate for 22 hours per day. Continued research into each component of the system will continue to increase yields, decrease operational costs and increase overall feasibility of biohydrogen production from *Chlamydomonas*.

CHAPTER SIX

General Conclusions and Recommendations for Future Research

6.1   Conclusions

The concept of waste to energy has shown to be very valuable in the production of renewable energy and simultaneous prevention of environmental damage. Renewable energy from biological organisms is by far the superior source with regards to environmental concerns and sustainability. Large bioprocessing plants are required to produce energy from biological means.

Bioprocessing involves numerous components that all require individual optimization to work effectively as a single system. Industrial applications are available to improve feasibility of pilot scale designs. These include industrial harvesters, low power and efficient LED lighting sources, computer equipment capable of automation as well as materials that are strong, durable and UV resistant. The designs can be predicted and modelled, however, the key to maximising hydrogen production using landfill leachate as the waste feedstock was the intermediary – *Chlamydomonas*. An improved understanding of the physiological changes that occurred during hydrogen production resulted in a novel pilot scale bioprocessing design capable of exploiting the physiology of *Chlamydomonas*, improving hydrogen yields and decreasing processing costs.

The biggest cost factor in microalgae cultivation per volume is the nutrient source. Landfill leachate was freely available at the landfill sites and as it is high in nutrients, showed potential as a suitable nutrient source. The use of a leachate supplemented media was found to increase biomass yields (Chapter 2). This process was occurring at an intra-cellular level where nitrogen and micronutrients were being assimilated and converted into biological chemicals. These were essential to increased photosynthesis and the subsequent cell division. Microalgal cells were also acclimatizing to hyper nutrient levels and using energy to maintain homeostasis. The optimum concentration was based on the equilibrium of these two processes where cells needed to assimilate nutrients and divide, while maintaining homeostasis. The optimum leachate concentration was found to increase overall feasibility as

less commercial growth media was used to produce greater amounts of biomass. *Chlamydomonas* cultured in a leachate supplemented media was found to produce more hydrogen gas and was able to produce hydrogen for a longer duration when compared to conventional methods. The addition of leachate was therefore used as a supplement for the bioprocessing plant during the cultivation stage to increase biomass yields (phase 1) and to increase hydrogen yields (phase 2).

Cultivation of biomass required aerobic conditions and the inclusion of sulphur in the growth media in contrast to hydrogen inducing conditions which required sulphur deprivation and anaerobic conditions. Clear differences were shown during the growth conditions compared to the hydrogen production conditions. During hydrogen production, photosystem II was shown to have reduced activity as was expected however photosystem I was shown to be up-regulated during hydrogen synthesis (Chapter 3). This shows the dominance of Photosystem I during hydrogen production as compared to the dominance of PSII during normal growth conditions. It was for this reason that a two phase system was utilized to be able to fully optimize each phase individually. The two phase reactor system also involved a novel modular design to allow for easy upgrade from pilot scale to large scale to possible commercial scale. Reactor units can be added to increase volume with the ability to be monitored without down-time of existing units and original reactors can be retained in the large scale production.

Cellular NADPH was found to be directly correlated to hydrogen production making it very effective as an indicator of hydrogen production (Chapter 4). This also prompted the concept that increased NADPH concentrations may increase hydrogen production and not only that the production of hydrogen increased NADPH concentrations. The role of NADPH as an indicator molecule is very valuable in a pilot scale system. Apart from indicating hydrogen production, NADPH provided instantaneous projected yields of hydrogen over the 10 day cycle, thus improving commercial productivity and preventing poor hydrogen yields.

During growth the inoculum has minimal turbidity and shading effects. As the culture grows density becomes inversely proportional to the light attenuation through the culture. Rapid light curves obtained from PAM fluorometry showed that light intensity is crucial for both biomass production and hydrogen synthesis. Therefore light levels need to be adjusted to maintain an intensity conducive of maximised electron flow, ATP production and growth. It is for this purpose that an internal LED light source was included in the reactor design.

Firstly, this removes the dark zone along the centre of the cylinder and secondly, light levels can be increased to maintain a constant intensity during biomass production. Light levels required for hydrogen production were found to be between 25 μE m^{-2}s^{-1} PAR (Kosourov et al., 2007, Tsygankov et al., 2006) and 200-250 μE m^{-2} s^{-1} (Antal et al., 2003). Since PS I is up-regulated during hydrogen production, light levels needs to be at an intensity to stimulate electron transport through PSI towards the hydrogenase enzyme. Rapid light curves showed that PSI has a maximised ETR at higher levels than suggested by literature (500 – 2000 μmol m^{-2}s^{-1}). Adjustable internal LED light sources were included in phase two to allow for PSI stimulation and improved hydrogen yields.

The monitoring of the bioprocessing plant is important to maintain maximised levels for all critical components of the hydrogen production process. These include, lighting, aerobic/anaerobic conditions, nitrogen levels, physiological functioning (PS I and PS II) and NADPH concentrations. A unique collection of probes formed part of the online monitoring system. These allowed for real-time conditions to be recorded and manipulated maintaining optimized levels. As PAM Fluorometry was used to optimize leachate concentration, monitor electron transport rate in both PS I and PS II as well as monitor NADPH concentrations. This tool proved invaluable from a monitoring aspect and was therefore included in the monitoring system of the bioprocessing plant. This will provide continual real-time information regarding the health of the culture, electron transport rates of both PS I and PS II and the detailed information on NADPH levels. Other probes worked in conjunction with the PAM to maintain maximised levels. The light meter was used to determine how the lighting needed to be adjusted to maintain light levels conducive of maximum electron transport. Nitrogen and Ammonium meters were used to maintain leachate levels conducive to maximum electron transport, homeostasis and growth.

The major output of the bioprocessing plant is charged batteries. These batteries have a multitude of uses. They can be stepped up to 220V to operate household appliances (kettles, fridges, microwaves etc) or they can be stepped down to operate portable smaller devices (cellular phones, laptop computers etc). The minor output of the bioprocessing plant is biomass. The design sells this biomass thereby creating an income stream for the plant assisting with running costs and adding to the overall feasibility.

This bioprocessing system demonstrates the potential for maximising hydrogen production from *Chlamydomonas*. The novel application of intra-cellular research towards a pilot

bioprocessing systems has allowed for major improvements in understanding the physiology of hydrogen production. This knowledge has then been used to design a pilot scale bioprocessing plant capable of exploiting the newly found technology in an attempt to improve feasibility of biohydrogen production from *Chlamydomonas* (Chapter 5). With this conceptual thinking, the rising fuel prices and continuous advancement in industrial biotechnology and bioprocessing, the potential for biomass to replace petroleum based fuels is inevitable.

6.2 Recommendations for future research

1. A Life Cycle Analysis needs to be conducted to determine the feasibility of the leachate to hydrogen waste to energy pilot scale bioprocessing project.

2. The construction of the modular pilot scale biohydrogen bioprocessing system would prove valuable to compare predicted vs. actual outputs of biomass and hydrogen.

3. As the leachate composition varies significantly from location to location and even daily, it would be worth investigating which specific chemical component(s) in the leachate really enhance hydrogen production.

4. It would be valuable to elucidate methods in which to enhance the activity of photosystem I. This should, in conjunction with a down-regulated photosystem II, increase hydrogen yields from *Chlamydomonas.*

5. A dedicated study into the exact role of NADPH in the hydrogen production process would prove invaluable. This would allow for possible genetic engineering studies to increase NADPH concentrations.

6. It would be useful to monitor cellular neutral lipids during incubation with landfill leachate to determine the potential for a biodiesel production facility in a multi-output approach from *Chlamydomonas*.

7. It would be informative to determine the effect that different colour LED's would have on PSI up-regulation and its subsequent effect on hydrogen production during sulphur deprivation.

REFERENCES

Aceves, S., Berry, G., Martinez-Frias, J. & Espinosa-Loza, F. 2006. Vehicular storage of hydrogen in insulated pressure vessels. International Journal of Hydrogen Energy 31, 2274-2283.

Alric, J., Lavergne, J. & Rappaport, F. 2010. Redox and ATP control of photosynthetic cyclic electron flow in *Chlamydomonas reinhardtii* (I) aerobic conditions. Biochimica et Biophysica Acta 1797, 44-51.

Amos, W. & Ghirardi, M. L. 2004. Renewable energy from green algae. Biocycle 45, 59.

Ananthachar, V. & Duffy, J. 2005. Efficiencies of hydrogen storage systems onboard fuel cell vehicles. Solar Energy 78, 687-694.

Antal, T. K., Krendeleva, T. E., Laurinavich, T. V., Makarova, V. V., Ghirardi, M. L., Rubin, A., B, Tsygankov, A. A. & Seibert, M. 2003. The dependence of algal H_2 production on Photosystem II and O_2 consumption activities in sulfur-deprived *Chlamydomonas reinhardtii* cells. Biochimica et Biophysica Acta (BBA) - Bioenergetics 1607, 153-160.

Bakare, A. A., Mosuro, A. A. & Osibanjo, O. 2005. An in vivo evaluation of induction of abnormal sperm morphology in mice by landfill leachate. Mutation Research 582, 28-34.

Baker, N. R. 2008. Chlorophyll Fluorescence: A probe of Photosynthesis In Vivo. Annual Review of Plant Biology 59, 89-113.

Balat, M. 2008. Potential important of hydrogen as a future solution to environmental and transportation problems. International Journal of Hydrogen Energy 33, 4013-4029.

Balmant, W., Oliveira, B., Mitchell, D., Vargas, J. & Ordonez, J. 2014. Optimal operating conditions for maximum biogas production in anaerobic bioreactors. Applied Thermal Engineering 62, 197-206.

Barrett, S. 2012. Turkish fuel cell boat powered, refuelled by Hydrogenics tech. Fuel Cell Bulletin 2-3.

Beardall, J., Young, E. & Roberts, S. 2001. Approaches for determining phytoplankton nutrient limitation. Aquatic Science 63, 44-69.

Bhatnagar, A., Chinnasamy, S., Singh, M. & Das, K. C. 2011. Renewable biomass production by mixotrophic algae in the presence of various carbon sources and wastewaters. Applied Energy 88, 3425-3431.

Blaby-Haas, C. & Merchant, S. 2012. The ins and outs of algal metal transport. Biochimica et Biophysica Acta 1823, 1531-1552.

Blaby-Haas, C. & Merchant, S. 2013. Iron sparing and recycling in a compartmentalized cell. Current Opinion in Microbiology doi: 10.1016/j.mib.2013.07.019.

Blanch, H. 2012. Bioprocessing for biofuels. Current Opinion in Biotechnology 23, 390-395.

Bolan, N., Thangarajan, R., Seshadri, B., Jena, U., Das, K., Wang, H. & Naidu, R. 2013. Landfills as a Biorefinery to produce biomass and capture biogas. Bioresource Technology 135, 578-587.

Bukhov, N., Samson, G. & Carpentier, R. 2001. Non photosynthetic reduction of the intersystem electron transport chain of chloroplasts following heat stress. The pool size of stromal reductants. Photochemistry and Photobiology 74, 438-443.

Butler, WL. 1978. Energy distribution in the photochemical apparatus of photosynthesis. Annual Review of Plant Physiology 29, 345-378.

Cai, T., Park, S., Li, Y. 2013. Nutrient recovery from wastewater streams by microalgae: status and prospects. Renewable and Sustainable Energy Reviews 19, 360-369.

Cardol, P., Forti, G. & Finazzi, G. 2011. Regulation of electron transport in microalgae. Biochimica et Biophysica Acta 1807, 912-918.

Cardol, P., Gonzalez-Halphen, D., Reyes-Prieto, A., Baurain, D., Matagne, R. & Remacle, C. 2005. The mitochondrial oxidative phosphorylation proteome of *Chlamydomonas reinhardtii* deduced from the Genome Sequencing Project. Plant Physiology 137, 447-459.

Chisti, Y. 2007. Biodiesel from Microalgae. Biotechnology Advances 25, 294-306.

Chisti, Y. 2008. Biodiesel from microalgae beats bioethanol. Trends in Biotechnology 26, 126-131.

Cho, S., Lee, N., Park, S. Y., Yu, J., Luong, T. T., Oh, Y. & Lee, T. 2013. Microalgae cultivation for bioenergy production using wastewaters from a municipal WWTP as nutritional sources. Bioresource Technology 131, 515-520.

Chochois, V., Constans, L., Dauvillee, D., Beyly, A., Soliveres, M., Ball, S., Peltier, G. & Cournac, L. 2010. Relationships between PSII-independent hydrogen bioproduction and starch metabolism as evidenced from isolation of starch catabolism mutants in the green alga *Chlamydomonas reinhardtii*. International Journal of Hydrogen Energy 35, 10731-10740.

Chou, C. H., Han, C. L., Chang, J. J. & Lay, J. J. 2011. Co-culture of *Clostridium beijerinckii* L9, *Clostridium butyricum* M1 and *Bacillus thermoamylovorans* B5 for converting yeast waste into hydrogen. International Journal of Hydrogen Energy 36, 13972-13983.

Christenson, L. & Sims, R. 2011. Production and harvesting of microalgae for wastewater treatment, biofuels and bioproducts. Biotechnology Advances 29, 686-702.

Chynoweth, D. P., Owens, J. M. & Legrand, R. 2001. Renewable methane from anaerobic digestion of biomass. Renewable Energy 22**,** 1-8.

Ciccoli, R., Cogolotti, V., LoProsti, R., Massi, E., PcPhail, S., Monteleone, G. 2010. Molten carobonate fuel cells fed with biogas: combating H_2S. Waste Management 33, 1648-1658.

Cimpan, C. & Wenzel, H. 2013. Energy implications of mechanical and mechanical-biological treatment compared to direct waste-to-energy. Waste Management 33, 1648-1658.

Clavier, J., Boucher, G., Chauvaud, L. & Fichez, C., S 2005. Benthic response to ammonium pulses in a tropical lagoon: implications for coastal environmental processes. Journal of Experimental Marine Biology and Ecology 316, 231-241.

Costa, J. A. V. & Greque De Morais, M. 2011. The role of biochemical engineering in the production of biofuels from microalgae. Bioresource Technology 102, 2-9.

Cottrell, C., Grasman, S., Thomas, M., Martin, K. & Sheffield, J. 2011. Strategies for stationary and portable fuel cell markets. International Journal of Hydrogen Energy 36, 7969-7975.

Cournac, L., Mus, F., Bernard, L., Guedeney, G., Vignais, P. & Peltier, G. 2002. Limiting steps of hydrogen production in *Chlamydomonas reinhardtii* and *Synechocystis* PCC 6803 as analysed by light-induced gas exchange transients. International Journal of Hydrogen Energy 27, 1229-1237.

Couth, R., Trois, C., Parkin, J., Strachen, L., Gilder, A. & Wright, M. 2011. Delivering and viability of landfill gas CDM projects in Africa - A South African experience. Renewable and Sustainable Energy Reviews 15, 392-403.

Da Fonseca, R., Bideaux, E., Gerard, M., Jeanneret, B., Desbois-Renaudin, M. & Sari, A. 2014. Control of PEMFC system air group using differential flatness approach: Validation by a dynamic fuel cell system model. Applied Energy 113, 219-229.

Daday, A., Mackerras, AH., Smith, GD. 1985. The effect of Nickel on hydrogen metabolism and nitrogen fixation in Cyanobacterium *Anabaena cyclindrica*. Journal of General Microbiology 131, 231-238.

Daimler, Ford, Gm/Opel, Honda, Hyundia/Kia, Renault/Nissan, T. A. & Toyota 2009. Letter of understanding on the developments and market introduction of fuel cell vehicles.

Das, D. & Veziroglu, T. N. 2001. Hydrogen production by biological processes: a survey of literature. International Journal of Hydrogen Energy 26, 13-28.

De Gioannis, G. & Muntoni, A. 2007. Dynamic transformations of nitrogen during mechanical-biological pre-treatment of municipal solid waste. Waste Management 27**,** 1479-1485.

De Gioannis, G., Muntoni, A., Cappai, G. & Milia, S. 2009. Landfill gas generation after mechanical biological treatment of municipal solid waste. Estimation of gas generation rate constants. Waste Management 29**,** 1026-1034.

De Gioannis, G., Muntoni, A., Polettini, A. & Pomi, R. 2013. A review of dark fermentative hydrogen production from degradable municipal waste fractions. Waste Management 33**,** 1345-1361.

Degrenne, B., Pruvost, J. & Legrand, J. 2011. Effect of prolonged hypoxia in autotrophic conditions in the hydrogen production by the green microalga *Chlamydomonas reinhardtii* in photobioreactor. Bioresource Technology 102, 1035-1043.

Del Mar Arxer, M. & Martinez Calleja, L. 2007. Hercules project: Contributing to the development of the hydrogen infrastructure. Journal of Power Sources 171, 224-227.

Dent, R., Han, M. & Niyogi, K. 2001. Functional genomics of plant photosynthesis in the fast lane using *Chlamydomonas reinhardtii*. Trends in Plant Science 6, 356-371.

Department of Environmental Affairs (2012) National Waste Information Baseline Report. Department of Envionmental Affairs. Pretoria, South Africa.

Di Profio, P., Arca, S., Rossi, F. & Filipponi, M. 2009. Comparison of hydrogen hydrates with existing hydrogen storage technologies: Energetic and economic evaluations. International Journal of Hydrogen Energy 34, 9173-9180.

El-Fadel, M., Abi-Esber, L. & Salhab, S. 2012. Emission assessment at the Burj Hammoud inactive municiapal landfill: Viability of landfill gas recovery under the clean development mechanism. Waste Management 32**,** 2106-2114.

Federov, A. S., Kosourov, S., Ghirardi, M. L. & Seibert, M. 2005. Continuous hydrogen photoproduction by *Chlamydomonas reinhardtii*: using a novel two stage sulfate-limited chemostat system. Applied Biochemistry and Biotechnolog, 121**,** 403-412.

Ferreira, A. F., Marques, A. C., Batista, A. P., Marques, P. A. S. S., Gouveia, L. & Silva, C. M. 2012. Biological hydrogen production by *Anabaena* sp. - Yield, energy and CO_2 analysis including fermentative biomass recovery. International Journal of Hydrogen Energy 37, 179-190.

Ferreira, A. F., Ortigueira, J., Alves, L., Gouveia, L., Moura, P. & Silva, C. M. 2013a. Biohydrogen production from microalgal biomass: Energy requirement, CO_2 emissions and scale-up scenarios. Bioresource Technology 144, 156-164.

Ferreira, A. F., Ortigueira, J., Alves, L., Gouveia, L., Moura, P. & Silva, C. M. 2013b. Energy requirement and CO emissions of bioH2 production from microalgal biomass. Biomass and Bioenergy 49**,** 249-259.

Finazzi, G. 2005. The central role of the green alga *Chlamydomonas reinhardtii* in revealing the mechanism of state transitions. Journal of Experimental Botany 56, 383-388.

Florin, L., Tsokoglou, A. & Happe, T. 2001. A novel type of [Fe]-hydrogenase in the green alga *Scenedesmus obliquus* is linked to the photosynthetical electron transport chain. Journal of Biological Chemistry 6125-6132.

Forsberg, C. 2007. Future hydrogen markets for large-scale hydrogen production systems. International Journal of Hydrogen Energy 32, 431-439.

Fouchard, S., Hemschemeier, A., Caruana, A., Pruvost, J., Legrand, J., Happe, T., Peltier, G. & Cournac, L. 2005. Autotrophic and mixotrophic hydrogen photoproduction in sulfur-deprived *Chlamydomonas* cells. Applied and Environmental Microbiology 71, 6199-6205.

Fouchard, S., Pruvost, J., Degrenne, B. & Legrand, J. 2008. Investigation of H_2 production using the green microalga *Chlamydomonas reinhardtii* in a fully controlled photobioreactor fitted with on-line gas analysis. International Journal of Hydrogen Energy 33, 3302-3310.

Fu, W., Gudmmundsson, O., Feist, A., Herjolfsson, G., Brynjolfsson, S. & Palsson, B. 2012. Maximizing biomass productivity and cell density of *Chlorella vulgaris* by using light-emitting diode-based photobioreactor. Journal of Biotechnology 161, 242-249.

Gaffron, H. & Rubin, J. 1942 Fermentative and photochemical production of hydrogen in algae. Journal of General Physiology 26, 219-240.

Gao, Y., Yang, M. & Wang, C. 2013. Nutrient deprivation enhances lipid content in marine microalgae. Bioresource Technology 147, 484-491.

Geigenberger, P., Kolbe, A. & Tiesson, A. 2005. Reox regulationof carbon storage and partitioning in response to light and sugars. Journal of Experimental Botany 56, 1469-1479.

Genty, B., Briantais, J. M. & Baker, N. R. 1989. The relationship between the quantum yield of photosynthesis electron transport and quenching of chlorophyll fluorescence. Biochimica et Biophysica Acta 990, 87-92.

Ghirardi, M. L. 2006. Hydrogen production by photosynthetic green algae. Indian Journal of Biochemistry and Biophysics 43, 201-210.

Ghirardi, M. L., Togasaki, R. K. & Seibert, M. 1997. Oxygen-sensitivity of algal H_2 production. Applied Biochemistry and Biotechnolog, 63, 141-151.

Ghirardi, M. L., Zhang, J., Lee, J., Flynn, T., Seibert, M., Greenbaum, E. & Melis, A. 2000. Microalgae: a green source of renewable H_2. Trends in Biotechnology 18, 506-511.

Giannelli, L. & Torzillo, G. 2012. Hydrogen production with the microalga *Chlamydomonas reinhardtii* grown in a compact tubular photobioreactor immersed in a scattering light nanoparticle suspension. International Journal of Hydrogen Energy 37, 16951-16961.

Gorman, D. & Levine, R. 1965 Cytochrome f and plastocyanin: their sequence in the photosynthetic electron transport chain of *Chlamydomonas reinhardtii*. PNAS 54, 1665-1669.

Greenwell, H. C., Laurens, M. L., Shields, R. J., Lovitt, R. W. & Flynn, K. J. 2009. Placing microalgae on the biofuels priority list: a review of the technological challenges. Journal of Royal Society Interface 7(46):703-26.

Grossman, A. R. 2000. Acclimation of *Chlamydomonas reinhardtii* to its Nutrient Environment. Protist 152, 201-224.

Grossman, A. R., Croft, M., Gladyshev, V., Merchant, S., Posewitz, M., Prochnik, S. & Spalding, M. 2007. Novel metabolism in *Chlamydomonas* through the lens of genomics. Current Opinion in Plant Biology 10, 190-198.

Guo, Q., Luo, Y. & Jiao, K. 2013. Modelling of assisted cold start processes with anode catalytic hydrogen-oxygen reaction in proton exchange membrane fuel cell. International Journal of Hydrogen Energy 38, 1004-1015.

Hamada, E., Dowiador, S. & Punnet, T. 2003. Influence of spectral range and carbon and nitrogen sources on oxygen evolution and Emerson enhancement in *Chlamydomonas reinhardtii*. Biologica Plantarium 46, 389-397.

Hartig, P., Wolfstein, K., Lippemeier, S. & Coljin, F. 1998. Photosynthetic activity of natural microphytobenthos populations measured by fluorescence (PAM) and ^{14}C-tracer methods: a comparison. Marine Ecology Press Series 166, 53-62.

Harun, R., Singh, M., Forde, G. M. & Danquah, M. K. 2010. Bioprocess engineering of microalgae to produce a variety of consumer products. Renewable and Sustainable Energy Reviews 14, 1037-1047.

Hassan, A., Carreras, A., Trincavelli, J. & Ticianelli, E. A. 2014. Effect of heat treatment on the activity and stability of carbon supported PtMo alloy electrocatalysts for hydrogen oxidation in proton exchange membrane fuel cells. Journal of Power Sources 247, 712-720.

Hausinger, R. 1987. Nickel Utilization by Micro organisms. Microbiological Review, 51, 22-42.

He, M., Li, L., Zhang, L. & Liu, J. 2012. The enhancement of hydrogen photoproduction in *Chlorella protothecoides* exposed to nitrogen limitation and sulfur deprivation. International Journal of Hydrogen Energy 37, 16903-16915.

Hemschemeier, A. & Happe, T. 2011. Alternative photosynthetic electron transport pathways during anaerobiosis in the green alga *Chlamydomonas reinhardtii*. Biochimica et Biophysica Acta 1807, 919-926.

Herlory, O., Bonzom, J. & Gilbin, R. 2013. Sensitivity evaluation of the green alga *Chlamydomonas reinhardtii* to uranium by pulse amplitude modulated (PAM) fluorometry. Aquatic Toxicology 140-141, 288-294.

Hoshino, T., Johnson, D. J. & Cuello, J. L. 2012. Design of new strategy for green algal photo-hydrogen production: Spectral-selective photosystem I activation and photosystem II deactivation. Bioresource Technology 120, 233-240.

Hosseini, M., Dincer, I., Naterer, G. & Rosen, M. A. 2012. Thermodynamic analysis of filling compressed gaseous hydrogen storage tanks. International Journal of Hydrogen Energy 37, 5063-5071.

Hou, Y., Shen, C., Hao, D., Liu, Y. & Wang, H. 2014. A dynamic model for hydrogen consumption of fuel cell stacks considering the effects of hydrogen purge operation. Renewable Energy 62, 672-678.

Hwang, J.-J. 2013. Sustainability study of hydrogen pathways for fuel cell vehicle applications. Renewable and Sustainable Energy Reviews 19, 220-229.

Inman, K., Ahmed, Z., Shi, Z. & Wang, X. 2011. Design of a proton exchange membrane portable fuel cell system for the 1st international association for hydrogen energy design competition. International Journal of Hydrogen Energy 36, 13868-13874.

Jahns P, Depka, B, & Trebst, A. 2000. Xanthophyll cycle mutants from *Chlamydomonas reinhardtii* indicate a role for zeaxanthin in the D1 protein turnover. Plant Physiology and Biochemistry 38, 371-376.

Jo, J. H., Lee, D. & Park, J. M. 2006. Modelling and optimization of photosynthetic hydrogen gas production by green alga *Chlamydomonas reinhardtii* in sulphur-deprived circumstance. Biotechnology Progress 22, 431-437.

Jorquera, O., Kiperstok, A., Sales, E. A., Embirucu, M. & Ghirardi, M. L. 2008. S-systems sensitivity analysis of the factors that may influence hydrogen production by sulfur-deprived *Chlamydomonas reinhardtii*. International Journal of Hydrogen Energy 33, 2167-2177.

Juneau, P., El Berdey, A. & Popovic, R. 2002. PAM Fluorometry in the Determination of the Sensitivity of *Chlorella vulgaris, Selenastrum capricornutum*, and *Chlamydomonas reinhardtii* to Copper. Archives of Environmental Contamination and Toxicology 42, 155-164.

Juneau, P., Green, B. R. & Harrison, P. J. 2005. Simulation of Pulse-Amplitude-Modulated (PAM) fluorescence: Limitations of some PAM-parameters in studying environmental stress effects. Photosynthetica 43, 75-83.

Kawai, M., Purwanti, I., Nagao, N., Slamet, A., Hermana, J. & Toda, T. 2012. Seasonal variation in chemical properties and degradability by anaerobic digestion of landfill leachate at Benowo in Surabaya, Indonesia. Journal of Environmental Management 110, 267-275.

Kim, H.-Y., Jeon, S., Song, M. & Kim, K. 2014. Numerical simulations of water droplet dynamics in hydrogen fuel cell gas channel. Journal of Power Sources 246, 679-695.

Kirk, J. 2003. The vertical attenuation of irradiance as a function of the optical properties of the water. Limnology and Oceanography 48, 9-17.

Kjeldsen, P., Barlaz, M. A., Rooker, A. P., Baun, A., Ledin, A. & Christensen, T. 2002. Present and long-term composition of MSW landfill leachate: a review. Critical Reviews in Environmental Science and Technology 32, 297-336.

Klughammer, C. & Schreiber, U. 2008. Saturation Pulse method for assessment of energy conversion in PS I. PAM Application Notes 1, 11-14.

Kosourov, S., Batyrova, K., Petushkova, E., Tsygankov, A., Ghirardi, M. L. & Seibert, M. 2012. Maximizing the hydrogen photoproduction yields in *Chlamydomonas reinhardtii* cultures: The effect of the H_2 partial pressure. International Journal of Hydrogen Energy 37, 8850-8858.

Kosourov, S., Patrusheva, E., Ghirardi, M. L., Seibert, M. & Tsygankov, A. 2007. A comparison of hydrogen photoproduction by sulfur-deprived *Chlamydomonas reinhardtii* under different growth conditions. Journal of Biotechnology 128, 776-787.

Kosourov, S., Seibert, M. & Ghirardi, M. L. 2003. Effects of extra-cellular pH on the metabolic pathways in sulphur-deprived H_2 producing *Chlamydomonas reinhardtii* cultures. Plant Physiology 44**,** 146-155.

Kosourov, S., Tsygankov, A., Seibert, M. & Ghirardi, M. L. 2002. Sustained Hydrogen Photoproduction by *Chlamydomonas reinhardtii*: Effects of Culture Parameters. Biotechnology and Bioengineering 78, 731-740.

Kothari, R., Tyagi, V. V. & Pathak, A. 2010. Waste-to-energy: A way from renewable energy sources top sustainable development. Renewable and Sustainable Energy Reviews 14**,** 3164-3170.

Kromkamp, J. & Peene, J. 1999. Estimation of phytoplankton photosynthesis and nutrient limitation in the Eastern Scheldt estuary using variable fluorescence. Aquatic Ecology 33, 101-104.

Kruse, O., Rupprecht, J., Bader, K., Thomas-Hall, S., Schenk, P. M., Finazzi, G. & Hankamer, B. 2005. Improved Photobiological H_2 Production in Engineered Green Algal Cells. The Journal of Biological Chemistry 280, 34170-34177.

Kuby, M., Lines, L., Schultz, R., Xie, Z., Kim, J.-G.& Lim, S. 2009. Optimization of hydrogen stations in Florida using the Flow-Refueling Location Model. International Journal of Hydrogen Energy 34, 6045-6064.

Kundu, K., Kulshrestha, M., Dhar, N. & Roy, A. 2012. Production of Hydrogen as a Potential Source of Renewable Energy from Green Algae - A review. *IPCSIT,* 28.

Kurniawan, T., Lo, W. & Chan, G. Y. S. 2006. Physico-chemical treatments for removal of recalcitrant contaminants from landfill leachate. Journal of Hazardous Materials 129**,** 80-100.

Kuster, A., Schaible, R. & Schobert, H. 2004. Light acclimation of photosynthesis in three charophyte species. Aquatic Botany 79, 111-124.

Laurinavichene, T. V., Federov, A. S., Ghirardi, M. L., Seibert, M. & Tsygankov, A. A. 2006. Demonstration of sustained hydrogen photoproduction by immobilized, sulfur-deprived *Chlamydomonas reinhardtii* cells. International Journal of Hydrogen Energy 31, 659-667.

Laurinavichene, T. V., Tolstygina, I. V., Galiulina, R. R., Ghirardi, M. L., Seibert, M. & Tsygankov, A. A. 2002. Dilution methods to deprive *Chlamydomonas reinhardtii* cultures of sulfur for subsequent hydrogen photoproduction. International Journal of Hydrogen Energy, 27, 1245-1249.

Leon-Banares, R., Gonzalez-Ballester, D., Galvan, A. & Fernandez, E. 2004. Transgenic microalgae as green cell factories. Trends in Biotechnology 22, 45-52.

Lesmana, S. O., Febriana, N., Soetaredjo, F. E., Sunarso, J. & Ismadji, S. 2009. Studies on potential applications of biomass for the separation of heavy metals from water and wastewater. Biochemical Engineering Journal 44, 19-41.

Levin, D., Pitt, L. & Love, M. 2004. Biohydrogen production: prospects and limitations to practical application. International Journal of Hydrogen Energy 27, 1217-1228.

Li, Q., Chen, W., Wang, Y., Jia, J. & Han, M. 2009. Nonlinear robust control of proton exchange membrane fuel cell by state feedback exact linearization. Journal of Power Sources 194, 338-348.

Li, Z., Pan, X., Sun, K. & Ma, J. 2013. Evaluation on the harm effects of accidental releases from cryo-compressed hydrogen tank for fuel cell cars. International Journal of Hydrogen Energy 38, 8199-8207.

Lin, L., Chan, G. Y. S., Jiang, B. L. & Lan, C. Y. 2007. Use of ammoniacal nitrogen tolerant microalgae in landfill leachate treatment. Waste Management 27, 1376-1382.

Lou, X. & Nair, J. 2009. The impact of landfilling and composting on greenhouse gas emissions - a review. Bioresource Technology 100, 3792-3798.

Ma, W., Chen, M., Wang, L., Wei, L. & Wang, Q. 2011. Treatment with $NaHSO_3$ greatly enhances photobiological H_2 production in the green alga *Chlamydomonas reinhardtii*. Bioresource Technology 102, 8635-8638.

Ma, W. & Mi, H. 2008. Effect of exogenous glucose on the expression and activity of NADPH dehydrogenase complexes in the cyanobacterium *Synechocystis* sp. strain PCC 6803. Plant Physiology and Biochemistry 46, 775-779.

Markov, S., Eivazova, E. & Greenwood, J. 2006. Photostimulation of H_2 production in the green alga *Chlamydomonas reinhardtii* upon photoinhibition of its O_2 evolving system. International Journal of Hydrogen Energy 31, 1314-1317.

Mathews, J. & Wang, G. 2009. Metabolic pathway engineering for enhanced biohydrogen production. International Journal of Hydrogen Energy 34, 7404-7416.

Maxwell, K. & Johnson, G. N. 2000. Chlorophyll fluorescence- a practical guide. Journal of Experimental Botany 51, 659-668.

Mckinlay, J. B. & Harwood, C. S. 2010. Photobiological production of hydrogen gas as a biofuel. Current Opinion in Biotechnology 21, 244-251.

Meherkotay, S. & Das, D. 2008. Biohydrogen as a renewable energy source - prospects and potentials. International Journal of Hydrogen Energy 33, 258-263.

Melis, A. 2007. Photosynthetic H_2 metabolism in *Chlamydomonas reinhardtii* (unicellular green algae). Planta 226, 1075-1086.

Melis, A. & Chen, H. C. 2005. Chloroplast sulfate transport in green algae - genes, proteins and effects. Photosynthetic Research 86, 299-307.

Melis, A. & HAPPE, T. 2004. Trails of Green Alga Hydrogen Research - from Hans Gaffron to New Frontiers. Photosynthesis Research 80, 401-409.

Melis, A., Zhang, L., Forestier, M., Ghirardi, M. L. & Seibert, M. 2000. Sustained Photobiological Hydrogen Production upon Reversible Inactivation of Oxygen Evolution in the Green Alga *Chlamydomonas reinhardtii*. Plant Physiology 122, 127-135.

Merchant, S., Allen, M., Kropat, J., Moseley, J., Long, J., Tottey, S. & Terauchi, A. 2006. Between a rock and a hard place: Trace element nutrition in *Chlamydomonas*. Biochimica et Biophysica Acta 1763, 578-594.

Merchant, S., Prochnol, S., Vallon, O., Harris, E., Karpowicz, S., Witman, G. & Al., E. 2007. The *Chlamydomonas* genome reveals the evolution of key animal and plant functions. Science 318, 245-250.

Midilli, A. & Dincer, I. 2008. Hydrogen as a renewable and sustainable solution in reducing global fossil fuel consumption. International Journal of Hydrogen Energy 33, 4209-4222.

Mignolet, E., Lecler, R., Ghysels, B., Remacle, C. & Franck, F. 2012. Function of the chloroplastic NAD(P)H dehydrogenase Nda2 for H_2 photoproduction in sulphur-deprived *Chlamydomonas reinhardtii*. Journal of Biotechnology 162, 81-88.

Morsi, I. & El-Din, L. 2014. SCADA System for Oil Refinery Control. Measurement 47, 5-13.

Muller, P., Li, X.-P.& Niyogi, K. 2001. Non-photochemical quenching. A response to excess light energy. Plant Physiology 1558-1566.

Munoz, R. & Guieysse, B. 2006. Algal-bacterial processes for the treatment of hazardous contaminants: A review. Water Research 40, 2799-2815.

Murata, N., Takahashi, S., Y, N. & Allakhverdiev, S. 2007. Photoinhibition of photosystem II under environmental stress. Biochimica et Biophysica Acta 1767, 414-421.

Murray, E. P., Tsai, T. & Barnett, S. A. 1999. A direct-methane fuel cell with a ceria-based anode. Letters to Nature 400, 649-651.

Mus, F., Cournac, L., Cardettini, V., Caruana, A. & Peltier, G. 2005. Inhibitor studies on non-photochemical plastoquinone reduction and H_2 photoproduction in *Chlamydomonas reinhardtii*. Biochimica et Biophysica Acta 1708, 322-332.

Mus, F., Dubini, A., Seibert, M., Posewitz, M. & Grossman, A. R. 2007. Anaerobic acclimation in *Chlamydomonas reinhardtii*: Anoxic gene expression, hydrogenase, induction, and metabolic pathways. Journal of Biological Chemistry 282, 25475-25486.

Neves Jr, N. & Pinto, C. 2013. Licensing a fuel cell bus and a hydrogen fuelling station in Brazil. International Journal of Hydrogen Energy 38, 8215-8220.

Norsker, N.-H., Barbosa, M. J., Vermue, M. & Wijffels, R. H. 2011. Microalgal production - A close look at the economics. Biotechnology Advances 29**,** 24-27.

Oh, Y., Mohan Raj, S., Jung, G. & Park, S. 2011. Current status of the metabolic engineering of microorganisms for biohydrogen production. Bioresource Technology 102, 8357-8367.

Oncel, S. 2013. Microalgae for a macroenergy world. Renewable and Sustainable Energy Reviews 26, 241-264.

Oncel, S. & Sabankay, M. 2012. Microalgal biohydrogen production considering light energy and mixing time as the two key features for scale-up. Bioresource Technology 121, 228-234.

Oncel, S. & Sukan, F. 2011. Effect of light intensity and the light: dark cycles on the long term hydrogen production of *Chlamydomonas reinhardtii* by batch cultures. Biomass and Bioenergy 35, 1066-1074.

Orhan, M. F., Dincer, I. & Rosen, M. A. 2011. Design of systems for hydrogen production based on the Cu-Cl thermochemical water decomposition cycle: Configurations and performance. International Journal of Hydrogen Energy 36, 11309-11320.

Oxborough, K., Hanlon, A. R. M., Underwood, G. J. C. & Baker, N. R. 2000. In vivo estimation of the photosystem II photochemical efficiency of individual microphytobenthos

cells using high resolution imaging of chlorophyll a fluorescence. Limnology and Oceanography 43, 1207-1221.

Ozdemir, E. & Karacor, M. 2006. Mobile phone based SCADA for industrial automation. ISA Transactions 45, 67-75.

Parmar, A., Singh, N. K., Pandey, A., Gnansounou, E. & Madamwar, D. 2011. Cyanobacteria and microalgae: A positive prospect for biofuels. Bioresource Technology 102, 10163-10172.

Parsons, T. R., Maita, Y. & Lalli, C. M. 1984. A manual of chemical and biological methods for seawater analysis, Pergamon Press.

Peters, R. & Samsun, R. 2013. Evaluation of multifunctional fuel cell systems in aviation using a multistep process analysis methodology. Applied Energy 111, 46-63.

Power, M. 1999. Recovery in Aquatic Ecosystems: Considerations for definition and measurement. Journal of Aquatic Ecosystems Stress and Recovery 6, 179-180.

Pratt, J., Klebanoff, L., Munoz-Ramos, K., Akhil, A., Curgus, D. & Schenkman, B. 2013. Proton exchange membrane fuel cells for electrical power generation on-board commercial airplanes. Applied Energy 101, 776-796.

Pulz, O. 2001. Photobioreactors: Production systems for phototrophic microorgansims. Applied Microbiology and Biotechnology 57, 287-293.

Raine, D. 2013. Hydrogen transport infrastructure: How industry is preparing for the arrival of affordable fuel cell vehicles. Fuel Cell Bulletin 12-14.

Rakopoulos, C., Scott, M., Kyritsis, D. & Giakoumis, E. 2008. Availability analysis of hydrogen/natural gas blends combustion in internal combustion engines. Energy 33, 248-255.

Ralph, P. J. & Gademann, R. 2005. Rapid light curves: A powerful tool to assess photosynthetic activity. Aquatic Botany 82, 222-237.

Rashid, N., Rehman, M., Memon, S., Rahman, Z., Lee, K. & Han, J. 2013. Current status, barriers and developments in biohydrogen production by microalgae. Renewable and Sustainable Energy Reviews 22, 571-579.

Richards, R. G. & Mullins, B. J. 2013. Using microalgae for combined lipid production and heavy metal removal from leachate. Ecological Modelling 249, 59-67.

Ritchie, R. J. 2008. Fitting light saturation curves measured using modulated fluorometry. Photosynthesis Research 96, 201-215.

Robinson, H., Knox, K., Bone, B. & Picken, A. 2005. Leachate quality from landfilled MBP waste. Waste Management, 25, 383-391.

Romeo, G., Borello, F., Correa, G. & Cestino, E. 2013. ENFICA-FC: Design of transport aircraft powered by fuel cell & flight test of zero emission 2-seater aircraft powered by fuel cells fuelled by hydrogen. International Journal of Hydrogen Energy 38, 469–479.

Rosner, V. & Wagner, H.-J. 2012. Life cycle assessment and process development of photobiological hydrogen production - from laboratory to large scale applications. Energy Procedia 29, 532-540.

Rupprecht, J. 2009. From systems biology to fuel — *Chlamydomonas reinhardtii* as a model for a systems biology approach to improve biohydrogen production. Journal of Biotechnology 142, 10-20.

Sakurai, H., Masukawa, H., Kitashima, M. & Inoue, K. 2013. Photobiological hydrogen production: Bioenergetics and challenges for its practical application. Journal of Photochemistry and Photobiology C: Photochemistry Reviews 17, 1-25.

Salomon, K. & Silva Lora, E. 2009. Estimate of the electric energy generating potential for different sources of biogas in Brazil. Biomass and Bioenergy 33, 1101-1107.

Santabarbara, S., Agostini, G., Casazza, A. P., Syme, C. D., Heathcote, P., Bohles, F., Evans, M. C. W., Jennings, R. C. & Carbonera, D. 2007. Chlorophyll triplet states associated with

Photosystem I and Photosystem II in thylakoids of the green alga *Chlamydomonas reinhardtii*. Biochimica et Biophysica Acta 1767, 88-105.

Schottler, M., Albus, C. & Bock, R. 2011. Photosystem I: Its biogenesis and function in higher plants. Journal of Plant Physiology 168, 1452-1461.

Schreiber, U. 2004. Pulse-amplitude-modulation (PAM) fluorometry and saturation pulse method: an overview, Kluwer Academic Publishers.

Schreiber, U. & Klughammer, C. 2009. New NADPH/9-AA module for the DUAL-PAM-100: Description, operation and examples of application. PAM Application Notes 2, 1-13.

Schreiber, U., Muller, J. F., Haugg, A. & Gademann, R. 2002. New type of dual-channel PAM chlorophyll fluorometer for highly sensitive water toxicity biotests. Photosynthesis Research 74, 317-330.

Schreiber, U., Quayle, P., Schmidt, S., Escher, B. & Mueller, J. 2007. Methodology and evaluation of a highly sensitive algae toxicity test based on multiwell chlorophyll fluorescence imaging. Biosensors and Bioelectronics 22, 2554-2563.

Scoma, A., Giannelli, L. & Faraloni, C. Torzillo., G. 2012. Outdoor H_2 production in a 50-L tubular photobioreactor by means of a sulfur-deprived culture of the microalga *Chlamydomonas reinhardtii*. Journal of Biotechnology 157, 620-627.

Scoma, A., Krawietz, D., Faraloni, C., Giannelli, L., Happe, T. & Torzillo, G. 2011. Sustained H_2 production in a *Chlamydomonas reinhardtii* D1 protein mutant. Journal of Biotechnology 157, 613-619.

Shaw, L., Pratt, J., Klebanoff, L., Johnson, T., Arienti, M. & Moreno, M. 2013. Analysis of H_2 storage needs for early market "man-portable" fuel cell applications. International Journal of Hydrogen Energy 38, 2810-2823.

Show, K., Lee, D., Tay, J., Lin, C. & Chang, J. 2012. Biohydrogen production: Current perspectives and the way forward. International Journal of Hydrogen Energy 37, 15616-15631.

Sims, R. E. H., Mabee, W., Saddler, J. N. & Talyor, M. 2010. An overview of second generation biofuel technologies. Bioresource Technology 101, 1570-1580.

Singh, S., Tang, W. & Tachiev, G. 2013. Fenton treatment of landfill leachate under different COD loading factors. Waste Management 33, 2116-2122.

Smith, P., Bingham, A. & Swartz, J. 2012. Generation of hydrogen from NADPH using a FeFe hydrogenase. International Journal of Hydrogen Energy 37, 2977-2983.

Spolaore, P., Joannis_Cassan, C., Duran, E. & Isambert, A. 2006. Commercial applications of microalgae. Journal of Biosciences and Bioengineering 101, 87-96.

Srisangan, K., Pyne, M. E. & Chou, C. P. 2011. Biochemical and genetic engineering strategies to enhance hydrogen production in photosynthetic algae and cyanobacteria. Bioresource Technology 102, 8589-8604.

Stephens-Romero, S., Brown, T., Carreras-Sospedra, M., Kang, J., Brouwer, J., Dabdub, D., Recker, W. & Samuelson, G. 2011. Projecting full build-out environmental impacts and roll-out strategies associated with viable hydrogen fuelling infrastructure strategies. International Journal of Hydrogen Energy 36, 14309-14323.

Stirbit, A. & Govindjee 2011. On the relation between the Kautsky effect (chlorophyll a fluorescence induction) and Photosystem II: Basics and applications of the OJIP fluorescence transient. Journal of Photochemistry and Photobiology B: Biology 104, 236-257.

Sybirna, K., Ezanno, P., Baffert, C., Leger, C. & Bottin, H. 2013. Arginine[171] of *Chlamydomonas reinhardtii* [Fe-Fe] hydrogenase HydA1 plays a crucial role in electron transfer to its catalytic centre. International Journal of Hydrogen Energy 38, 2998-3002.

Tolstygina, I., Antal, T. K., Kosourov, S., Krendeleva, T. E., Rubin, A., B & Tsygankov, A. 2009. Hydrogen production by photoautotrophic sulphur-deprived *Chlamydomonas reinhardtii* pre-grown and incubated under high light. Biotechnology and Bioengineering 102, 1055-1061

Trois, C., Coulon, F., Polge De Combret, C., Martins, J. M. F. & Oxarango, L. 2010a. Effect of pine bark and compost on the biological denitrification process of non-hazardous landfill leachate: Focus on the microbiology. Journal of Hazardous Materials 181, 1163-1169.

Trois, C., Griffith, M., Brummack, J. & Mollekopf, N. 2007. Introducing mechanical biological waste treatment in South Africa; a comparative study. Waste Management 27, 1706-1714.

Trois, C., Pisano, G. & Oxarango, L. 2010b. Alternative solutions for the bio-denitrification of landfill leachates using pine bark and compost. Journal of Hazardous Materials 178, 1100-1105.

Tsygankov, A., Kosourov, S., Seibert, M. & Ghirardi, M. L. 2002. Hydrogen photoproduction under continuous illumination by sulfur-deprived, synchronous *Chlamydomonas reinhardtii* cultures. International Journal of Hydrogen Energy 27, 1239-1244.

Tsygankov, A. A., Kosourov, S. N., Tolstygina, I. V., Ghirardi, M. L. & Seibert, M. 2006. Hydrogen production by sulfur-deprived *Chlamydomonas reinhardtii* under photoautotrophic conditions. International Journal of Hydrogen Energy 31, 1574-1584.

Wang, M., Wang, Z., Gong, X. & Guo, Z. 2014. The intensification technologies to water electrolysis for hydrogen production - A review. Renewable and Sustainable Energy Reviews 29, 573-588.

Weinert, J., Shaojun, L., Ogden, J. & Jianxin, M. 2007. Hydrogen refuelling costs in Shanghai. International Journal of Hydrogen Energy 32, 4089-4100.

White, S., Anandraj, A. & Bux, F. 2011. PAM Fluorometry as a tool to assess microalgal nutrient stress and monitor cellular neutral lipids. Bioresource Technology 102, 1675-1682.

White, S., Anandraj, A. & Trois, C. 2013. The effect of landfill leachate on hydrogen production in *Chlamydomonas reinhardtii* as monitored by PAM Fluorometry. International Journal of Hydrogen Energy 38, 14214-14222.

Wykoff, D. D., Davies, J. P., Melis, A. & Grossman, A. R. 1998. The regulation of photosynthetic electron transport during nutrient deprivation in *Chlamydomonas reinhardtii*. Plant Physiology 117, 129-139.

Xu, Y., Zhou, Y., Wang, D., Chen, S., Liu, J. & Wang, Z. 2008. Occurrence and removal of organic micro pollutants in the treatment of landfill leachate by combined anaerobic-membrane bioreactor technology. Journal of Environmental Sciences 20**,** 1281-1287.

Yang, S.-T. 2007. Chapter 1.Bioprocessing - from Biotechnology to Biorefinery.IN YANG, S.-T. (Ed.) Bioprocessing for Value-Added products from Renewable Resources. Elsevier.

Yeager, C. M., Milliken, C. E., Bagwell, C. E., Staples, L., Berseth, P. A. & Sessions, H. T. 2011. Evaluation of experimental conditions that influence hydrogen production among heterocystous *Cyanobacteria*. *Intern*ational Journal of Hydrogen Energy 36, 7487-7499.

Yuksel, I. & Kaygusuz, K. 2011. Renewable energy sources for clean and sustainable energy policies in Turkey. Renewable and Sustainable Energy Reviews 15**,** 4132-4144.

Zhang, L., Happe, T. & Melis, A. 2002. Biochemical and morphological characterization of sulphur-deprived and H_2 producing *Chlamydomonas reinhardtii* (green algae). Planta 214**,** 552-561.

Zhang, T., Ding, L. & Ren, H. 2009. Pretreatment of ammonium removal from landfill leachate by chemical precipitation. Journal of Hazardous Materials 166, 911-915.

Zhevago, N., Denisov, E. & Glebov, V. 2010. Experimental investigation of hydrogen storage in capillary arrays. International Journal of Hydrogen Energy*,* 35, 169-175.

APPENDIX 1: Technical Article 1

The effect of landfill leachate on hydrogen production in *Chlamydomonas reinhardtii* as monitored by PAM Fluorometry

Sarah White [a,b,*], Akash Anandraj [a], Cristina Trois [b]

[a] Centre for Algal Biotechnology, Mangosuthu University of Technology, PO Box 12363, Jacobs, 4026 Durban, South Africa

[b] School of Engineering, College of Agriculture, Engineering and Science, University of KwaZulu-Natal, Howard College Campus, Durban 4041, South Africa

ABSTRACT

This study investigated the effect of landfill leachate on biomass and biohydrogen production from *Chlamydomonas reinhardtii*. Maximum biomass and cell viability was recorded in 16% leachate medium with a corresponding growth rate of 927 $\mu g/l$ chl a d^{-1} as compared to the control of 688 $\mu g/l$ chl a d^{-1}. *Chlamydomonas* cultured in leachate-supplemented medium was subsequently induced to produce 37% more biohydrogen compared to the control culture. The spurge in growth can be a consequence of abundant essential elements in the diluted leachate. Energy Dispersive X-ray analysis of cells in a 16% leachate medium had the highest accumulation of Cr, Mn, Fe, Co, Ni, Mo and Cd. The benefits of the leachate medium were further shown during the hydrogen production phase using Pulse Amplitude Modulated Fluorometry. This period was extended to 8 days in comparison to the control. Leachate therefore increases both the biomass and biohydrogen yield of *Chlamydomonas*.

Copyright © 2013, Hydrogen Energy Publications, LLC. Published by Elsevier Ltd. All rights reserved.

1. Introduction

Hydrogen has always been thought of as the fuel of the future, mainly due to its high conversion efficiency, recyclability and non-polluting nature [1]. Hydrogen is used in fuel cells which constitute an attractive power generation technology, converting chemical energy into electricity at a high efficiency (60%—70%) [2]. Sustainability and renewability of hydrogen production can be achieved if the source is biological, such as bacteria (*Rhodopseudomonas palustris, Clostridium butyricum* and *Bacillus thermoamylovorans*) [3] or algae (*Scenedesmus obliquus*,

Chlamydomonas reinhardtii and cyanobacteria) [4]. Biohydrogen has been found to be less energy intensive and environmentally friendly compared the current thermochemical and electrochemical processes [5].

Microalgae have been identified as a leading feedstock for biodiesel and jet fuel [6] and recently extensive research has been undertaken to produce biohydrogen [7,8]. For the production of biohydrogen, photosynthetic microalgae are cultured in conditions to induce an anaerobic environment where, microalgae use solar energy to split water into protons and electrons, producing hydrogen as the proton carrier [9].

* Corresponding author. Centre for Algal Biotechnology, Mangosuthu University of Technology, PO Box 12363, Jacobs, 4026 Durban, South Africa. Tel: +27 31 907 7627; fax: +27 865 188012.
E-mail address: sez.white@gmail.com (S. White).

APPENDIX 2: Technical Article 2

Available online at www.sciencedirect.com

ScienceDirect

journal homepage: www.elsevier.com/locate/he
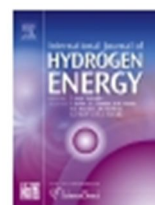
NADPH fluorescence as an indicator of hydrogen production in the green algae *Chlamydomonas reinhardtii*

S. White [a,b,*], A. Anandraj [b], C. Trois [a]

[a] School of Engineering, College of Agriculture, Engineering and Science, Howard College Campus, University of KwaZulu-Natal, Durban 4041, South Africa
[b] Centre for Algal Biotechnology, Mangosuthu University of Technology, PO Box 12363, Jacobs, 4026 Durban, South Africa

ARTICLE INFO

ABSTRACT

This study investigated cellular Nicotinamide Adenine Dinucleotide Phosphate (NADPH) fluorescence as a potential indicator of biohydrogen production in *Chlamydomonas reinhardtii* and a β-NADPH standard. NADPH fluorescence profiles of cultures grown in TAP-S (Tris-acetate phosphate minus sulphur) media, TAP (Tris-acetate phosphate) media and TAP + 3-(3,4-dichlorophenyl)-1,1-dimethylurea (DCMU) were subsequently compared. Hydrogen production induced from sulphur depletion was found to correlate directly ($r = 0.941$) with NADPH over the ten day period. The addition of leachate was used to increase hydrogen yields, and subsequently increased the NADPH concentration by 50%–70%. A direct correlation was observed ($r = 0.929$) between NADPH and hydrogen when the leachate supplemented media was used. As NADPH is the terminal electron acceptor in the photosynthetic chain, results show that NADPH has a pivotal role in hydrogen production as a carrier molecule. Under sulphur depletion, cellular NADPH fluorescence can be used as an indicator of hydrogen production.

1. Introduction

Hydrogen is envisioned to play a pivotal role as a clean renewable fuel in the hydrogen driven economy of the future [1]. Hydrogen can be used as a feedstock for Proton Exchange Membrane Fuel Cells (PEMFC) which are shown to have a high energy efficiency [2]. Hydrogen causes less to no effect on the environment [3]. Hydrogen has shown to have attractive characteristics during its use with regard to exergetic performance [4]. Hydrogen cannot be depleted and if used carefully it can provide a reliable and sustainable energy source [3]. Microalgae have shown to be a sustainable source of hydrogen and numerous strains have been found to produce hydrogen such as cyanobacteria, *Scenedesmus obliquus* [5] and *Chlamydomonas reinhardtii* [6].
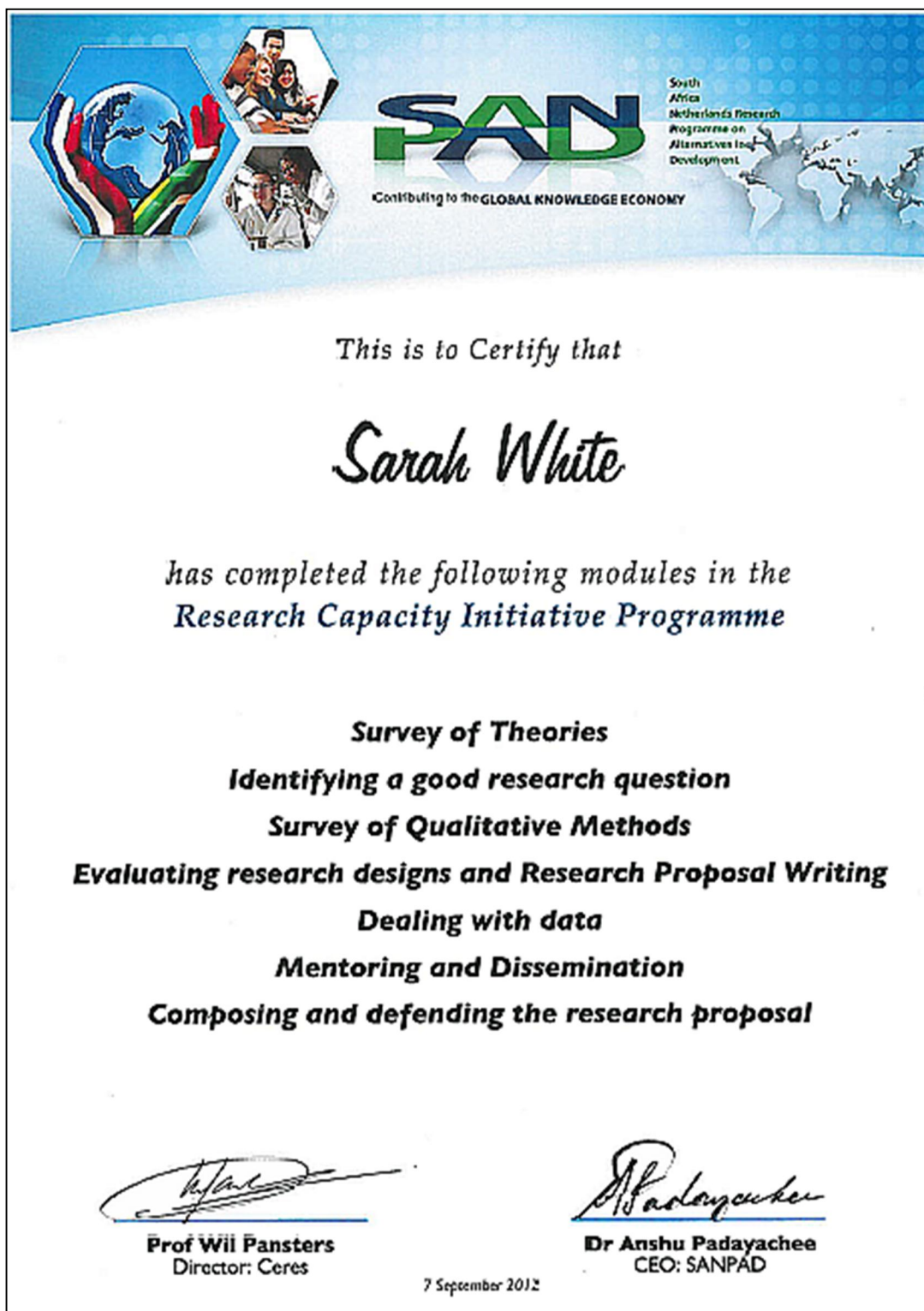
Chlamydomonas is one of the best reference organisms for studying algal biology, physiology and photosynthesis [7]. This is due to the fact that its genome has retained genes from the last common ancestor to both the plant and animal lineages [8]. It can be grown into very high cell densities in a few

APPENDIX 3: SANPAD Certificate

APPENDIX 4: Turnitin Originality Report

turnitin **Turnitin Originality Report**

Sarah White PhD Thesis- Environmental Engineering by Sarah White

From Papers (Prd Papers)

Processed on 25-Oct-2013 11:32 AM CAT
ID: 365971882
Word Count 32858

Similarity Index	Similarity by Source	
	Internet Sources:	5%
10%	Publications:	8%
	Student Papers:	4%

sources:

1 2% match (publications)

White, S., "PAM fluorometry as a tool to assess microalgal nutrient stress and monitor cellular neutral lipids", Bioresource Technology, 201101

2 1% match (student papers from 01-Mar-2012)

Submitted to Royal Melbourne Institute of Technology on 2012-03-01

3 1% match (publications)

Kosourov, S., "A comparison of hydrogen photoproduction by sulfur-deprived Chlamydomonas reinhardtii under different growth conditions", Journal of Biotechnology, 20070310

4 < 1% match (student papers from 14-May-2009)

Submitted to University of KwaZulu-Natal on 2009-05-14

5 < 1% match (Internet from 07-Jan-2013)

http://www.ncbi.nlm.nih.gov/pmc/articles/PMC2777220/?tool=pubmed

6 < 1% match (Internet from 05-Aug-2012)

http://crida.academia.edu/ArunShanker/Books/1188570/Abiotic_Stress_In_Plants_-_Mechanisms_and_Adaptations

7 < 1% match (Internet from 24-Dec-2012)

http://walz.asia/products/chl_p700/dual-pam-100/spec_modular_version.html

8 < 1% match (Internet from 17-Mar-2012)

http://web1.sssup.it/pubblicazioni/ugov_files/306260_2011%20New%20Phytol%20Whitney%20et%20al.pdf

9 < 1% match (Internet from 16-Dec-2012)

http://www.scribd.com/doc/79249515/2011-Biological-Hydrogen-Production-by-the-Algal-Biomass-Chlorella-Vulgaris-MSU-01

10 < 1% match (publications)

Taras K. Antal. "Acclimation of green algae to sulfur deficiency: underlying mechanisms and

https://turnitin.com/newreport_printview.asp?eq=1&eb=1&esm=10&oid=365971882&sid=0&n=0&...   2013/11/06